Image Recovery from Partial Fresnel Zone Information

by

Robert J. Rolleston

Submitted in Partial Fulfillment

of the

Requirements for the Degree

DOCTOR OF PHILOSOPHY

Supervised by Dr. Nicholas George

The Institute of Optics

University of Rochester

Rochester, New York

1988

UNCLASSIFIED
SECURITY CLASSIFICATION OF THIS PAGE

REPORT DOCUMENTATION PAGE

1a. REPORT SECURITY CLASSIFICATION Unclassified	1b. RESTRICTIVE MARKINGS
2a. SECURITY CLASSIFICATION AUTHORITY	3. DISTRIBUTION/AVAILABILITY OF REPORT Approved for public release; distribution unlimited.
2b. DECLASSIFICATION/DOWNGRADING SCHEDULE	
4. PERFORMING ORGANIZATION REPORT NUMBER(S)	5. MONITORING ORGANIZATION REPORT NUMBER(S) ARO 24749.3-PH
6a. NAME OF PERFORMING ORGANIZATION University of Rochester 6b. OFFICE SYMBOL (If applicable)	7a. NAME OF MONITORING ORGANIZATION U. S. Army Research Office
6c. ADDRESS (City, State, and ZIP Code) The Institute of Optics Rochester, New York 14627	7b. ADDRESS (City, State, and ZIP Code) P. O. Box 12211 Research Triangle Park, NC 27709-2211
8a. NAME OF FUNDING/SPONSORING ORGANIZATION U. S. Army Research Office 8b. OFFICE SYMBOL (If applicable)	9. PROCUREMENT INSTRUMENT IDENTIFICATION NUMBER DAAL03-87-K-0084
8c. ADDRESS (City, State, and ZIP Code) P. O. Box 12211 Research Triangle Park, NC 27709-2211	10. SOURCE OF FUNDING NUMBERS PROGRAM ELEMENT NO. / PROJECT NO. / TASK NO. / WORK UNIT ACCESSION NO
11. TITLE (Include Security Classification) Image recovery from partial Fresnel zone information	
12 PERSONAL AUTHOR(S) Robert J. Rolleston	
13a. TYPE OF REPORT Technical 13b. TIME COVERED FROM _____ TO _____	14. DATE OF REPORT (Year, Month, Day) March 1988 15. PAGE COUNT 191
16. SUPPLEMENTARY NOTATION The view, opinions and/or findings contained in this report are those of the author(s) and should not be construed as an official Department of the Army position, policy, or decision, unless so designated by other documentation.	

17. COSATI CODES		
FIELD	GROUP	SUB-GROUP

18. SUBJECT TERMS (Continue on reverse if necessary and identify by block number)
Image recovery; phase retrieval; Fresnel Zone; magnitude retrieval

19 ABSTRACT (Continue on reverse if necessary and identify by block number)

The problem of reconstructing an unknown image from partial data in the Fresnel zone region is discussed. An iterative method of reconstructing an unknown image from either the phase-only or magnitude-only data in the transform domain, is investigated through the use of digital calculations. From the Fourier transform plane through the Fresnel region, it is demonstrated that the phase-only information in the transform allows for a very good reconstruction in just a few iterations. While reconstructing an image from the magnitude of the Fourier transform is very difficult, as one moves further into the Fresnel zone region, good reconstructions are obtained in only several iterations.

20. DISTRIBUTION/AVAILABILITY OF ABSTRACT ☐ UNCLASSIFIED/UNLIMITED ☐ SAME AS RPT. ☐ DTIC USERS	21. ABSTRACT SECURITY CLASSIFICATION Unclassified
22a. NAME OF RESPONSIBLE INDIVIDUAL Nicholas George	22b. TELEPHONE (Include Area Code) 716-275-2417 22c. OFFICE SYMBOL

DD FORM 1473, 84 MAR 83 APR edition may be used until exhausted. All other editions are obsolete.

SECURITY CLASSIFICATION OF THIS PAGE
UNCLASSIFIED

Image Recovery from Partial Fresnel Zone Information

by

Robert J. Rolleston

Submitted in Partial Fulfillment

of the

Requirements for the Degree

DOCTOR OF PHILOSOPHY

Supervised by Dr. Nicholas George

The Institute of Optics

University of Rochester

Rochester, New York

1988

VITAE

Robert Rolleston [redacted] was awarded the Most Outstanding Science Student in the graduating class of Trinity High School, where he graduated with honors in 1977. After high school he entered Carnegie-Mellon University, where he obtained a Bachelor of Science in Computational Physics with University Honors in 1981. During the summers of his college years, he worked for NCR Corporation in Cambridge, Ohio, where his interest in optics was nurtured.

In the fall of 1981, Robert Rolleston was in the first group of Master Co-op students at The Institute of Optics, University of Rochester. In 1982 he worked for Xerox Corporation in Webster, New York as part of the Co-op program, and returned to The Institute of Optics in the fall of 1982 to pursue his doctorate under the supervision of Professor Nicholas George. He was awarded his Master of Science in Optics in the spring of 1983. He served as the Graduate Student Representative in 1984, and during the summer of 1987 took time off from his studies to ride a bicycle across the United States.

During his stay at The Institute of Optics Robert Rolleston has been supported by several assistantships including one from the New York State Center for Advanced Optical Technology.

ACKNOWLEDGMENTS

It is a pleasure to formally acknowledge and thank the many people who have made my time here at The Institute of Optics not only possible, but an enjoyable experience as well.

Thanks are due my advisor, Dr. Nicholas George, for his support on this project. In working with him I have learned a great deal more than the research presented in this dissertation.

I acknowledge the financial support of the U.S. Army Research Office and the New York State Center for Advanced Optical Technology.

The many individuals I have known and worked with here have all contributed something in their own way. A few deserve special thanks. Mal, for not only proof reading this dissertation, but along with Paul and Keith, making our office a pleasure to work in. Joan, Ben, Greg, Phil, and Tony for all those lunches under the optics tree. Leo and Anne for joining me and being witness to the continuous live entertainment of Kathleen. These names are just some of the people I knew I could count on, to those of you not mentioned explicitly, I thank you and appreciate your help and friendship.

Some of the images used as examples were photographs taken by Mike Garner. A special thanks for putting up with the pain in the butt and documenting the summer of 1987.

Finally, my parents, without whose love and support I would not be who I am today.

with love and respect for my mother and father.

ABSTRACT

The problem of reconstructing an unknown image from partial data in the Fresnel zone region is discussed. The Fresnel region of a coherent optical processing system is used as a basis for the definition of a Fresnel zone transform pair. An iterative method of reconstructing an unknown image located in the object domain, from either the phase-only or magnitude-only data in the transform domain, is investigated through the use of digital calculations.

The Fresnel zone transform is implemented digitally using a fast Fourier transform routine. The number of Fresnel zones, which is a measure of how far out of the Fourier transform plane one is located, is limited by certain sampling considerations which are discussed. From the Fourier transform plane through the Fresnel region, it is demonstrated that the phase-only information in the transform allows for a very good reconstruction in just a few iterations of the reconstruction algorithm. While reconstructing an image from the magnitude of the Fourier transform is very difficult, as one moves further into the Fresnel zone region, good reconstructions are obtained in only several iterations.

The success of the magnitude-only reconstructions from data far into the Fresnel region is explained. An approximation of the Fresnel zone transform integral is derived which is valid for a large number of Fresnel zones. This approximation is used to show that the first iterative guess is approximately equal to the unknown image.

Phase-only information in the Fresnel zone transform leads to very good reconstructions throughout the Fresnel zone region. For a given number of iterations, there is a slight degradation in the quality of the reconstructed image as the number of Fresnel zones is increased. The phase of the Fresnel zone transform preserves the structure of the sharp edges in the image, the ability of the phase information to preserve the edge information is demonstrated analytically.

A degradation in the reconstructed image results if noise is present in the given data. The probability density functions of the magnitude and phase of a signal in the presence of coherently additive noise are derived. The effects of both signal independent and signal dependent noise are investigated.

An error in the number of Fresnel zones is investigated. A method of searching through the Fresnel region to find the correct location of the Fresnel zone transform is discussed.

In reconstructing an image from either the phase-only or magnitude-only data of the Fresnel zone transform, the iterative reconstruction algorithms which are used are shown to be stable both in the presence of noise and in an error in the number of Fresnel zones. In addition, while there is only a slight degradation in the quality of the reconstruction from phase-only data, there is a dramatic improvement in the quality of the magnitude-only reconstruction as one moves out of the Fourier transform plane and into the Fresnel region.

The novel aspect of this research is the extension of the reconstruction algorithm into the Fresnel zone region. With the formulation presented

in the appendix, the Fresnel zone transform is seen to be a particular case of a more general reconstruction problem. It is demonstrated in this dissertation that for a set number of iterations, the reconstructions are much improved if the illuminating wavefront is known and non-trivial (i.e. contains terms of higher order than constant and linear).

TABLE OF CONTENTS

LIST OF TABLES

LIST OF FIGURES

Chapter 1

Introduction

1.1 Statement of the Problem and Objectives

Down through history, people have been trying to get something for nothing. It may be as simple as a free lunch or as complicated as the reconstruction of an unknown image from partial information of the transform. It is worthwhile to begin this discussion with an explanation of image reconstruction and how it relates to other fields such as image enhancement, image restoration, image synthesis, and image recovery. The fact that all of these areas are of active interest is affirmed by the recent publication of two books dedicated to these subjects [Stark, (1987); Bates and McDonnell, (1986)], and the success of recent conferences [see for example, *Signal Recovery and Synthesis with Incomplete Information and Constraints Technical Digest*, (Optical Society of America, Washington D.C., 1983); *Topical Meeting on Signal Recovery and Synthesis II Technical Digest*, (Optical Society of America, Washington D.C., 1986); *SPSE's 40th Annual Conference and Symposium on Hybrid Imaging Systems*, (SPSE - The Society for Imaging Science and Technology, Springfield VA, 1987)] and special issue journal publications dedicated to these topics [see for example, J. Opt. Soc. Am., 73, (1983); J. Opt. Soc. Am. A , 4, (1987)].

Manipulating the tone reproduction curve, adjusting color maps for the display of a digital image, and changing the development process when printing a picture are just some examples of image enhancement.

"Image enhancement processes consist of a collection of techniques that seek to improve the visual appearance of an image, or to convert the image to a form better suited to human or machine analysis" [Pratt, (1978), p. 307]. Many image enhancement techniques lack a rigorous derivation as a basis for the methods which are used. This is quite often the case because the end result, the improved appearance of an image, is very subjective.

Image restoration is very similar to image enhancement, in that the result is an improved image. "Image restoration involves estimating the properties of the distortion and using them to refurbish the original information" [Bates and McDonnell, (1986), p. 5]. The techniques used in image restoration generally have a mathematical basis and involve estimation, statistics, and the modeling of physical processes. Some typical image restoration procedures involve estimating the statistical properties of various noise processes in an attempt to read a signal through the noise, or the modeling of the physical effects of varnish and shellac over time to restore ancient artwork [Asmus, (1987)].

In both the enhancement and restoration of images, one is given an image and work is done to improve that image for its intended use. Image synthesis differs from these procedures because there is no original image given; "the synthesis problem is concerned with the determination of a signal, such as an image, which is consistent with the known constraints" [Hayes, (1987)]. "An image restoration problem involves the recovery of an actual image that has been distorted by a given imaging system. Image synthesis, on the other hand, aims at discovering an input

image which, when distorted by a given imaging system (e.g. a display device), yields a desired output pattern. The sought image is discovered (designed, constructed, or synthesized), rather than recovered, reconstructed, or restored" [Saleh, (1987)]. A direct application of these synthesis techniques is in the design of a mask used for the manufacture of integrated circuits. In this instance, there is a very definite structure desired after the imaging of a mask onto a substrate, and the subsequent etching of that substrate.

"Stated in its most general form, the signal recovery problem is described like this: Given data g, determine the source f, that produced g" [Stark, (1987), p. xi]. This definition of image recovery is indeed very general, and may better be viewed as just one topic under the wider field of inverse source problems. In the image enhancement and image restoration problems discussed above, one is given an image of some type, and the procedures will alter the image in some way, but the general structure and form of the image is known and not changed. In the case of image recovery, the given data may differ quite a bit from the sought after solution to the problem. Literature concerning both the larger areas of study investigating various aspects of of the inverse source problem, and inverse scattering problem (see for example: Baltes, ed., (1978); Baltes, ed., (1980)], and the general field of image recovery will not be reviewed here.

The work contained in this thesis is best placed in the area of image reconstruction. "The reconstruction problem ... is concerned with the unique recovery of a signal given a partial Fourier domain description

along with a signal model, or a set of signal constraints" [Hayes, (1987)]. The reconstruction of a signal from partial Fourier domain information includes the areas of computer aided tomography, image retrieval, phase retrieval, and magnitude retrieval. The use of Fresnel zone information as opposed to Fourier domain information is a novel aspect of the research discussed in this dissertation.

While the Fresnel zone transform pair will be defined in Sect. 2.2, it is worthwhile to define the Fourier transform pair. Given a function (or image), g(x,y), defined in the object domain (or image plane), the Fourier transform, $G(f_x, f_y)$, is given by

$$G(f_x, f_y) = \int_{-\infty}^{+\infty}\int_{-\infty}^{+\infty} g(x,y)\, e^{-i2\pi(f_x x + f_y y)}\, dxdy\,, \tag{1-1}$$

where x and y are spatial coordinates and f_x and f_y are spatial frequencies. The inverse Fourier transform is given by

$$g(x,y) = \int_{-\infty}^{+\infty}\int_{-\infty}^{+\infty} G(f_x, f_y)\, e^{+i2\pi(f_x x + f_y y)}\, df_x df_y\,. \tag{1-2}$$

Throughout this thesis, lower case letters will be used to represent functions (or images) in the object domain (or image plane), and upper case letters will represent the transform of the corresponding lower case function. Writing the complex valued function, $G(f_x,f_y)$, in polar form

$$G(f_x, f_y) = |G(f_x, f_y)|\, exp\{i\theta(f_x, f_y)\}\,, \tag{1-3}$$

the magnitude (or modulus), $|G(f_x, f_y)|$, is given by

$$|G(f_x, f_y)| = [G(f_x, f_y)\;\; G^*(f_x, f_y)]^{\frac{1}{2}}\,, \tag{1-4}$$

where * represents a conjugate complex. The phase, $\theta(f_x, f_y)$, is defined to satisfy the simultaneous equations

$$\cos[\theta(f_x,f_y)] = \frac{RE[G(f_x,f_y)]}{|G(f_x,f_y)|} \quad , \tag{1-5a}$$

$$\sin[\theta(f_x,f_y)] = \frac{IM[G(f_x,f_y)]}{|G(f_x,f_y)|} \tag{1-5b}$$

where $RE[G(f_x,f_y)]$ and $IM[G(f_x,f_y)]$ are the real and imaginary parts, respectively, of $G(f_x,f_y)$.

The terms magnitude-only reconstruction and phase retrieval are both used to describe the problem when only the magnitude information, $|G(f_x,f_y)|$, is known. The problem is then one of reconstructing the image from this magnitude-only information, or retrieving the the phase which corresponds to the given magnitude. The terms phase-only reconstruction and magnitude retrieval are both used to describe the problem when only the complex phase, $\exp\{ i\,\theta(f_x, f_y) \}$, is known. The problem is then one of reconstructing the image from this phase-only information, or retrieving the magnitude which corresponds to the given phase information. A third type of problem is posed when both the magnitude and phase are known, but only over a partial region of the transform space. This is the problem often encountered in computer aided tomography. All of these problems generally make certain assumptions about the unknown image such as constraints on its spatial extent or non-negativity.

1.2 Background

The problem of reconstructing a function from partial Fourier domain information was first investigated by A.A. Michelson [1891, 1892] and

Lord Rayleigh [1892]. The problem originally arose in trying to determine the spectrum of a source from a measurement of the visibility curves of the interference pattern. The measured visibility curve represented only the modulus of the Fourier transform of the unknown spectrum [see also Born and Wolf, §7.5.8, (1980)].

The phase retrieval problem was investigated by Wolf [1962], who introduced the idea of using some of the analytic properties of the functions involved. This method used the locations of the complex zeros in the analytically continued functions to reconstruct the complete Fourier spectra.

The dispersion relations [Toll, (1956)], which relate the real and imaginary parts of a complex function that is analytic and regular in the lower half plane, are used to reconstruct the Fourier phase from knowledge of the log of the Fourier magnitude. Problems arise however, when there are zeros located in the lower half plane of the analytically continued Fourier magnitude. In this case there is a multiplicity of solutions due to the Blaschke factor which is used to remove these zeros. The position of the zeros and their physical interpretation was investigated by Nussenvieg [1966]. In addition, it has been shown [Nieto-Vesperinas, (1980)] that the extension of the dispersion relations to two dimensions yields a pair of equations that in general have no solution.

Techniques which made use of the fact that the functions are band-limited, which is the case for imaging, were investigated by Walther [1962]. This method dealt with only the one dimensional diffraction

problem, and Walther expected that "the extension to the real two-dimensional case will probably be fraught with difficulties."

Methods of modifying the experimental measurement were first suggested by Kohler and Mandel [1969, 1972], and Mehta [1965, 1968]. These methods suggested the use of an additional point source or reference beam, which is analogous to the use of a reference beam in holography, and the use of exponential filters on the source, which would change the locations of the zeros in the analytically continued complex plane. The conditions under which the support of the unknown object allow for the successful reconstruction were also investigated [Greenaway, (1977)].

Using the location of the zeros not only in the Fourier transform magnitude, but in the Fresnel region as well, has also been suggested [Ross *et al* (1980)], along with an interpretation of the importance of the zeros throughout the Fresnel region [Fiddy *et al*, (1982)].

While the early work on phase retrieval from the Fourier transform modulus data concentrated on one-dimensional functions, the problem for the case of two-dimensional data was introduced by Napier and Bates [1974]. For the most common case of sampled data, the problem can be stated in terms of the ability to factorize polynomials [Bruck and Sodin, (1979)]. By the fundamental theorem of algebra, any polynomial of degree two or more of a single variable can always by factored, but there is no guarantee of the ability to factorize polynomials of more than one variable. This basic difference between the one-dimensional and two-dimensional problems was one aspect in the questions about ambiguity

and uniqueness of any reconstruction [Bates, (1982); Garden and Bates, (1982); Fright and Bates, (1982)]. These questions will not be addressed here, but rather the reader is directed to some of the extensive literature on this subject [Huiser and vanToorn, (1980); Fiddy *et al*, (1983); Brames, (1985, 1986); Hayes and McClellan, (1982); Kierdron, (1981); Sanz and Huang, (1983); Scivier and Fiddy, (1985)].

Along with the many analytic techniques mentioned above, computer algorithms were also developed. Most of the computer algorithms were based upon an iterative procedure first described by Gerchberg and Saxton [1971, 1973]. The original procedure outlined by Gerchberg and Saxton used the intensity in both the image plane and the Fourier plane to find the phase function in each domain. The algorithm is iterative, and transforms back and forth between the two domains. At each iteration the known magnitude information is applied in the appropriate domain, while the phase functions are allowed to iterate to a value which is consistent with the known information.

It should be noted that this procedure can be easily generalized to many other situations. The basic idea of the algorithm is simply to transform between two domains, and apply any known information in each domain as appropriate. One such generalization was developed by Misell [1972, 1973a, 1973b, 1973c] for the case of information recorded in the image plane and in one defocused plane. Although a non-iterative solution to the phase problem is possible when data from two different locations is known [Dallas, (1975); (1976)], Boucher [1980a, 1980b] has

shown that these techniques are much more sensitive to noise and errors than are the iterative techniques.

Modified versions of the Gerchberg-Saxton algorithm have been developed by Fienup [1978, 1979, 1981a, 1981b, 1982, 1983]. The basic modification to the algorithm is in the use of only one intensity measurement (in the Fourier plane), and the use of non-negativity and spatial extent constraints in the object domain. Other modifications involve variations on how the known information and constraints are applied in each domain. Variations of these reconstruction algorithms require from 60 to 200 iterations for a satisfactory solution. A nice summary and comparison of these different techniques has been given by Fienup [1982]. Current forms of Fienup's algorithm are concerned with overcoming the common problems of stagnation, improving the convergence time (i.e. number of iterations) of the reconstruction [Fienup and Wackerman, (1986); Fienup, (1986)], and working with complex valued objects [Fienup, (1986a)].

All of the reconstruction techniques discussed above have dealt with the problem of phase retrieval. The corresponding problem of magnitude retrieval was first investigated by Hayes, Lim and Oppenheim, [1980] and others [Oppenheim *et al*, (1980); Hayes, (1981, 1982); Oppenheim *et al*, (1982); Oppenheim *et al*, (1983); Oppenheim and Lim, (1983)]. Although in many cases of interest a closed form solution to the problem of reconstructing an image from Fourier transform phase information is possible, the large set of equations which must be solved simultaneously makes these methods of solution very difficult. Using only the phase

information of the Fourier transform as the known data in a Gerchberg-Saxton type algorithm leads to a recognizable image in just one iteration, and a fairly good reconstruction in just several iterations [Hayes, (1982)]. Good reconstructions were found even when only one bit of the phase information was combined with the magnitude information [Van Hove, (1982); Van Hove *et al*, (1983)].

The theory and method of projections onto convex sets [Youla and Webb, (1982); Sezan and Stark, (1982)] present a rigorous mathematical basis for many of the iterative reconstruction techniques discussed above. The method of alternating projections onto convex sets has been applied to both the phase retrieval [Levi and Stark, (1984)] and the magnitude retrieval [Levi and Stark, (1983)] problems.

Other methods of image reconstruction have been investigated [Frieden, (1972); Kiedron, (1980); Arsenault and Chalasinka-Macukow, (1983); Bortz, (1983); Deighton *et al*, (1985); Harque and Meyer, (1986); Fienup, (1986b)] but will not be described here since our main interest is in a reconstruction method based upon the Gerchberg-Saxton algorithm.

1.3 Overview of this Dissertation

The problem of reconstructing an unknown image from partial data in the Fresnel zone region is discussed. The Fresnel region of a coherent optical processing system is used as a basis for the definition of a Fresnel zone transform pair. An iterative method of reconstructing an unknown image located in the object domain, from either the phase-only or

magnitude-only data in the transform domain, is investigated through the use of digital calculations.

In Chapt. 2, the Fresnel zone transform is implemented digitally using a fast Fourier transform routine. The number of Fresnel zones, which is a measure of how far out of the Fourier transform plane the original (or available) data is obtained, is introduced as a dimensionless parameter used throughout this dissertation. The number of Fresnel zones is limited by certain sampling considerations which are discussed. From the Fourier transform plane through the Fresnel region, it is demonstrated that the phase-only information in the transform allows for a very good reconstruction in just a few iterations of the reconstruction algorithm. While reconstructing an image from the magnitude of the Fourier transform is very difficult, as one moves further into the Fresnel zone region good reconstructions are obtained in only several iterations [Rolleston and George, (1986)].

Chapter 3 presents an explanation for the success of the magnitude-only reconstructions from data far into the Fresnel region. An approximation of the Fresnel zone transform integral is derived which is valid for a large number of Fresnel zones. The stationary phase approximations which are used are developed for the case of one-dimensional functions, with a summary given for the case of two-dimensional images. Critical points of the second kind are also calculated for the case of two dimensional images. These approximations are used to show that the first iterative guess is approximately equal to the unknown image [Rolleston and George, (1987)].

As evidenced by the reconstruction experiments in Chapt. 2, phase-only information in the Fresnel zone transform leads to very good reconstructions throughout the Fresnel zone region. It has been shown that, for a given number of iterations, there is a slight degradation in the quality of the reconstructed image as the number of Fresnel zones is increased, but that the phase of the Fresnel zone transform preserves the structure of the sharp edges in the image. Through several illustrative examples presented in Chapt. 4, the ability of the phase information to preserve the edge information is demonstrated analytically.

Chapter 5 concerns itself with a discussion of the effects of noise on the reconstruction process. A degradation in the reconstructed image results if noise is present in the given data. A model for coherently additive noise, and the resulting probability density functions of the magnitude and phase of a signal, are derived. The effects of both signal independent additive and signal dependent multiplicative noise are investigated.

Another possible source of error is the incorrect number of Fresnel zones used in the reconstruction algorithm. Chapter 6 discusses the effects of using the incorrect number of Fresnel zones and describes a method of searching through the Fresnel region to find the correct location of the Fresnel zone transform.

An alternate point of view of the Fresnel zone transform, as defined in the context of the coherent optical processor discussed in Chapt. 2, is described in App. A. This alternate point of view allows for a generalization of the Fresnel zone transform to include the case of illumination by a general aberrated wavefront. An example of this type

of reconstruction is presented.

Chapter Two

Image Reconstruction from Partial Fresnel Zone Information

2.1 Introduction

Many of the methods used for reconstructing an object from partial Fourier transform information discussed in Chapt. 1 use a modified Gerchberg-Saxton algorithm. There are instances when only the undistorted phase or magnitude of the Fourier transform is known, and a reconstruction of the original object is desired. It is generally assumed in these reconstructions that the original object is real valued.

In this chapter a method for the reconstruction of an image from partial data in the Fresnel zone region is presented. The ability to obtain excellent image reconstructions using either phase-only or magnitude-only data from the Fresnel zone transform of a real-valued, non-negative object will be demonstrated with the use of computer simulations.

The standard 4-F canonical optical processor discussed in Sect. 2.2 is used as the basis for the derivation of the optical Fresnel zone transform [see Goodman, (1968) §5.2 and §7.4 for a further discussion of coherent optical processors]. From this groundwork in coherent optical processors, a generalized Fourier transform pair is defined. The numerical methods used to calculate the Fresnel zone transforms, as well as the sampling considerations, are discussed. A dimensionless parameter, Z_F (the number of Fresnel zones), is introduced as a measure of how far out of the Fourier transform plane the Fresnel zone transform is located.

An alternate point of view of the Fresnel zone transform is described in App. A. The presentation in App. A formulates the reconstruction problem in the context of Fourier transforms. The problem is to reconstruct the magnitude of an image; given either the magnitude-only or phase-only data of the Fourier transform, and the phase part of the original complex image. In this context, the Fresnel zone transform discussed in this dissertation is a special case of the reconstruction problem presented in App. A.

Section 2.3 presents an algorithm used for reconstructing an image from phase-only data. The results of reconstructions from several different Fresnel zone locations, as well as measures of the error in these reconstructions, are presented. Magnitude-only reconstructions are discussed in Sect. 2.4, which includes error measurements, and examples of several reconstructions.

It is shown that for this type of reconstruction, as one moves away from the Fourier transform plane, very good reconstructions are obtained in just a few iterations using phase-only data. For the same number of iterations, reconstructions from magnitude-only information improve as one moves farther from the Fourier plane.

2.2. Optical Fresnel Zone Transform and Digital Calculation

Consider the standard 4-F canonical optical processor shown in Fig. 2-1. It consists of an input plane (x,y), a generalized transform plane (u,v), a Fourier transform plane located midway between the two lenses, and an output plane (r,s). Throughout this section we adopt the notation that g(x,y) is the scalar component of the field in the input plane and G(u,v) is the scalar component in the transform plane. Note that the transform plane is not constrained to a location midway between the two lenses, so it is not necessarily a Fourier transform. If the input, with amplitude transmittance g(x,y), is illuminated by a monochromatic plane wave, then the scalar component of the field in the transform plane a distance d_1 behind the first lens will be given by

$$G(u,v) = c_1 \int_{-\infty}^{+\infty} \int_{-\infty}^{+\infty} g(x,y)\, K_1(x,y;\, u,v)\, dx\, dy \ , \tag{2.2-1}$$

where the transfer kernel $K_1(x,y;\, u,v)$ is as follows:

$$K_1(x,y;\, u,v) = e^{-i\pi a_1 (x^2+y^2)}\, e^{-i2\pi (f_x x + f_y y)} \ . \tag{2.2-2}$$

For simplicity of notation, we have defined the complex constant c_1 by

$$c_1 = \frac{i e^{-ik(d_1 + F)}}{\lambda F} \tag{2.2-3}$$

and the spatial frequency variables f_x and f_y by

$$f_x = -u/\lambda F \quad and \quad f_y = -v/\lambda F \ . \tag{2.2-4}$$

The convenient offset parameter a_1, used in Eq. (2.2-2), is defined as follows:

$$\alpha_1 = \left(1 - \frac{d_1}{F}\right) / \lambda F \,. \tag{2.2-5}$$

If $d_1 = F$, then $\alpha_1 = 0$. and the well known Fourier transform relationship between the front and back focal planes of a convex lens is obtained. If $d_1 \neq F$, then the generalized transform plane is in the Fresnel zone of the optical processor; this is the region of central interest in this discussion. The terminology optical Fresnel zone transform will be used to describe Eq. (2.2-1).

If the scalar component of the field, G(u,v), is propagated a distance d_2 to the second lens and then to the output plane (r,s), the scalar component of the output is given by

$$g_{out}(r,s) = c_2 \int_{-\infty}^{+\infty} \int_{-\infty}^{+\infty} G(u,v)\, K_2(u,v;\, r,s)\, du\, dv \,, \tag{2.2-6}$$

where the transfer kernel $K_2(u,v; r,s)$ is as follows:

$$K_2(u,v;r,s) = e^{-i\pi\alpha_2(r^2+s^2)}\, e^{-i2\pi(f_x r + f_y s)} \,. \tag{2.2-7}$$

The complex constant c_2 is given by

$$c_2 = \frac{i e^{-ik(d_2 + F)}}{\lambda F} \,, \tag{2.2-8}$$

and the spatial frequencies f_x and f_y are defined in Eq. (2.2-4). A convenient offset parameter α_2, used in Eq. (2.2-6), is defined as follows:

$$\alpha_2 = \left(1 - \frac{d_2}{F}\right) / \lambda F \,. \tag{2.2-9}$$

For the case when $d_1 + d_2 = 2F$, the output $g_{out}(r,s)$ is given by

$$g_{out}(r,s) = -e^{-ik4F} g(-r,-s) \,. \tag{2.2-10}$$

Aside from a phase retardation term, the output is an inverted image of the input.

2.2.2 The Fresnel Zone Transform Pair

It is convenient to summarize the above discussion with the following definition of a Fresnel-zone transform pair. Consider a general function, g(x,y), and its associated Fresnel zone transform $G(f_x, f_y)$. The Fresnel-zone transform of g(x,y) is given by

$$G(f_x, f_y) = \int_{-\infty}^{+\infty}\int_{-\infty}^{+\infty} g(x,y)\,K(x,y;\, f_x, f_y)\,dx\,dy\,, \tag{2.2-11}$$

and the inverse Fresnel zone transform is given by

$$g(x,y) = \int_{-\infty}^{+\infty}\int_{-\infty}^{+\infty} G(f_x, f_y)\,K^{*}(x,y;\, f_x, f_y)\,df_x\,df_y\,. \tag{2.2-12}$$

The Fresnel-zone transform kernel $K(x,y;\, f_x, f_y)$ is given as

$$K(x,y;\, f_x, f_y) = e^{-i\pi\alpha_1(x^2+y^2)}\; e^{-i2\pi(f_x x + f_y y)}\,, \tag{2.2-13}$$

and * denotes a conjugate complex. In this mathematical definition of a Fresnel-zone transform pair the phase retardation and image inversion that occur in the optical transform have been suppressed.

This Fresnel-zone transform pair is very closely related to the well known Fourier transform pair. A Fresnel zone transform is easily calculated by using the analytic properties of Fourier transform theory as well as the numerical methods associated with the fast Fourier transform. To calculate the Fresnel zone transform of an input object g(x,y), first multiply the object by the complex Gaussian phase term, $\exp[-i\pi\alpha_1(x^2 + y^2)]$, and then take the Fourier transform of this product. This

multiplication followed by a Fourier transform is much easier and faster than convolving the Fourier transform of the object with the Fourier transform of the complex Gaussian phase term. The Fresnel zone transform of a digitized image can be calculated easily using a fast Fourier transform (FFT) routine.

If the Fresnel zone transform $G(f_x,f_y)$ is known, then an inverse Fresnel zone transform can be used to find the unknown image. To calculate an inverse Fresnel zone transform, first perform an inverse Fourier transform, and then multiply by the complex Gaussian phase term $\exp[i\pi\alpha_1(x^2 + y^2)]$. If it is known that the object is real valued and non-negative, then the modulus of the inverse Fourier transform can be used as the inverse Fresnel-zone transform rather than multiplying by the complex Gaussian. The inverse Fresnel zone transform can be calculated using an inverse fast Fourier transform (IFFT) routine, followed by a multiplication or absolute value operation.

Throughout this dissertation the Fresnel zone transform pair defined in Eqs. (2.2-11) and (2.2-12) will be used, rather than the optical transform described in Eqs. (2.2-1) and (2.2-6). This prevents the resultant image from being inverted and suppresses the constant phase retardation that occurs in the optical transform. Since the input functions are limited to real valued non-negative objects, the complex Gaussian, $\exp[i\pi\alpha_1(x^2 + y^2)]$, used to calculate an inverse Fresnel zone transform is not needed.

2.2.3 Sampling Considerations

In the numerical computation of the Fresnel-zone transform defined in Eq. (2.2-11) a consideration of the sampling interval must be made. The sampling interval is controlled both by the spectrum of g(x,y) and by the oscillatory nature of the complex Gaussian multiplier. This discussion will investigate the sampling limits based upon the oscillations of the complex Gaussian term, and not on the spectrum of g(x,y).

Consider the sampling of the input in more detail. From Eqs. (2.2-11) and (2.2-13), it is seen that the process of calculating a Fresnel zone transform is the same as calculating the Fourier transform of the product

$$g(x,y)\, e^{-i\pi a_1 (x^2 + y^2)} \tag{2.2-14}$$

If this function is sampled at x = mT and y = nT, where T is the sampling interval, m = -N/2, − N/2 + 1, ... , + N/2-1, and n = -N/2, -N/2 + 1, ..., + N/2-1, Eq. (2.2-14) becomes

$$g(mT, nT)\, e^{-i\pi a_1 T^2 (m^2 + n^2)} \tag{2.2-15}$$

The total number of samples is NxN. An FFT can be used on this sampled data only if the function has been sampled at a sufficient frequency. The term g(mT, nT) will be a digitized picture of finite extent and it is assumed that T can be chosen so that the finest detail of interest in the image will be properly sampled. However, the term $\exp[-i\pi a_1 T^2(m^2 + n^2)]$ can oscillate very rapidly near the edge of the image. To obtain an estimate of how large a_1 can be, let n = 0 and assume that the argument of the complex Gaussian is to change by no more than $\pi/4$ from one sample point to the next at the edge of the image. Under these constraints, the

following inequality must be satisfied:

$$\left| \pi a_1 T^2 \left(\frac{-N}{2} \right)^2 - \pi a_1 T^2 \left(\frac{-N}{2} + 1 \right)^2 \right| \leq \frac{\pi}{4} . \tag{2.2-16}$$

With N>>1 this reduces to

$$|a_1| \leq \frac{1}{4NT^2} . \tag{2.2-17}$$

Combining Eqs. (2.2-5) and (2.2-17) we find that the distance d_1 must satisfy the constraint:

$$\left| 1 - \frac{d_1}{F} \right| \leq \frac{\lambda F}{4NT^2} . \tag{2.2-18}$$

These constraints are based upon the assumption that the argument of the complex Gaussian should change by no more than π/4 from one sample point to the next. To compare this sampling criterion with the Nyquist sampling rate, consider the real part of the complex Gaussian given in Eq. (2.2-15):

$$\cos(\pi a_1 T^2 m^2), \tag{2.2-19}$$

where along the x-axis, n is equal to zero. This expression can be written as

$$\cos(2\pi [\frac{a_1}{2} T^2 m] m), \tag{2.2-20}$$

where the term in square brackets can be viewed as an instantaneous frequency, f_I.

At the edge of the image (i.e. n = ± N/2), the instantaneous frequency is at a maximum and is given by

$$f_I = \frac{a_1 T^2 N}{4} . \tag{2.2-21}$$

The Nyquist sampling interval of a sinusoid of this frequency is at least $1/(2f_I)$, but since the sampling interval is already given by $\Delta m = 1$, there will be a limit on the magnitude of f_I. The Nyquist limit on this instantaneous frequency is given by

$$f_I \leq \frac{1}{2} . \tag{2.2-22}$$

Combining Eqs. (2.2-21) and (2.2-22) gives an upper bound on a_1,

$$|a_1| \leq \frac{2}{NT^2} , \tag{2.2-23}$$

which is eight times the limit given by Eq. (2.2-17). This factor of eight is the result of using the change in the total argument of the complex Gaussian, and limiting this change to $\pi/4$ rather then π in the derivation of Eq. (2.2-17).

2.2.4 Definition of Z_F

In going from the center to the edge of the image, the argument of the complex Gaussian in Eq. (2.2-15) either increases or decreases quadratically, depending upon the sign of a_1. Each multiple of 2π that the argument goes through will be counted as one Fresnel zone. Along either the x or y axis the maximum value of this argument will be

$$\pi |a_1| T^2 \left(\frac{N}{2}\right)^2 . \tag{2.2-24}$$

Dividing this quantity by 2π gives the total number of Fresnel zones. For any given value of a_1, as defined in Eq. (2.2-5), the corresponding number of Fresnel zones, Z_F, is given by:

$$Z_F = \frac{\alpha_1}{2}\left(\frac{NT}{2}\right)^2 . \qquad (2.2\text{-}25)$$

The dimensionless parameter Z_F will be used throughout this dissertation to denote how far into the Fresnel zone the transform plane is located. It is important to remember that as the magnitude of Z_F increases, the transform plane is moving farther away from the Fourier transform plane, and further into the Fresnel zone region of the optical processor.

Using the maximum value for α_1 given in Eq. (2.2-17), the argument of the complex Gaussian changes from zero to $2\pi(N/32)$ in moving from the center to the edge of the image. The maximum number of Fresnel zones that can be sampled is thus defined as N/32. The constraint on d_1 given in Eq. (2.2-18) is equivalent to a constraint requiring that the number of Fresnel zones, Z_F, satisfy the equation:

$$|Z_F| \leq \frac{N}{32} . \qquad (2.2\text{-}20)$$

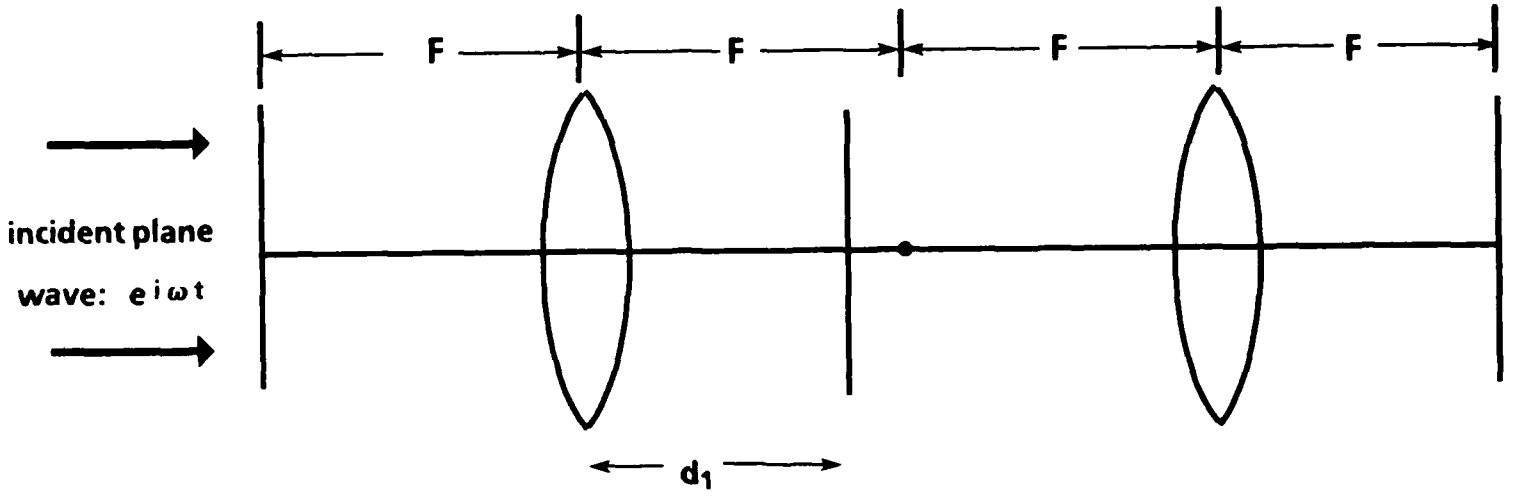

Fig. 2-1 Canonical optical processor. If the distance $d_1 = F$, the scalar component of the field in the transform plane corresponds to the Fourier transform of the scalar component of the field in the input plane. If $d_1 \neq F$, the scalar field in the transform plane corresponds to a Fresnel zone transform of the scalar field at the input plane.

2.3. Reconstruction from Fresnel Zone Phase Information

An iterative method of reconstructing an object from Fresnel zone transform phase information will be discussed in this section. In this reconstruction technique it is assumed that the phase of the Fresnel zone transform is known and that the original object is real and non-negative. It is also assumed that the phase information is free from noise and that the value of Z_F is known, i.e. the location in the Fresnel zone region at which the phase information was obtained is known. A block diagram illustrating this iterative algorithm is shown in Fig. 2-2.

The algorithm starts with an NxN object of random values, taken from a uniform distribution with a range of 0 to 255, as the initial guess for the object. The guess for the object is multiplied by the known complex Gaussian phase term and then padded with zeros to a size of 2Nx2N. An FFT is performed to calculate a guess for the Fresnel-zone transform. The modulus of this guess is multiplied by the known phase information and an IFFT is performed. Taking the modulus of the central NxN pixels yields the new guess for the object. The algorithm continues by transforming back and forth between the object domain and the Fresnel zone while applying the known information or constraints in each domain.

A direct measure of the error between the known phase information and the phase of the Fresnel zone transform of the current guess is given by the absolute phase error, $E_P^{(i)}$. The absolute phase error is defined by

$$E_P^{(i)} = \frac{1}{N^2} \sum_{m=0}^{N-1} \sum_{n=0}^{N-1} \left| \exp\{i\,\theta(m,n)\} - \exp\{i\,\theta_i(m,n)\} \right| , \qquad (2.3\text{-}1)$$

where $\exp\{i\theta(m,n)\}$ is the known phase information, and $\exp\{i\theta_i(m,n)\}$ is the phase of the Fresnel zone transform of the guess for the image after i iterations.

At each iteration an analytic measure of the relative squared error in the image plane, $E_I^{(i)}$, is given by

$$E_I^{(i)} = \frac{\sum_{m=0}^{N-1}\sum_{n=0}^{N-1} \left| g_i(m,n) - g_i'(m,n) \right|^2}{\sum_{m=0}^{N-1}\sum_{n=0}^{N-1} \left| g_i(m,n) \right|^2} \qquad (2.3\text{-}2)$$

where i is the iteration number, $g_i(m,n)$ is the calculated guess for the image after i iterations and before the image plane constraints have been imposed, and $g_i'(m,n)$ is the result of applying the image plane constraints on $g_i(m,n)$. Although this error is very difficult to relate to the known transform magnitude information, this error does give an indication as to how much the guess for the image must be modified at each iteration to fulfill the image plane constraints.

Figure 2-3 shows the original 256x256x8-bit digitized image used in the reconstruction experiments. The structure of the two railroad cars on the left-hand side of the picture provide a good reference for two different spatial frequencies, as does the low contrast fine detail at the back of the railroad car in the center of the picture. The uniform illumination of the sky and the hard edge of the coal pile against the background of the sky are also good reference structures.

A 256x256 complex Gaussian was calculated for several different Fresnel zone transforms. The known phase information that was used in

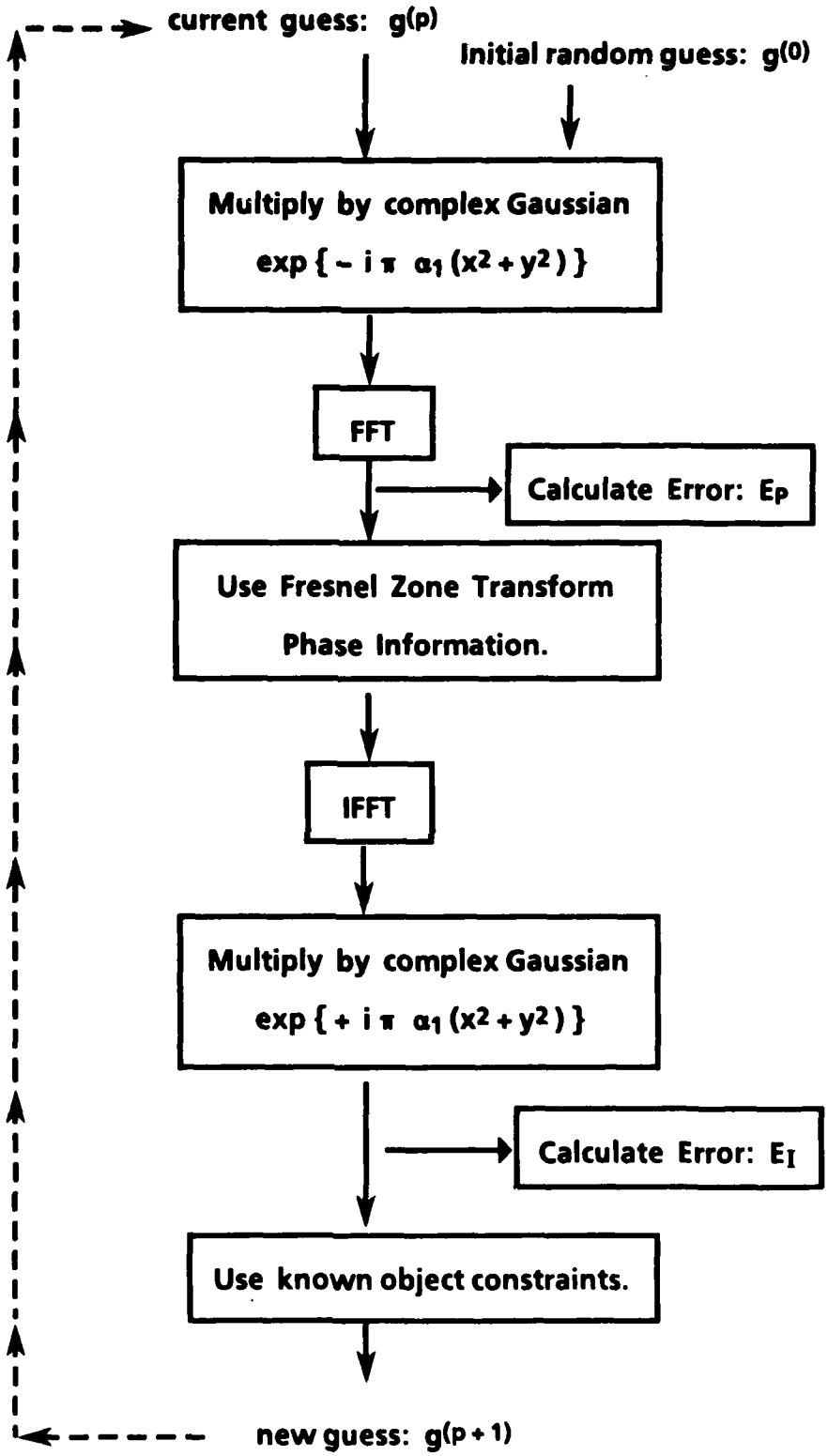

Fig. 2-2 Block Diagram showing the iterative technique of image reconstruction from Fresnel zone phase-only information

Fig. 2-3 Original digitized image used in the reconstruction experiments. The image has 256 X 256 pixels with 8 bits/pixel.

the iterative reconstruction was calculated by multiplying the known image by the corresponding complex Gaussian, padding this product with zeros to obtain a 512x512 image, performing an FFT with this data, and then setting the magnitude equal to unity at every pixel. This known Fresnel zone phase information from four different Fresnel zone transforms is shown in Fig. 2-4. This phase information was calculated for Z_F = 0.0, 0.5, 3.0, and 8.0 and is shown in Figs. 2-4(a), 2-4(b), 2-4(c), and 2-4(d) respectively. The phase is represented by 256 grey levels, with a phase which is just greater than $-\pi$ corresponding to black, and a phase which is equal to π being shown as white.

The reconstructions for the object after the fifth iteration using different values of d_1 are shown in Fig. 2-5. The reconstruction in Fig. 2-5(a) corresponds to $Z_F = 0.0$, which is the Fourier transform plane.

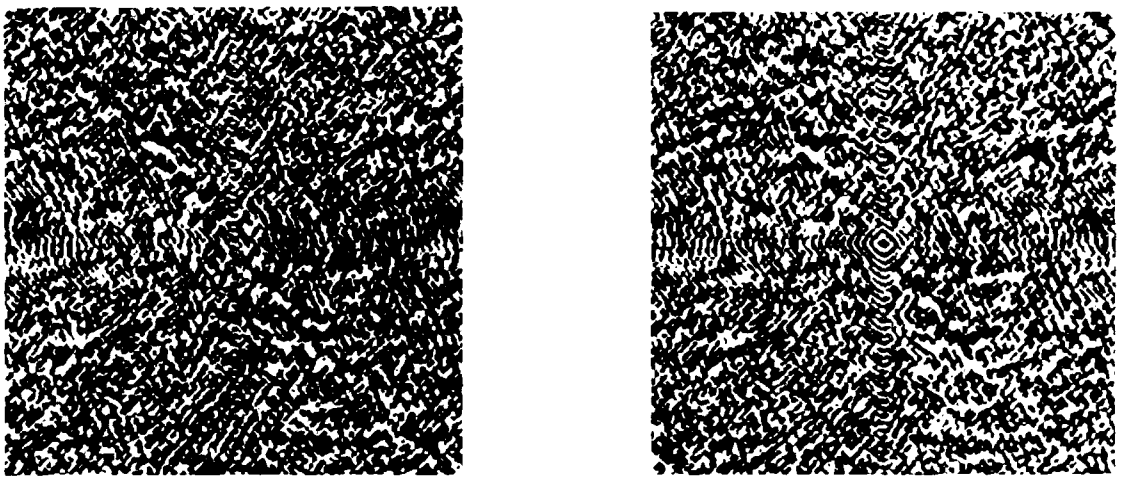

(a) $Z_F = 0.0$ (b) $Z_F = 0.5$

(c) $Z_F = 3.0$ (d) $Z_F = 8.0$

Fig. 2-4 Known phase information from four different Fresnel zone transforms. As defined in Eqs. (2.2-5) and (2.2-25), Z_F is the number of Fresnel zones, or a measure of the distance away from the Fourier plane. Phase values from $-\pi$ to $+\pi$ are mapped to a grey scale from black to white.

(a) $Z_F = 0.0$

(b) $Z_F = 0.5$

(c) $Z_F = 3.0$

(d) $Z_F = 8.0$

Fig. 2-5 Results of reconstructing an object from phase-only data at four different locations in the Fresnel zone region. The reconstructions are shown after five iterations. There are excellent reconstructions from this phase-only data at locations throughout the Fresnel zone region.

Reconstructions limited to the Fourier transform plane have been discussed in prior work by Hayes, Lim, and Oppenheim [1980, 1982] and Hayes [1982], where they demonstrated that a good reconstruction is obtained after only one iteration. It has been found that good reconstructions are obtained in only one iteration from phase-only Fresnel zone data as well. For the purpose of comparing phase-only reconstructions with magnitude-only reconstructions, the results of reconstructions after five iterations are shown.

Figures 2-5(b), 2-5(c), and 2-5(d) show the reconstructions in the Fresnel zone region. These reconstructions are shown with $Z_F = 0.5$, $Z_F = 3.0$, and $Z_F = 8.0$ respectively. Note that an increase in the number of Fresnel zones corresponds to an increase in the distance away from the Fourier transform plane. The high frequency detail and edges are very well preserved in all of these reconstructions. As the number of Fresnel zones increases, the uniformity of the sky is degraded, but overall there is still a very good reconstruction. From these results we see that this type of reconstruction is fairly insensitive to a shift out of the Fourier transform plane.

Figure 2-6 is a plot of the absolute phase error, $E_P(i)$, for iterations 2 through 20 at several different Fresnel zone locations. The error at the first iteration is approximately .5, and is omitted here to provide for a more detailed vertical scale. There is a slight increase in the absolute phase error as the number of Fresnel zones increases; this agrees with the slight degradation in the visual quality of the images shown in Fig. 2-5.

A plot of the relative squared error in the image plane at several different Fresnel zone locations is shown for iterations 2 through 20 in Fig. 2-7. The error after the first iteration is approximately .10 to .14 and is omitted in this plot to allow for greater resolution in the vertical scale. There is very little difference in the error as the transform plane moves away from the Fourier plane and further into the Fresnel zone region. The relative squared error in the image plane is independent of the number of Fresnel zones.

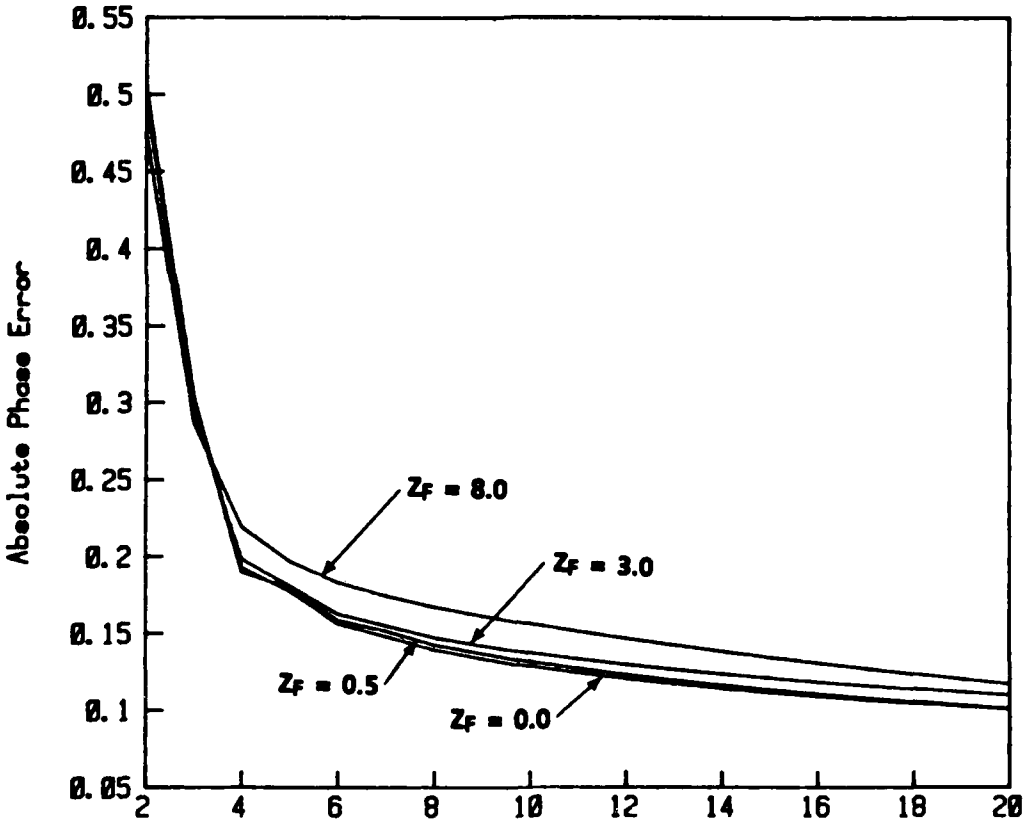

Fig. 2-6 Error in transform plane, $E_P^{(i)}$, vs. iteration number for phase-only reconstruction at Fresnel zones equal to 0.0, 0.5, 3.0, and 8.0.

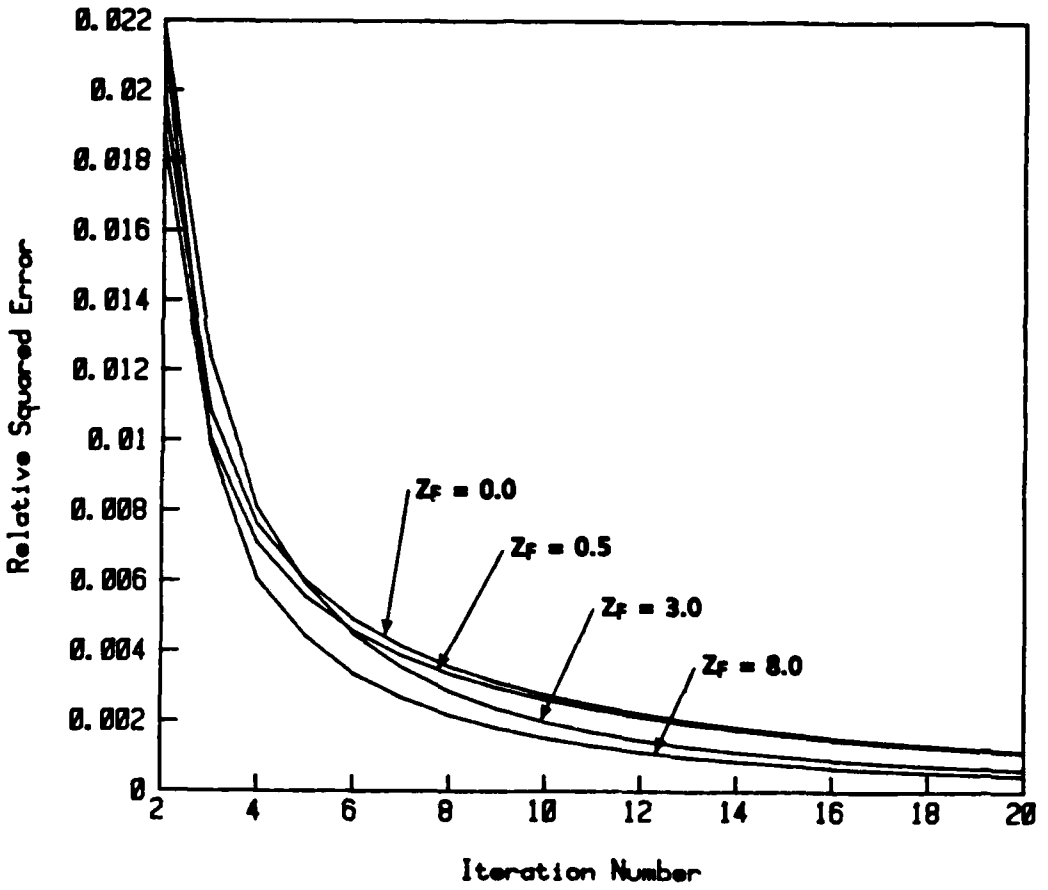

Fig. 2-7 Error in image plane, $E_I^{(i)}$, vs. iteration number for phase-only reconstructions at Fresnel zones equal to 0.0, 0.5, 3.0, and 8.0.

As the reconstruction algorithm progresses, there is a steady decrease in both the image plane error and the transform plane error. The reconstruction after the first iteration is an edge enhanced (almost to the point of being binary) outline of the unknown image. As the reconstruction progresses, the low frequency areas of the image are slowly filled in. In reconstructing an image from phase-only data, the quality of the reconstruction is essentially independent of the number of Fresnel zones. In locations throughout the Fresnel zone, the high contrast,

high frequency edges which dominate the first few iterative guesses are slowly worn down so that the low frequency, low contrast areas of the image may be recovered. The slight degradation in the quality of the reconstructed image as the number of Fresnel zones increases is reflected in a small increase in the value of the absolute phase error.

2.4 Reconstruction from Fresnel Zone Magnitude Information

The iterative method of reconstructing an object from Fresnel zone magnitude-only information is very similar to the algorithm discussed earlier for reconstructing an object from Fresnel zone phase-only information. The only difference is in the information that is known about the Fresnel zone transform. In this reconstruction it is assumed that the magnitude of the Fresnel zone transform is known, and that the original object is real and non-negative. It is also assumed that we know where in the Fresnel zone region the magnitude information was calculated. A block diagram showing this iterative algorithm is presented in Fig. 2-8.

This iteration also starts with an initial random guess for the object. The earlier algorithm is modified so that for this reconstruction, the known magnitude of the Fresnel zone transform is multiplied by the current calculated guess for the Fresnel zone transform phase. An IFFT is performed, and the modulus of the central NxN pixels yields a new guess for the object in the same manner as the previous algorithm.

At each iteration, an analytic measure of the relative squared error in the image plane (as defined by Eq. 2.3-2) is calculated. The absolute error in the transform plane, $E_M^{(i)}$, is given by

$$E_M^{(i)} = \frac{1}{N^2} \sum_{m=0}^{N-1} \sum_{n=0}^{N-1} \left| \, |G(m,n)| - |G_i(m,n)| \, \right| , \qquad (2.4\text{-}1)$$

where i is the iteration number, $|G(m,n)|$ is the measured magnitude data, and $|G_i(m,n)|$ is the magnitude data calculated from the Fresnel zone transform of the guess for the image after i iterations. This error is a direct

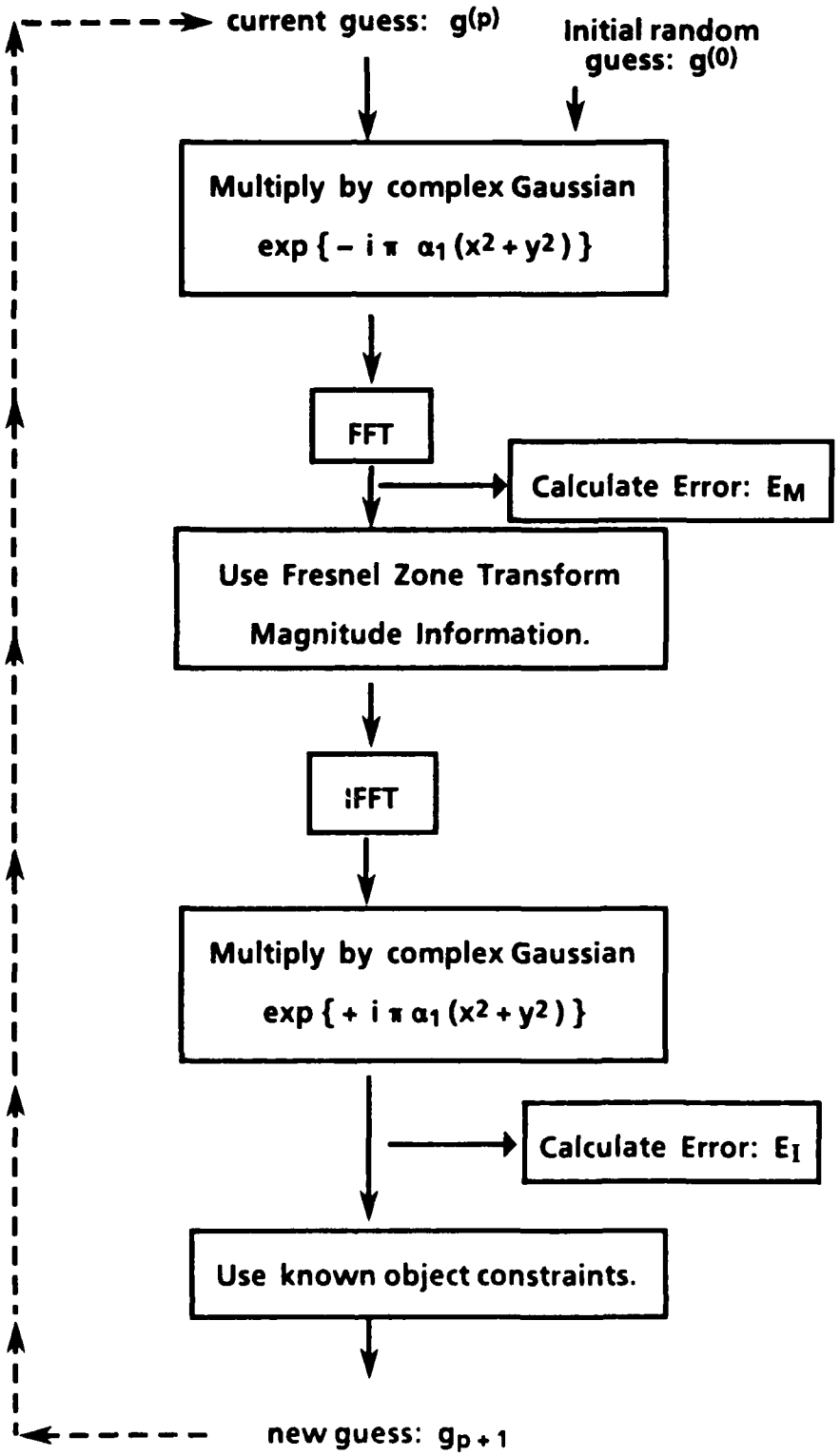

Fig. 2-8 Block Diagram showing the iterative technique of image reconstruction from Fresnel zone magnitude-only information.

measure of how well the iteration is progressing in terms of being consistent with the known magnitude information.

The original image shown in Fig. 2-3 was also used in this set of experiments. The known magnitude information was calculated by multiplying the image by the correct complex Gaussian, padding the data with zeros, calculating the FFT, and then setting the phase equal to zero at each pixel. The known Fresnel zone magnitude information from four different Fresnel zone transforms is shown in Fig. 2-9. This magnitude information was calculated for $Z_F = 0.0$, 0.5, 3.0, and 8.0 and is shown in Figs. 2-9(a), 2-9(b), 2-9(c), and 2-9(d) respectively. The magnitude is displayed with 256 grey levels such that the maximum value of $\log_e(1. + |G|)$ is shown as white and $|G| = 0$ is shown as black. The dynamic range of the computer is much larger than zero to 255, so this logarithmic scaling gives a much better representation of the data than a direct linear scaling of the magnitude. From this figure we can see that there is a spreading of the transform pattern as we move further into the Fresnel region.

The reconstructions for the object after the fifth iteration using different values of d_1 are shown in Fig. 2-10. The reconstruction in Fig. 2-10(a) corresponds to $Z_F = 0.0$, which is the Fourier transform plane. More sophisticated methods can be used to reduce the number of iterations required for a given quality of reconstruction, but will not be investigated here. In the results discussed here, we are concerned principally with the effect of moving into the Fresnel region, and not with the use of different iterative algorithms.

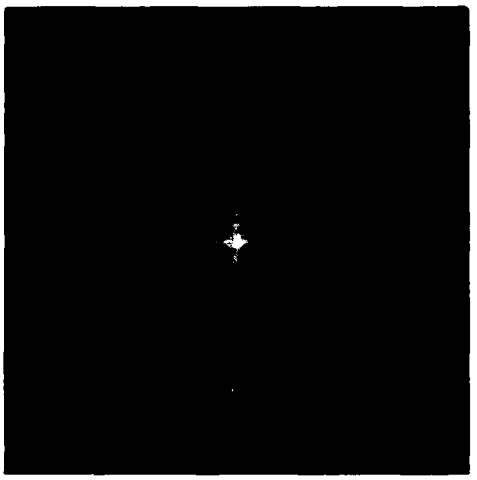

(a) $Z_F = 0.0$

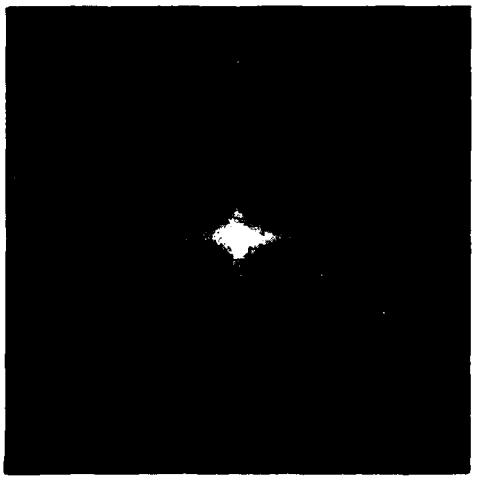

(b) $Z_F = 0.5$

(c) $Z_F = 3.0$

(d) $Z_F = 8.0$

Fig. 2-9. Known magnitude information from four different Fresnel zone transforms. Data is displayed such that the maximum value of $\log_e(1. + |G|)$ is shown as white, and $|G| = 0.$ is shown as black.

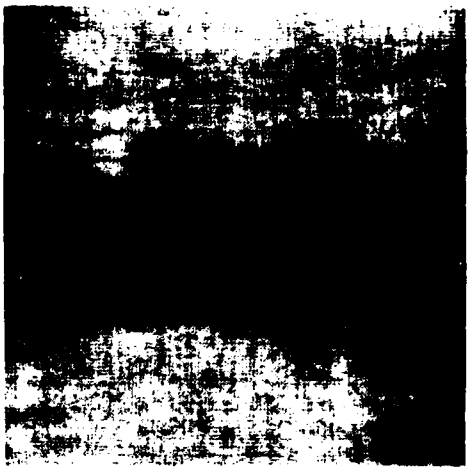

(a) $Z_F = 0.0$

(b) $Z_F = 0.5$

(c) $Z_F = 3.0$

(d) $Z_F = 8.0$

Fig. 2-10. Results of reconstructing an object from magnitude-only data at four different locations in the Fresnel zone region. The reconstructions are shown after five iterations. As we move further away from the Fourier transform plane the reconstructions improve.

Figures 2-10(b), 2-10(c), and 2-10(d) show the reconstructions as we move further away from the Fourier plane. These reconstructions from the Fresnel zone region are shown for $Z_F = 0.5$, $Z_F = 3.0$, and $Z_F = 8.0$ respectively. Recall that an increase in the number of Fresnel zones corresponds to an increase in the quantity $|1-d_1/F|$. The reconstruction at 0.5 Fresnel zones shows the location of the high contrast edges as well as the uniform illumination of the sky. At 3.0 Fresnel zones, some of the high frequency detail is starting to appear and the high contrast edges are well defined. There is a very good reconstruction at $Z_F = 8.0$. In this reconstruction much of the high frequency detail, as well as the low contrast fine detail at the back of the railroad car in the center of the picture, have been resolved . From these results we see that this type of algorithm gives a better reconstruction as the transform plane moves further away from the Fourier transform plane, and further into the Fresnel zone region of the optical processor.

Figure 2-11 is a plot of the absolute error in the transform plane at several different Fresnel zone locations for iterations 2 through 75. The error changes the most in the first several iterations; from this point on the rate of change in the error is directly proportional to the number of Fresnel zones. After 75 iterations, the error at 8.0 Fresnel zones has decreased rapidly to near zero value, at 3.0 Fresnel zones the error is still decreasing steadily, and at 0.5 Fresnel zones the error is decreasing very slowly. The error at 0.0 Fresnel zones (the Fourier transform plane) has stagnated after approximately 50 iterations.

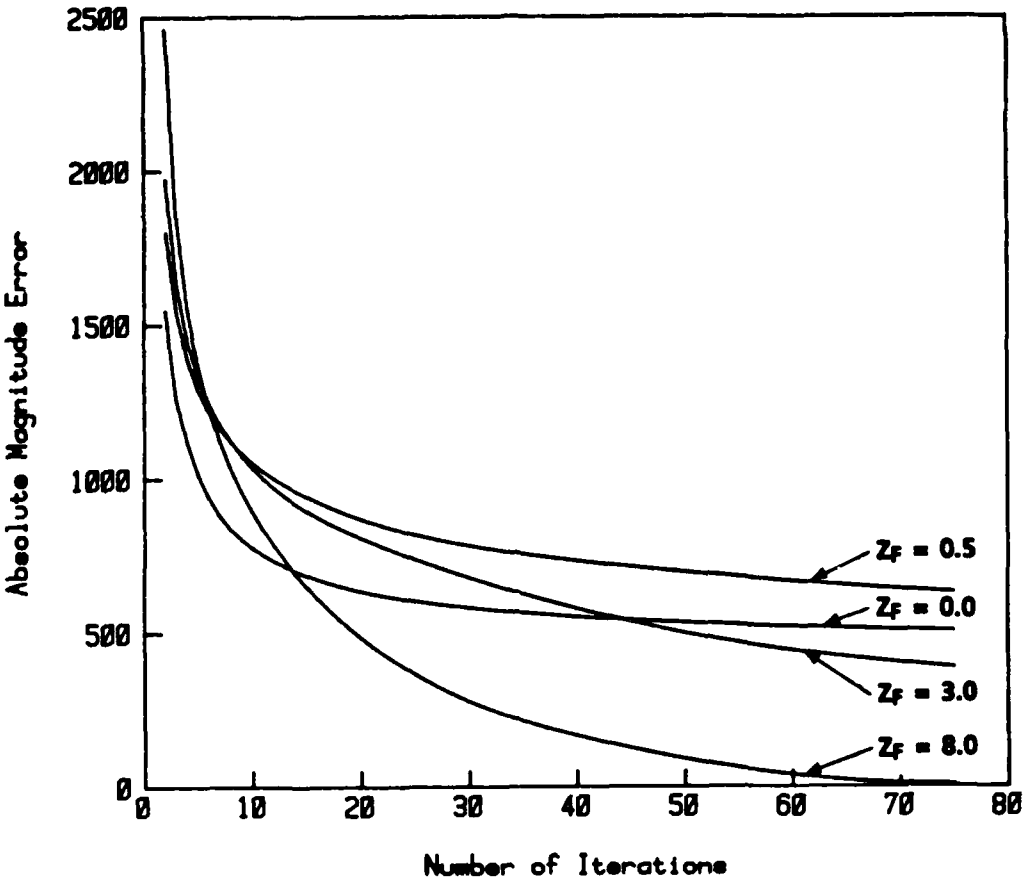

Fig. 2-11 Error in transform plane, $E_P^{(i)}$, vs. iteration number for Fresnel zones equal to 0.0, 0.5, 3.0, and 8.0.

A plot of the relative squared error for iterations 2 through 75 at several different Fresnel zones is shown in Fig. 2-12. The error decreases the most during the first several iterations at all Fresnel zone locations. The value of the error after the first iteration is inversely proportional to the number of Fresnel zones. For a given number of iterations, the error is lower for a larger number of Fresnel zones. This agrees well with the reconstructions shown in Fig. 2-10.

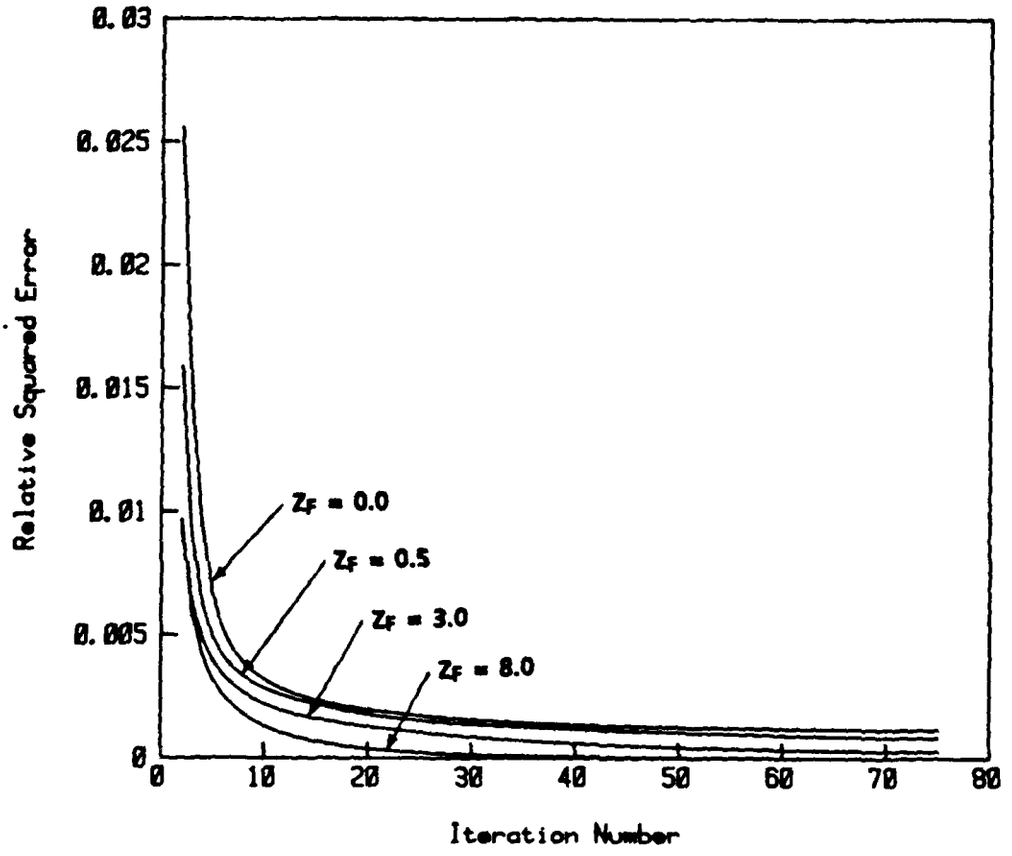

Fig. 2-12 Error in image plane, $E_I^{(i)}$, vs. iteration number for Fresnel zones equal to 0.0, 0.5, 3.0, and 8.0.

The quality of the image in Fresnel zone magnitude-only reconstructions is not only a function of the error in the image and transform domains, but also depends on the rate of change in the absolute error in the transform domain.

Chapter Three

Stationary Phase Approximations in Fresnel Zone Magnitude-only Reconstructions

3.1 Introduction

It was shown in Chapt. 2 that there is a very noticeable improvement in the quality of the magnitude-only reconstructions as the number of Fresnel zones increases. Moving a small distance into the Fresnel region aids in the reconstruction process in that the number of iterations needed to produce a good image is fewer than in the case of reconstructing an image from Fourier transform magnitude-only data. Data from deep in the Fresnel zone region leads to good reconstructions in just a few iterations.

An analytic explanation of why data obtained with a large number of Fresnel zones yields a good reconstruction in just a few iterations is the subject of this chapter. The analytic techniques used in the approximations discussed below are part of the general area of asymptotic expansions. A good general discussion of asymptotic expansions is given by Erdelyi [1956] and by Copson [1965], while a more applicable discussion concerning the case of two-dimensional integrals is given by Born and Wolf [1980]. The case of two-dimensional diffraction integrals has also been discussed by VanKampen [1949, 1950] and Seligson [1981].

In Sect. 3.2 the definition of the Fresnel zone transform is formulated so that the integral can be approximated by the method of stationary phase. This method of approximating the Fresnel zone transform is then used to form an estimate of the first guess for the Fresnel zone transform. The first iterative guess for the unknown image is shown to be approximately equal to the unknown image.

The discussion in Sect. 3.2 uses the one-dimensional Fresnel zone transform. A summary for the case of two-dimensional images is given in Sect. 3.3. While the analytic expressions given in Sects. 3.2 and 3.3 lead to a better understanding of the process of reconstructing an image from Fresnel zone magnitude-only data, Sect. 3.4 presents a geometrical derivation of the stationary phase point, and discusses the existence of a stationary phase point.

Critical points of the second kind are calculated in Sect. 3.5, and the associated term in the asymptotic expansion of the Fresnel zone transform integral is derived. The first term in the asymptotic expansion, due to the critical points of the first kind discussed in Sects. 3.2 and 3.3, are of the order $(Z_F)^{-1}$, while the term in the asymptotic expansion due to critical points of the second kind goes as $(Z_F)^{-3/2}$.

An illustrative example of the Fresnel zone transform for a large number of Fresnel zones, and the magnitude-only reconstruction after one iteration is given in Sect. 3.6. The structure of the Fresnel zone transform is shown to be dominated by the effects of critical points of the first kind.

3.2. Critical Points of the First Kind

In this section only the one-dimensional case of the Fresnel zone transform will be considered. The results and derivations presented in the following discussion are easily extended to two dimensions, and a summary of the results for the two-dimensional case are given in Sect. 3.3.

Consider a general function, g(x), and its associated Fresnel zone transform $G(f_x)$. The Fresnel zone transform of g(x) is given by

$$G(f_x) = \int_{-\infty}^{+\infty} g(x) K(x; f_x)\, dx \,. \tag{3.2-1}$$

By direct calculation, one can readily verify the following inversion relationship:

$$g(x) = \int_{-\infty}^{+\infty} G(f_x) K^*(x; f_x)\, df_x \,. \tag{3.2-2}$$

Where * denotes a complex conjugate, and the Fresnel-zone transform kernel $K(x; f_x)$ is given as

$$K(x; f_x) = e^{-i\pi\alpha x^2} e^{-i2\pi f_x x} \,. \tag{3.2-3}$$

The constant α is related to the distance away from the Fourier plane. The generalized frequency, f_x, will be equal to the Fourier spatial frequency only when $\alpha = 0$.

Consider a function g(x) that is non-zero only over a finite region, say

$$g(x) = 0 \quad for \quad |x| > b \;; \tag{3.2-4}$$

then the complex Gaussian term in the transform kernel will oscillate a finite number of times as we move from x = 0 to x = b. The argument of the complex Gaussian must be continuously increasing or decreasing, depending upon the sign of α. The number of multiples of 2π that this argument goes through is the number of Fresnel zones, Z_F, associated with a particular Fresnel zone transform. An increase in the magnitude of Z_F corresponds to a location in the Fresnel zone region which is farther away from the Fourier plane. The number of Fresnel zones is given by:

$$Z_F = \frac{\alpha b^2}{2}, \tag{3.2-5}$$

or

$$\alpha = \frac{2 Z_F}{b^2}. \tag{3.2-6}$$

Combining Eqs. (3.2-1), (3.2-3), and (3.2-6), the expression for a Fresnel zone transform with Z_F Fresnel zones can be expressed in terms of the number of Fresnel zones as:

$$G(f_x) = \int_{-b}^{+b} g(x)\, e^{-i\pi x^2 2Z_F/b^2}\, e^{-i2\pi f_x x}\, dx. \tag{3.2-7}$$

The bounds of integration reflect the non-zero region of g(x) defined by Eq. (3.2-4).

To formulate the expression for evaluation by the stationary phase approximation, rewrite Eq. (3.2-7) as

$$G(f_x) = e^{i\pi f_x^2 b^2/(2Z_F)} \int_{-b}^{+b} g(x)\, e^{-iZ_F(2\pi/b^2)\left(x + \frac{b^2 f_x}{2Z_F}\right)^2} dx \,. \qquad (3.2\text{-}8)$$

3.2.2. Stationary Phase Approximation

In this application, the principle of stationary phase makes use of the fact that if Z_F is large enough, and g(x) is slowly varying compared with the complex exponential, then the value of the integral in Eq. (3.2-8) is determined primarily by the behavior of the integrand at certain critical points. Critical points of the first kind, which will be considered in this section, are very similar for both one- and two-dimensional integrals. An analysis of critical points of the second kind will be discussed in Sect. 3-3.2.

Let the argument of the complex exponential be written as

$$i|Z_F|\Phi(x) \quad , \qquad (3.2\text{-}9)$$

where

$$\Phi(x) = -sgn[Z_F]\,(2\pi/b^2)\left(x + \frac{b^2 f_x}{2Z_F}\right)^2 \quad , \qquad (3.2\text{-}10)$$

and sgn[Z_F] is equal to the sign of Z_F. Critical points of the first kind are located in regions where

$$|x| < b \,, \qquad (3.2\text{-}11a)$$

and

$$\frac{\partial \Phi(x)}{\partial x} = 0. \qquad (3.2\text{-}11b)$$

Evaluating these conditions using the phase given in Eq. (3.2-10), one critical point, x_1, is found to be located at

$$x = x_1 = -\frac{b^2 f_x}{2 Z_F} . \tag{3.2-12}$$

Using a critical point of the first kind, the integral in Eq. (3.2-8) can be approximated by

$$G_s(f_x) = e^{i\pi f_x^2 b^2/(2Z_F)} \left(\frac{2\pi}{|Z_F|}\right)^{\frac{1}{2}} \left(\frac{i}{\phi''(x_1)}\right)^{\frac{1}{2}} g(x_1)\, e^{i|Z_F|\,\phi(x_1)} , \tag{3.2-13}$$

where the subscript (s) is used to denote the stationary phase approximation to $G(f_x)$. By direct calculation, the stationary phase approximation to the Fresnel zone transform is given by

$$G_s(f_x) = e^{i\pi f_x^2 b^2/(2Z_F)} \left(\frac{-i\,b^2}{2Z_F}\right)^{\frac{1}{2}} g\left(-\frac{b^2 f_x}{2Z_F}\right) \tag{3.2-14}$$

for large values of $|Z_F|$.

In the image reconstruction experiments discussed in Chapt. 2 it was shown that after only a few iterations, the magnitude-only reconstructions improve further away from the Fourier transform plane. From Eq. (3.2-14) we see that for large values of $|Z_F|$, or equivalently an increase in the distance away from the Fourier plane, the magnitude of the Fresnel zone transform is approximated by a scaled version of the unknown image. As the offset from the Fourier plane increases, the given Fresnel zone transform magnitude data more closely resemble the unknown image data.

3.2.3 Analytic Image Reconstruction

The iterative method of image reconstruction from magnitude-only data starts with an initial random guess, $g^{(0)}(x)$, for the object which fulfills any known object constraints. This random guess is denoted by $r(x)$, the Fresnel zone transform is denoted by $R(f_x)$, and can be written in polar form as $|R(f_x)|\exp\{i\theta(f_x)\}$. The algorithm continues by combining the known transform magnitude information, $|G(f_x)|$, with a guess for the phase of the Fresnel zone transform. The starting guess, $G^{(0)}(f_x)$, for the Fresnel zone transform is given by

$$G^{(0)}(f_x) = |G(f_x)| e^{i\theta^{(0)}(f_x)} , \qquad (3.2\text{-}15)$$

where $\exp\{i\theta^{(0)}(f_x)\}$ is the initial guess for the phase, which is set equal to the phase of $|R(f_x)|\exp\{i\theta(f_x)\}$.

The first iterative guess for the image, $g^{(1)}(x)$, is now obtained by first calculating the inverse Fresnel zone transform of $G^{(0)}(f_x)$,

$$g^{(1)}(x) = e^{i\pi x^2 2 Z_F / b^2} \int_{-\infty}^{+\infty} |G(f_x)| e^{i\theta^{(0)}(f_x)} e^{i2\pi f_x x} df_x , \qquad (3.2\text{-}16)$$

and then imposing any known image constraints. An illustrative example showing the result of this first iteration is discussed in Sect. 3.6.

The iteration continues by using $g^{(1)}(x)$ as the new guess for the image and calculating the Fresnel zone transform of this new guess. The phase from this Fresnel zone transform, $\exp\{i\theta^{(1)}(f_x)\}$, is then combined with the known magnitude, $|G(f_x)|$, to form a new guess, $G^{(1)}(f_x)$, for the Fresnel zone transform. Imposing any image constraints on the inverse Fresnel

zone transform of $G^{(1)}(f_x)$ yields a new guess for the image, $g^{(2)}(x)$. The algorithm continues to transform back and forth while applying any known image constraints and/or any known transform information.

3.2.4 Approximation of Reconstructed Image

Using the approximation to the Fresnel zone transform developed in Sect. 3.2.2 it is possible to estimate the quantities needed for the first iterative guess defined by Eq. (3.2-16). By using these estimates, an analytic approximation to the first iterative guess for the unknown image will be obtained. Let $g_s^{(1)}(x)$ denote an estimate of the first iterative guess for the image, $g^{(1)}(x)$. This estimate is then given by

$$g_s^{(1)}(x) = e^{i\pi x^2 2Z_F/b^2} \int_{-\infty}^{+\infty} |G_s(f_x)| e^{i\theta_s^{(0)}(f_x)} e^{i2\pi f_x x} df_x , \qquad (3.2\text{-}17)$$

in which the stationary phase approximation to the known magnitude information and the initial guess for the unknown phase are denoted by $|G_s(f_x)|$ and $\exp(i\theta_s^{(0)}(f_x))$ respectively. Using Eq. (3.2-14) as an estimate for the known magnitude information, $|G(f_x)|$ is given by

$$|G_s(f_x)| = \left(\frac{b^2}{2Z_F}\right)^{\frac{1}{2}} g\left(-\frac{b^2 f_x}{2Z_F}\right) . \qquad (3.2\text{-}18)$$

An estimate for the initial guess for the phase of the Fresnel zone transform, $\exp\{i\theta^{(0)}(f_x)\}$, is given by

$$e^{i\theta_s^{(0)}(f_x)} = e^{-i\pi/4} e^{i\pi f_x^2 b^2/(2Z_F)} \qquad (3.2\text{-}19)$$

Using the estimates given in Eqs. (3.2-18) and (3.2-19), Eq. (3.2-17) can be written as

$$g_s^{(1)}(x) = e^{i\pi x^2 2Z_F/b^2} \left(\frac{-ib^2}{2Z_F}\right)^{\frac{1}{2}} \times$$

$$\int_{-\infty}^{+\infty} e^{i\pi f_x^2 b^2/(2Z_F)} \; g\left(-\frac{b^2 f_x}{2Z_F}\right) \; e^{i2\pi f_x x} \; df_x \,. \qquad (3.2\text{-}20)$$

If this inverse Fresnel zone transform is viewed as the inverse Fourier transform of a product, which is equal to the convolution of the inverse Fourier transforms, Eq. (3.2-20) can be expressed as

$$g_s^{(1)}(x) = \left(\frac{-ib^2}{2Z_F}\right)^{\frac{1}{2}} e^{i\pi x^2 2Z_F/b^2} \times$$

$$\left\{e^{i\pi/4} \left|\frac{2Z_F}{b^2}\right|^{\frac{1}{2}} e^{-i\pi x^2 2Z_F/b^2}\right\} \otimes \left\{\left|\frac{2Z_F}{b^2}\right| G_F\left(\frac{2Z_F x}{b^2}\right)\right\}, \qquad (3.2\text{-}21)$$

where $G_F(f)$ is the Fourier transform of g(x) and $\otimes$ denotes a convolution. This convolution can be written out explicitly as

$$g_s^{(1)}(x) = \left(\frac{-ib^2}{2Z_F}\right)^{\frac{1}{2}} e^{i\pi/4} \left|\frac{2Z_F}{b^2}\right|^{3/2} e^{i\pi x^2 2Z_F/b^2} \times$$

$$\int_{-\infty}^{+\infty} G_F\left(\frac{2Z_F x'}{b^2}\right) \; e^{-i\pi(x-x')^2 2Z_F/b^2} \; dx', \qquad (3.2\text{-}22)$$

which when expressed in the form of an inverse Fourier transform becomes

$$g_s^{(1)}(x) = \left(\frac{-ib^2}{2Z_F}\right)^{\frac{1}{2}} e^{i\pi/4} \left|\frac{2Z_F}{b^2}\right|^{3/2} \times$$

$$\int_{-\infty}^{+\infty} G_F\left(\frac{2Z_F x'}{b^2}\right) e^{-i\pi x'^2 2Z_F/b^2} e^{i2\pi(x 2Z_F/b^2)x'} dx' . \qquad (3.2\text{-}23)$$

Again this inverse Fourier transform of a product can be written as the convolution of the inverse Fourier transforms, or

$$g_s^{(1)}(x) = \left(\frac{-ib^2}{2Z_F}\right)^{\frac{1}{2}} g(x) \otimes e^{i\pi x^2 2Z_F/b^2} . \qquad (3.2\text{-}24)$$

Writing this convolution out explicitly as

$$g_s^{(1)}(x) = \left(\frac{-ib^2}{2Z_F}\right)^{\frac{1}{2}} \int_{-\infty}^{+\infty} g(x') e^{iZ_F 2\pi(x-x')^2/b^2} dx' \qquad (3.2\text{-}25)$$

presents the integral in a form which can be approximated by the method of stationary phase. In this case the argument of the complex exponential is given by $i|Z_F|\Phi(x')$, where

$$\Phi(x') = sgn[Z_F](2\pi/b^2)\left(x - x'\right)^2 . \qquad (3.2\text{-}26)$$

The stationary phase point is found by evaluating the expression

$$\frac{\partial\Phi(x')}{\partial x'} = 0. \qquad (3.2\text{-}27)$$

The stationary phase point is located at

$$x' = x. \tag{3.2-28}$$

Using the stationary phase approximation for the integral in Eq. (3.2-25) leads to the approximation for the first iterative guess for the image:

$$g_s^{(1)}(x) \sim \frac{b^2}{2 Z_F} g(x) \quad . \tag{3.2-29}$$

Recall that $g_s^{(1)}(x)$ is an analytic estimate for the first iterative guess, $g^{(1)}(x)$. By the approximation given in Eq. (3.2-29), it has been shown that for large values of $|Z_F|$, the reconstruction after the first iteration is approximately equal to the unknown image.

3.3 Summary of Results for Two Dimensions

The results of the approximations if using a two-dimensional image are directly analogous to the one-dimensional case discussed above.

Consider a general function, g(x,y), and its associated Fresnel-zone transform $G(f_x, f_y)$. The Fresnel-zone transform of g(x,y) is given by

$$G(f_x, f_y) = \int_{-\infty}^{+\infty} \int_{-\infty}^{+\infty} g(x,y) K(x, y; f_x, f_y)\, dx dy \,. \tag{3.3-1}$$

By direct calculation, one can readily verify the following inversion relationship

$$g(x,y) = \int_{-\infty}^{+\infty} \int_{-\infty}^{+\infty} G(f_x, f_y) K^*(x,y; f_x, f_y)\, df_x df_y \,. \tag{3.3-2}$$

The Fresnel-zone transform kernel $K(x,y; f_x, f_y)$ is given as

$$K(x, y; f_x, f_y) = e^{-i\pi\alpha(x^2+y^2)}\, e^{-i2\pi(f_x x + f_y y)}, \tag{3.3-3}$$

The conjugate complex is denoted by *, and α is a constant which is a measure of the distance away from the Fourier plane and is defined in Eq. (2.2-5).

Consider a function g(x, y) which is non-zero only over a finite region, say

$$g(x,y) = 0 \quad for \quad |x| > b \quad or \quad |y| > b \,. \tag{3.3-4}$$

The number of Fresnel zones, Z_F, is defined as the number of multiples of 2π that the argument of the complex Gaussian goes through while moving along either the x or y axis from x = y = 0 to either x = b or y = b.

The two-dimensional Fresnel zone transform given in Eqs. (3.3-1) and (3.3-3) can be rewritten as

$$G(f_x,f_y) = e^{i\pi(f_x^2+f_y^2)b^2/(2Z_F)} \quad \times$$

$$\int_{-b}^{+b}\int_{-b}^{+b} g(x,y)\, e^{-iZ_F 2\pi/b^2\left\{\left(x+\frac{b^2 f_x}{2Z_F}\right)^2+\left(y+\frac{b^2 f_y}{2Z_F}\right)^2\right\}} dxdy \qquad (3.3\text{-}5)$$

where the non-zero region of g(x, y) is reflected in the bounds of integration.

The argument of the complex Gaussian in this two dimensional integral is equal to $i|Z_F|\Phi(x, y)$, where $\Phi(x, y)$ is given by

$$\Phi(x,y) = -sgn[Z_F](2\pi/b^2)\left\{\left(x+\frac{b^2 f_x}{2Z_F}\right)^2+\left(y+\frac{b^2 f_y}{2Z_F}\right)^2\right\} . \qquad (3.3\text{-}6)$$

The stationary phase points are found at locations where

$$|x| < b\,,\ |y| < b\,, \qquad (3.3\text{-}7a)$$

and

$$\frac{\partial\Phi(x)}{\partial x} = \frac{\partial\Phi(y)}{\partial y} = 0. \qquad (3.3\text{-}7b)$$

One stationary phase point is found to be located at

$$x = x_1 = -\frac{b^2 f_x}{2Z_F}\,,\ y = y_1 = -\frac{b^2 f_y}{2Z_F}\,. \qquad (3.3\text{-}8)$$

Using the method of stationary phase to evaluate the double integral in Eq. (3.3-5) leads to the approximation

$$G_s(f_x, f_y) = e^{i\pi (f_x^2 + f_y^2) b^2/(2Z_F)} \left(\frac{-i\, b^2}{2 Z_F} \right) g \left(\frac{-b^2 f_x}{2 Z_F} , \frac{-b^2 f_y}{2 Z_F} \right) \qquad (3.3\text{-}9)$$

for large values of $|Z_F|$. This expression is the two dimensional form of Eq. (3.2-14).

If $|G_S(f_x, f_y)|$ is used for an estimate of $|G(f_x, f_y)|$, and $\exp\{i\theta_s^{(1)}(f_x, f_y)\}$ for an estimate of $\exp\{i\theta^{(1)}(f_x, f_y)\}$ in a single iteration of the reconstruction algorithm, the same derivation that was discussed in Sect. 3.2.4 leads to the relation

$$g_s^{(1)}(x, y) \sim \left(\frac{b^2}{2 Z_F} \right)^2 g(x, y) \ . \qquad (3.3\text{-}10)$$

This expression is directly analogous to Eq. (3.2-29) in Sect. 3.2.4. For large values of $|Z_F|$, the first iteration of the reconstruction algorithm produces an image which is a close estimate to the unknown image.

3.4 Geometrical Interpretation of Stationary Phase

It is possible to derive the location of the stationary phase point given in Eq. (3.2-12) using an argument based upon the principles of geometrical optics. The expression for the number of Fresnel zones, Z_F, can be written

$$Z_F = \frac{b^2}{2} \frac{(1 - d_1/F)}{F} \frac{1}{\lambda} . \tag{3.4-1}$$

In the geometrical optics limit, i.e. as the wavelength λ goes to zero, the number of Fresnel zones goes to infinity (assuming $d_1 \neq F$). So the requirement for the stationary phase approximation, that the number of Fresnel zones be very large, is equivalent to having the wavelength go to zero.

The method for performing an optical Fresnel zone transform is shown in Fig. 3-1 with a geometrical ray originating at a point x_o and propagating parallel to the optical axis. After being refracted by the lens of focal length F, this ray intersects the u,v-plane (i.e. the Fresnel zone transform plane) at a height u_o. By similar triangles, the relationship

$$\frac{x_o}{F} = \frac{u_o}{F - d_1} \tag{3.4-2}$$

is obtained. This relationship can be solved for x_o, to give

$$x_o = \frac{u_o}{1 - d_1/F} . \tag{3.4-3}$$

Using the definition for the number of Fresnel zones given by Eq. (3.4-1) and the generalized frequency variable,

$$f_x = - \frac{u_o}{\lambda F} , \tag{3.4-4}$$

an expression for the stationary phase point, x_o, is given by

$$x_o = -\frac{f_x \lambda F}{2 Z_F \lambda F / b^2} , \tag{3.4-5}$$

or

$$x_o = -\frac{f_x b^2}{2 Z_F} . \tag{3.4-6}$$

This is equivalent to the stationary phase point given by Eq. (3.2-12).

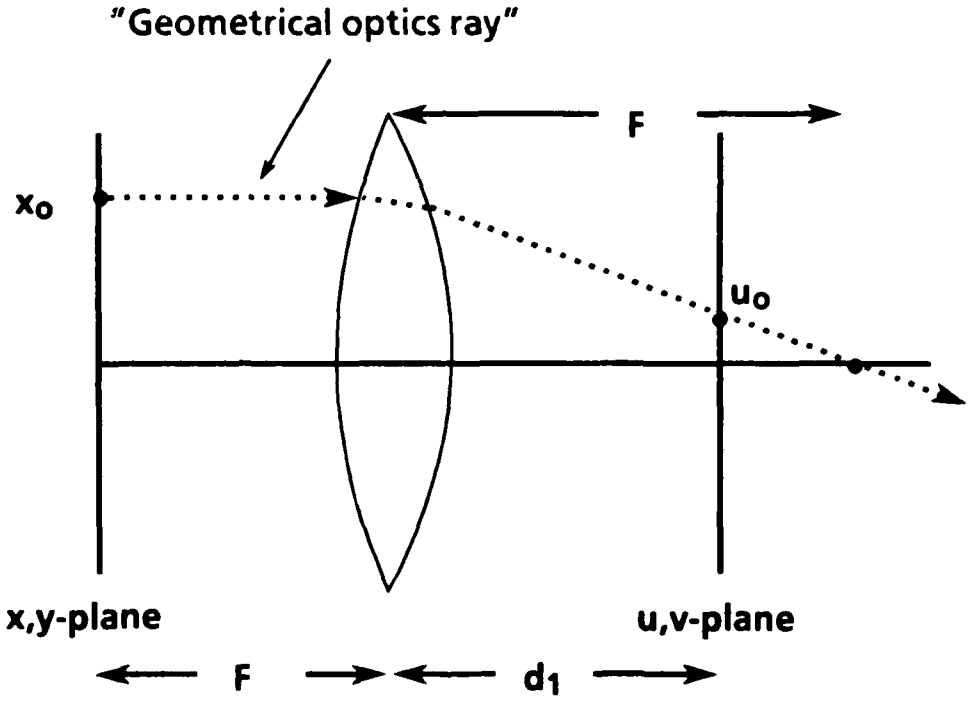

Fig. 3-1 Optical Fresnel zone transform system showing geometrical optics ray.

In the asymptotic expansion of the Fresnel zone transform, the leading term is attributed to stationary phase points. The location of these stationary phase points are the same as the points obtained by tracing an undiffracted geometrical optics ray through the imaging system. The existence of a stationary phase point is easily verified by tracing a

geometrical optics ray through the system, rays which are not obstructed give rise to stationary phase points.

3.5 Critical Points of the Second Kind

Section 3.3 discussed critical points of the first kind, or stationary phase points. The stationary phase approximation given in Eq. (3.3-9) is only the first term in an asymptotic expansion of the Fresnel zone transform integral. This section will discuss critical points of the second kind, which constitute a higher order term in the asymptotic expansion. Although there is a close similarity between one- and two-dimensional integrals for critical points of the first kind, there is not such an easy transition for critical points of the second kind. For this reason only the case of a two-dimensional image will be discussed here.

Consider once again the function given in Eq. (3.3-6):

$$\Phi(x,y) = -sgn[Z_F]\,\frac{2\pi}{b^2}\left\{\left(x+\frac{b^2 f_x}{2Z_F}\right)^2+\left(y+\frac{b^2 f_y}{2Z_F}\right)^2\right\}\ , \qquad (3.5\text{-}1)$$

Critical points of the second kind are located along the boundary curve of the region of integration. If a displacement along the boundary curve is denoted by ∂l, a critical point of the second kind is located where the function $\Phi(x,y)$, is stationary along the boundary curve, or

$$\frac{\partial \Phi(x,y)}{\partial l} = 0\ . \qquad (3.5\text{-}2)$$

A rectangular region with $|x| \leqq b$ and $|y| \leqq b$ is shown in Fig. 3-2. The calculation of the critical points is now done by finding points along the rectangular boundary where

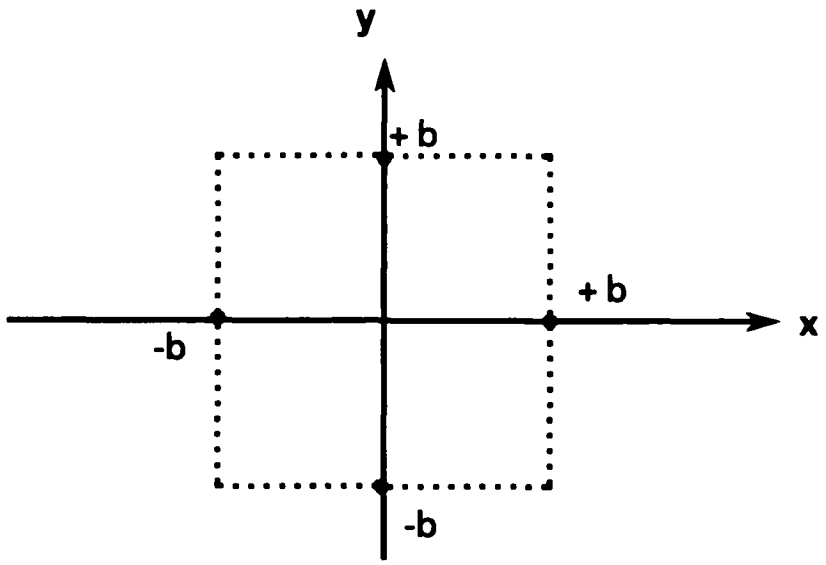

Fig. 3-2 Rectangular region of integration in the x,y plane.

$$\frac{\partial \phi(x,y)}{\partial l} = \frac{\partial \phi(x,y)}{\partial x}\,\frac{\partial x}{\partial l} + \frac{\partial \phi(x,y)}{\partial y}\,\frac{\partial y}{\partial l} = 0\,. \tag{3.5-3}$$

Considering the direction of travel to be counterclockwise along the boundary of integration, the partial derivatives are calculated

up the right hand side: $\frac{\partial x}{\partial l} = 0\,, \quad \frac{\partial y}{\partial l} = +1,$ (3.5-4a)

across the top: $\frac{\partial x}{\partial l} = -1\,, \quad \frac{\partial y}{\partial l} = 0,$ (3.5-4b)

down the left hand side: $\frac{\partial x}{\partial l} = 0\,, \quad \frac{\partial y}{\partial l} = -1,$ (3.5-4c)

and across the bottom: $\frac{\partial x}{\partial l} = +1 , \quad \frac{\partial y}{\partial l} = 0 .$ (3.5-4d)

The remaining partial derivatives are given by

$$\frac{\partial \phi(x,y)}{\partial x} = -2sgn[Z_F] \frac{2\pi}{b^2} (x + \frac{b^2 f_x}{2 Z_F}) , \quad (3.5\text{-}5a)$$

and

$$\frac{\partial \phi(x,y)}{\partial y} = -2sgn[Z_F] \frac{2\pi}{b^2} (y + \frac{b^2 f_y}{2 Z_F}) . \quad (3.5\text{-}5b)$$

Each side is found to contain one critical point of the second kind. These four points are located at:

$$x_a = +b , \; y_a = -\frac{b^2 f_y}{2 Z_F} , \quad (3.5\text{-}6a)$$

$$x_b = -\frac{b^2 f_x}{2 Z_F} , \; y_b = +b , \quad (3.5\text{-}6b)$$

$$x_c = -b , \; y_c = -\frac{b^2 f_y}{2 Z_F} , \quad (3.5\text{-}6c)$$

$$x_d = -\frac{b^2 f_x}{2 Z_F} , \; y_d = -b . \quad (3.5\text{-}6d)$$

The Fresnel zone transform given in Eq. (3.3-5) is now approximated by the first two terms in an asymptotic series as

$$G(f_x, f_y) \sim G_s (f_x, f_y) + G_2 (f_x, f_y) , \quad (3.5\text{-}7)$$

where $G_s(f_x, f_y)$ is due to critical points of the first kind and is given in Eq. (3.3-9). $G_2(f_x, f_y)$ is equal to the sum of the contributions from each of the four critical points of the second kind. The contribution from each of these critical points, (x_i, y_i), is given by:

$$\frac{(2\pi)^{1/2} i \varepsilon \eta}{|Z_F|^{3/2} \Omega^{1/2}} g(x,y) \exp\{i |Z_F| \Phi(x,y)\} \Big|_{(x_i, y_i)}, \tag{3.5-8}$$

where

$$\Omega = \frac{\partial^2 \Phi}{\partial x^2} \left(\frac{\partial \Phi}{\partial y}\right)^2 - 2 \frac{\partial^2 \Phi}{\partial x \partial y} \frac{\partial \Phi}{\partial x} \frac{\partial \Phi}{\partial y} + \frac{\partial^2 \Phi}{\partial y^2} \left(\frac{\partial \Phi}{\partial x}\right)^2,$$

$$+ \frac{\eta}{R} \left[\left(\frac{\partial \Phi}{\partial x}\right)^2 + \left(\frac{\partial \Phi}{\partial y}\right)^2 \right]^{3/2}, \tag{3.5-9}$$

$$\varepsilon = \begin{cases} \exp\{+i\pi/4\} & \Omega > 0 \\ \exp\{-i\pi/4\} & \Omega < 0 \end{cases}, \tag{3.5-10}$$

$$\eta = \begin{cases} +1 \text{ if } \dfrac{\partial x}{\partial l} \dfrac{\partial \Phi}{\partial y} > 0 \\ -1 \text{ if } \dfrac{\partial x}{\partial l} \dfrac{\partial \Phi}{\partial y} < 0 \end{cases} \text{ and } \frac{\partial x}{\partial l} \frac{\partial \Phi}{\partial y} \neq 0 \\ \begin{cases} +1 \text{ if } \dfrac{\partial y}{\partial l} \dfrac{\partial \Phi}{\partial x} < 0 \\ -1 \text{ if } \dfrac{\partial y}{\partial l} \dfrac{\partial \Phi}{\partial x} > 0 \end{cases} \text{ and } \frac{\partial x}{\partial l} \frac{\partial \Phi}{\partial y} = 0 \end{cases}, \tag{3.5-11}$$

and R is the radius of curvature (which is infinite for this rectangular region of integration).

Evaluating Eq. 3.5-8 at each critical point and summing, gives

$$\sum_{\text{over ponts } (x_i, y_i)} = Q \frac{g(b, -\frac{b^2 f_y}{2 Z_F})}{b + \frac{b^2 f_x}{2 Z_F}} exp\left\{ -i Z_F \frac{2\pi}{b^2} \left(b + \frac{b^2 f_x}{2 Z_F} \right)^2 \right\}$$

$$+ Q \frac{g(-\frac{b^2 f_x}{2 Z_F}, b)}{b + \frac{b^2 f_y}{2 Z_F}} exp\left\{ -i Z_F \frac{2\pi}{b^2} \left(b + \frac{b^2 f_y}{2 Z_F} \right)^2 \right\}$$

$$- Q \frac{g(-b, -\frac{b^2 f_y}{2 Z_F})}{-b + \frac{b^2 f_x}{2 Z_F}} exp\left\{ -i Z_F \frac{2\pi}{b^2} \left(-b + \frac{b^2 f_x}{2 Z_F} \right)^2 \right\}$$

$$- Q \frac{g(-\frac{b^2 f_x}{2 Z_F}, -b)}{-b + \frac{b^2 f_y}{2 Z_F}} exp\left\{ -i Z_F \frac{2\pi}{b^2} \left(-b + \frac{b^2 f_y}{2 Z_F} \right)^2 \right\}, \qquad (3.5\text{-}12)$$

where

$$Q = \frac{(2\pi)^{1/2} i}{|Z_F|^{3/2} (2K)^{3/2}} sgn[Z_F] \; exp\{ +i \pi/4 \} . \qquad (3.5\text{-}13)$$

Note that these terms, which are due to the contributions of the critical points of the second kind, are of the order $(Z_F)^{-3/2}$. The term due to critical points of the first kind goes as $(Z_F)^{-1}$. For a very large number of Fresnel

zones, the Fresnel zone transform is dominated by the term $G_s(f_x, f_y)$, which is due to critical points of the first kind.

In Eq. 3.3-9 it is very easy to see the behavior of the magnitude and phase of the Fresnel zone transform due to the critical points of the first kind. It is not so easy to understand the structure of the Fresnel zone transform due to critical points of the second kind. One feature that can be seen readily is the impact of the rectangular shape of the image on the transform. By looking along the f_x axis, i.e. by letting $f_y = 0$, the contributions from the points (x_a, y_a) and (x_c, y_c) depend only on the image points at $x = \pm b$ and $y = 0$, the contributions due to the critical points (x_b, y_b) and (x_d, y_d), are proportional to the magnitude of the image along the edges $y = +b$ and $y = -b$. Thus, critical points of the second kind, which lie at the edge of the image, yield contributions to the Fresnel zone transform which contain information about the edges of the image.

3.6 Illustrative Example

As described in Sect. 2.2, the numerical computation of a Fresnel zone transform is done using a fast Fourier transform (FFT) routine. The object to be transformed is multiplied by the complex Gaussian corresponding to a particular Fresnel zone; the FFT of this product is equal to the Fresnel zone transform. Although the stationary phase approximation discussed above improves as the parameter $|Z_F|$ increases, the sampling requirements of the numerical calculation of the Fourier transform place an upper limit on the practical size of $|Z_F|$. A discussion of sampling considerations is given in detail in Sect. 2.2.3.

Figure 3-3 shows the original digitized image of a sailboat that was used in this example of magnitude-only image reconstruction. In this experiment the 256×256 image is padded with zeros to give a 512×512 image. For display purposes, Fig. 3-3 shows only the central 256×256 pixels.

The phase and magnitude of a Fresnel zone transform of the image shown in Fig. 3-3 are shown in Figs. 3-4(a) and (b) respectively. Figures 3-4(a) and (b) are each displayed with 512×512 pixels. This Fresnel zone transform was calculated for 16 Fresnel zones. Note that both the phase and magnitude have structures which are similar to that predicted by Eq. (3.3-9). The phase of the Fresnel zone transform shown in Fig. 3-4(a) is dominated by the ring-like structure associated with a complex Gaussian. The magnitude of the Fresnel zone transform shown in Fig. 3-4(b) has a rough outline of the sails from the sailboat, and the light sky and dark sea are transposed. This general structure of the magnitude of the Fresnel zone transform was previously predicted and can be verified by simply

Fig. 3-3. Original digitized image used in the reconstruction experiments.

rotating Fig. 3-4(b) by 180°; i.e., as shown, the sailboat is upside down and reduced in size.

In the iterative method of reconstruction, the given magnitude information shown in Fig 3-4(b) is multiplied by the phase from the Fresnel zone transform of a random guess for the unknown image. An inverse Fresnel zone transform then gives the first iterative guess that is shown in Fig. 3-5(a). For display purposes, only the central 256×256 pixels, out of a field of 512×512 pixels, are shown. In this first iterative reconstruction the sailboat is easily recognized, and even the small details of the lighthouse can be discerned. This example is a demonstration of the fact that the reconstruction after the first iteration is a very good approximation to the original image, as was predicted by the relationship given in Eq. (3.3-10). For comparison with the reconstructions discussed in Chapt. 2, the iterative reconstruction after five iterations is shown in Fig. 3-5(b).

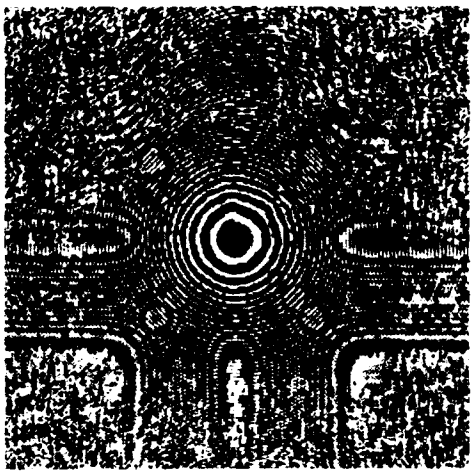

(a) Phase

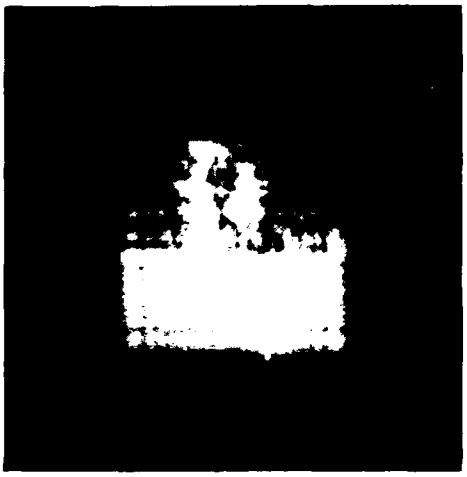

(b) Magnitude

Fig. 3-4. (a)Fresnel zone transform phase, at 16 Fresnel zones, of the image shown in Fig. 3-3. The phases from $-\pi$ to $+\pi$ are shown as grey levels from black to white. (b)Fresnel zone transform magnitude, at 16 Fresnel zones, of the image shown in Fig. 3-3. The magnitude is shown on a linear scale such that $|G(f_x, f_y)| = 0$ is black and the maximum value of $|G(f_x, f_y)|$ is white.

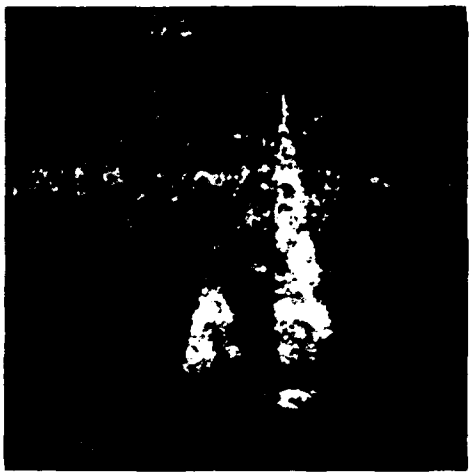

(a) First Iteration

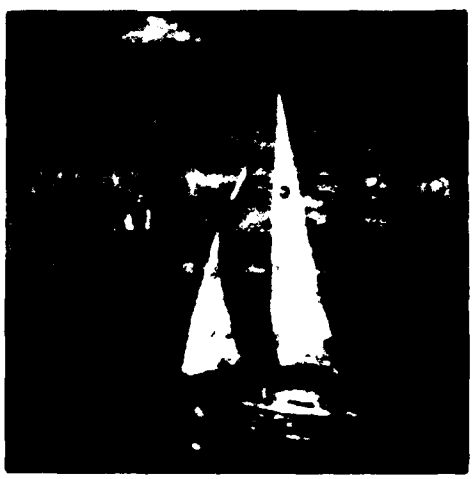

(b) Fifth Iteration

Fig. 3-5. Modulus of the (a)first and (b)fifth iterative guesses for the magintude-only reconstruction.

Chapter Four

The Importance of Edges in Phase-only Reconstructions

4.1 Introduction

The importance of the phase information in image formation and signal processing has been discussed in the literature [see for example, O'Neil and Walther, 1963; Huang *et al*, 1975; Oppenheim *et al*, 1979; Oppenheim and Lim, 1981] The Kinoform, a device which operates only on the phase of an incident wave, has been developed [Lesem *et al*, 1969]. Kermisch [1970] has given a quantitative analysis of image reconstruction from phase-only data for the case of a diffusely reflecting, coherently illuminated surface. For the case of Fourier transform data compression, Pearlman and Gray [1978] have shown that the real and imaginary parts of the data should be encoded with equal precision, but that in polar form the phase angle is more important than the magnitude. Using only the phase information in correlation filters has also been investigated [Horner and Gianino, 1984; Gianino and Horner, 1984]

A simple reconstruction experiment can be used to illustrate the importance of the phase information in the Fourier transform. Figure 4-1(a) is the original 256 X 256 X 8-bit image denoted by g(x, y). The Fourier transform of this image is denoted by $G(f_x, f_y)$, and is a complex quantity with both a magnitude and phase. This complex quantity can be represented in polar form as

$$G(f_x, f_y) = |G(f_x, f_y)| \exp\{i\theta(f_x, f_y)\}, \qquad (4.1\text{-}1)$$

where $|G(f_x, f_y)|$ is the magnitude of the transform, and $\exp\{i\theta(f_x, f_y)\}$ is the exponential phase of the transform.

The resulting image of a phase-only inverse transform is shown in Fig. 4-2(b). This image is obtained by taking the inverse Fourier transform of the quantity $\exp\{i\theta(f_x, f_y)\}$. The magnitude information has been discarded by setting the magnitude equal to unity in the transform plane. The fact that the edges are the significant features which are retained in this experiment is easily seen. This type of experiment was first reported by Oppenheim, Lim, Kopec, and Pohlig [1979].

One idea which would explain this phenomenon is based upon the technique of edge enhancement through high-pass filtering. For a wide class of interesting images, the magnitude of the Fourier transform generally behaves as 1/r for $r \neq 0$, where $r^2 = f_x^2 + f_y^2$ [Scott, 1963; Kinzly *et al*, 1968]. Dividing both sides of Eq. (4.1-1) by $|G(f_x, f_y)|$ gives

$$\frac{G(f_x, f_y)}{|G(f_x, f_y)|} = \exp\{i\theta(f_x, f_y)\}. \qquad (4.1\text{-}2)$$

Filtering the Fourier transform by $|G(f_x, f_y)|^{-1}$ amplifies the high frequencies and attenuates the low frequencies. In the image domain this has the effect of enhancing the edges.

While setting the magnitude equal to unity leads to a very edge enhanced image, it is also interesting to combine the phase from one image with the magnitude of a second image. In this case, the resulting image contains many of the features of the image from which the phase was taken [Oppenheim and Lim, 1981]. The features which are preserved are again the high-contrast edges of the image.

(a) Original Image

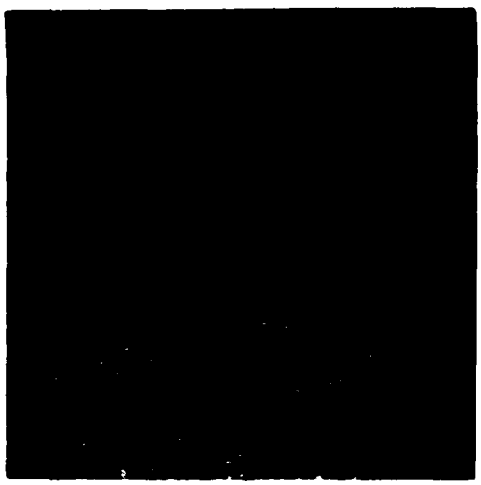

(b) Phase-only Inverse Transform

Fig. 4-1 (a) Original digitized image used in this reconstruction demonstration.
(b) Magnitude of the phase-only reconstruction obtained by setting the Fourier transform magnitude equal to unity and calculating an inverse Fourier transform.

Section 4.2 contains a discussion of two examples of phase-only reconstructions which can be done analytically. These examples demonstrate the preservation of the edges in the Fourier transform phase information.

Reconstructions from Fresnel zone transform phase information have been shown in Sect. 2.3. There is a slight degradation in the quality of these reconstructions as the number of Fresnel zones is increased. Section 4.3 will present two analytic reconstructions from Fresnel zone transform phase-only data. The approximations used in these examples will assume that the number of Fresnel zones is small. For a small number of Fresnel zones, the phase information in the Fresnel zone transform preserves information about the edges in the image.

4.2 Analytic Fourier Transform Phase-only Reconstructions

The rectangle function, shown in Fig. 4-2, is a simple, non-negative

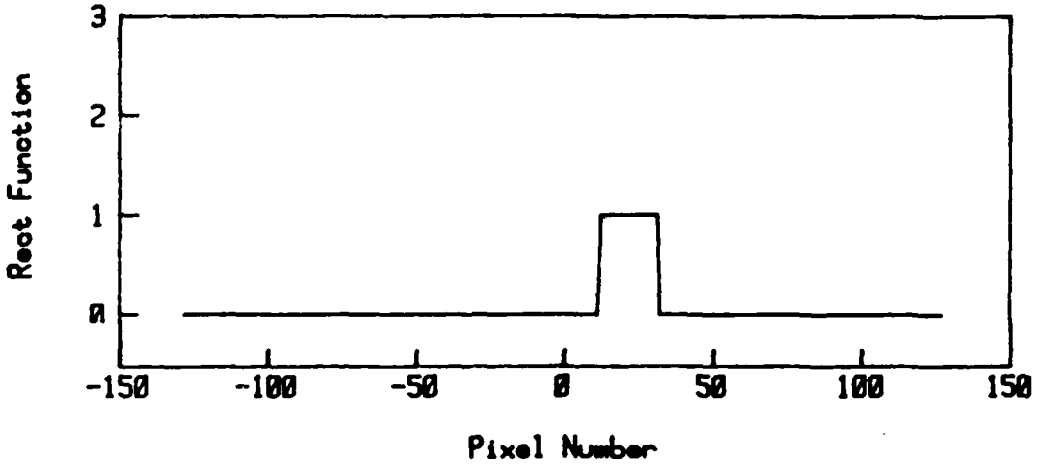

Fig. 4-2 Rectangle function denoted by rect[(x-x_0)/b].

function of finite extent which has sharp edges. This function is denoted by:

$$g(x) = rect\left(\frac{x-x_0}{b}\right). \tag{4.2-1}$$

The Fourier transform of g(x), G(f), is given by

$$G(f) = exp\{-i2\pi f x_0\}\, b\, \frac{sin(\pi b f)}{\pi b f}. \tag{4.2-2}$$

This can be written as a magnitude,

$$|G(f)| = \frac{1}{\pi}\, \frac{|sin(\pi b f)|}{|f|}, \tag{4.2-3}$$

and a phase

$$exp\{i\theta(f)\} = exp\{-i2\pi f x_0\}\, sgn(f) \left\{-1 + 2rect(bf) \otimes \frac{b}{2} comb\left(\frac{f-\frac{1}{2b}}{2/b}\right)\right\}, \tag{4.2-4}$$

where $\otimes$ denotes a convolution. This way of expressing the phase

function will prove useful in the computation of the phase-only reconstruction.

An expression for the phase-only reconstruction is found by taking the inverse Fourier transform of Eq. 4-6, and is given by

$$\frac{1}{in(x-x_0)} - \frac{1}{inx} \otimes \left\{ sinc\left(\frac{x-x_0}{b}\right) \frac{2}{b} comb\left(\frac{x-x_0}{b/2}\right) exp\{-i\pi(x-x_0)/b\} \right\}. \qquad (4.2\text{-}5)$$

The magnitude of this expression is shown in Fig 4-3. Note that the

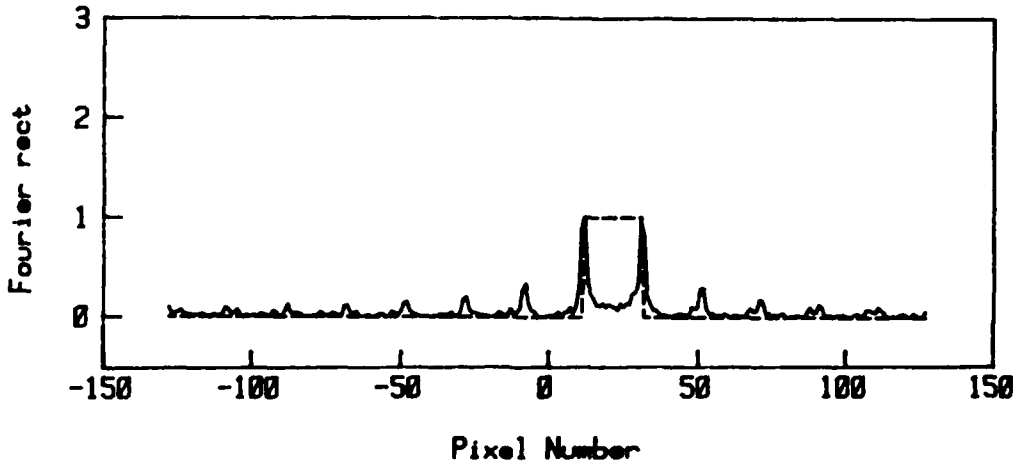

Fig. 4-3 Magnitude of the Fourier transform phase-only reconstruction (solid line) and the original rectangle function (dashed line).

structure is dominated by the presence of large spikes at $x = x_0 \pm b/2$, the location of the edges in the original rectangle function. There is no spike at the center of the sinc{(x-x0)/b} envelope, and the higher order spikes are attenuated by this envelope function.

As a second example which shows the importance of edges in the phase data, consider the hat function shown in Fig 4-4. This function is generated by adding two rectangle functions together, as

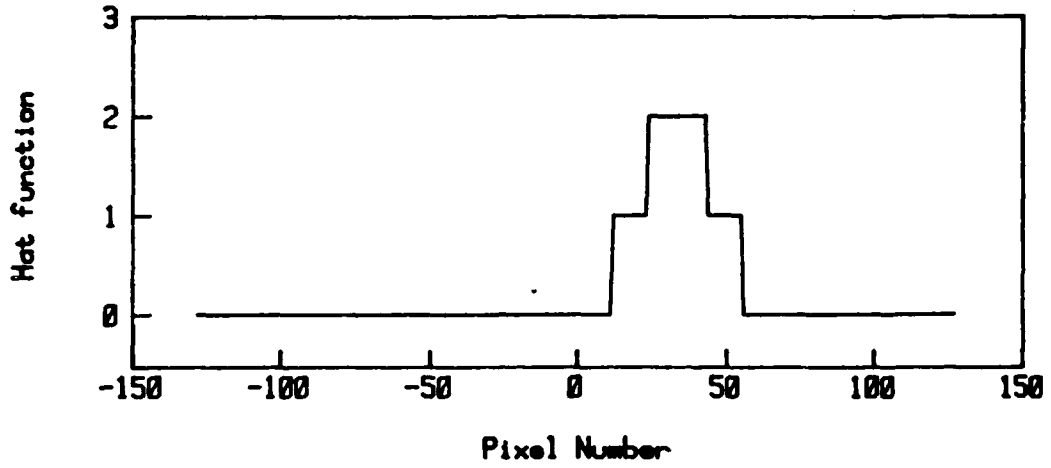

Fig. 4-4 Sum of rectangle functions, producing the hat function.

$$g(x) = rect\left(\frac{x-x_1}{b}\right) + rect\left(\frac{x-x_2}{b}\right) . \tag{4.2-6}$$

The Fourier transform of Eq. (4.2-6) can be written as a magnitude

$$|G(f)| = \frac{2}{\pi}\ \frac{|sin(\pi b f)|}{|f|}\ \left|\ cos\left\{2\pi f \frac{(x_2 - x_1)}{2}\right\}\right| , \tag{4.2-7}$$

and a phase

$$exp\{i\theta(f)\} = exp\left\{-i2\pi f\frac{(x_1 + x_2)}{2}\right\}\ sgn(f)\left\{-1 + 2rect(bf) \otimes \frac{b}{2} comb\left(\frac{f - \frac{1}{2b}}{2/b}\right)\right\}\ \times$$

$$\left\{-1 + 2rect\left(2\frac{(x_2 - x_1)}{2} f\right) \otimes \frac{(x_2 - x_1)}{2} comb\left(\frac{x_2 - x_1}{2} f\right)\right\} . \tag{4.2-8}$$

The inverse Fourier transform of Eq. (4.2-8) is given by:

$$\delta\left(x - \frac{x_1 + x_2}{2}\right) \otimes \frac{-1}{i\pi x} \otimes \left\{-\delta(x) + sinc\left(\frac{x}{b}\right)\ \frac{2}{b} comb\left(\frac{2x}{b}\right) exp\{i\pi x/b\}\right\}$$

$$\otimes \left\{-\delta(x) + sinc\left(\frac{x}{x_2 - x_1}\right)\ \frac{2}{(x_1 - x_2)}\ comb\left(\frac{2x}{x_2 - x_1}\right)\right\} , \tag{4.2-9}$$

and the magnitude is shown in Fig. 4-5. Notice that once again, the

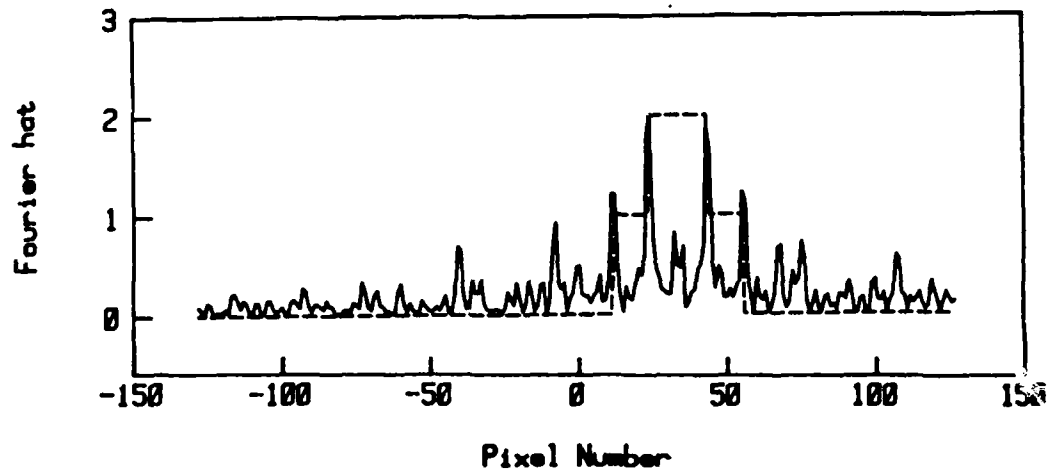

Fig. 4-5 Magnitude of the Fourier transform phase-only reconstruction (solid line) and the original hat function (dashed line).

general structure of the phase-only reconstruction is dominated by the appearance of large spikes at the same locations of the edges of the original function.

Both of these one-dimensional examples have shown how the information about the edges in an object is preserved in the phase of the Fourier transform. In performing a phase-only reconstruction, the edge itself is not reconstructed, but rather a strong discontinuity arises at the location of the edge.

4.3 Analytic Fresnel-zone Transform Phase-only Reconstructions

Now consider the case of the rectangle function shown in Fig. 4-2 under the process of a Fresnel-zone transform phase-only reconstruction. The Fresnel-zone transform of Eq. 4-3 is written as

$$G(f) = \int_{-\infty}^{+\infty} rect\left(\frac{x-x_0}{b}\right) exp(-i\pi a x^2)\ \ exp(-i2\pi fx)\,dx\ . \tag{4.3-1}$$

Using the convolution property of Fourier transforms, this integral can be treated as the Fourier transform of a product. The result is a convolution of Fourier transforms given by,

$$G(f) = \left\{exp\{-i2\pi fx_0\}\, b\, sinc(bf)\right\} \otimes \ \frac{1}{(ia)^{\frac{1}{2}}}\ exp(i\pi f^2/a)\ , \tag{4.3-2}$$

which when written in integral form becomes

$$G(f) = \frac{exp(-i\pi a x_0^2)}{\pi(ia)^{\frac{1}{2}}}\ exp\{-i2\pi fx_0\}\int_{-\infty}^{+\infty}\frac{sin(\pi b f')}{f'}\ exp\{i\frac{\pi}{a}[f'-(ax_0+f)]^2\}df'\ . \tag{4.3-3}$$

A useful approximation to this integral is possible with the assumption that a is small, i.e. the Fresnel zone is located close to the Fourier transform plane. It is then possible to use a stationary phase approximation (see also Sect. 3.2) to evaluate the integral in Eq. (4.3-3). The stationary phase approximation leads to an approximate expression for the Fresnel-zone transform of rect{(x-x_0)/b) :

$$G(f) \sim exp(-i\pi a x_0^2)\ exp\{-i2\pi fx_0\} b\frac{sin[\pi b(ax_0+f)]}{\pi b(ax_0+f)}\ . \tag{4.3-4}$$

Which can be separated into a magnitude;

$$|G(f)| \sim \frac{1}{\pi}\ \frac{|\ sin[\pi b(ax_0+f)]\ |}{|\ ax_0+f\ |}\ , \tag{4.3-5}$$

and a phase;

$$exp\{i\theta(f)\} \sim exp(-i\pi a x_0^2)\, exp\{-i2\pi f x_0\}\, sgn[ax_0+f] \;\times$$

$$\left\{-1 + 2rect(fb) \otimes \frac{b}{2}\, comb\left(\frac{f + ax_0 - \frac{1}{2b}}{2/b}\right)\right\} . \qquad (4.3\text{-}6)$$

Setting the magnitude equal to unity and taking the inverse Fresnel-zone transform of the phase leads to the expression for the phase-only reconstruction:

$$\frac{exp\{-i2\pi a x_0(x-x_0)\}}{i\pi(x-x_0)} - \frac{exp\{-i2\pi a x_0 x\}}{i\pi x} \otimes$$

$$\left\{ sinc\left(\frac{x-x_0}{b}\right) \frac{2}{b}\, comb\left(\frac{x-x_0}{b/2}\right) exp\{-i2\pi(x-x_0)(\frac{1}{2b} - ax_0\}\right\} , \qquad (4.3\text{-}7)$$

The magnitude of this complex-valued expression is shown in Fig. 4-6. The

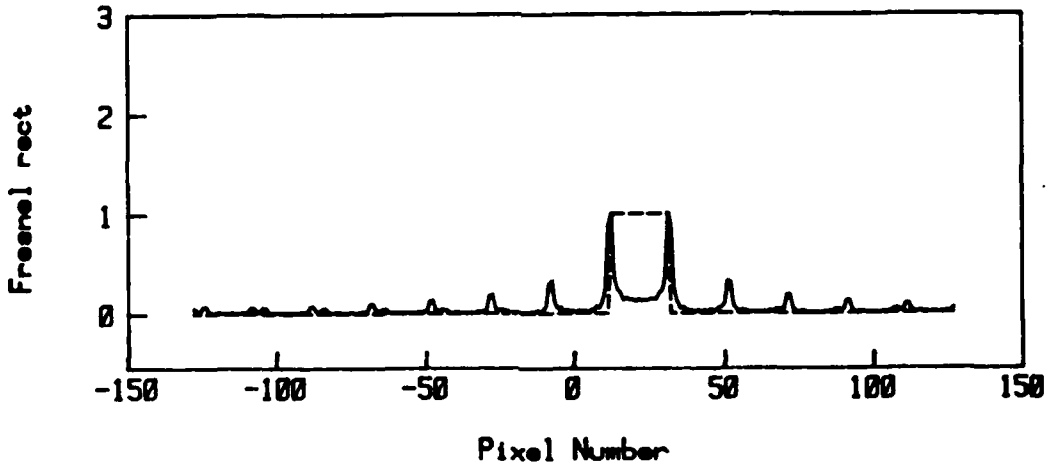

Fig. 4-6 Magnitude of the Fresnel-zone transform phase-only reconstruction (solid line) and the original rectangle function (dashed line).

result is a structure which is very similar to the Fourier transform phase-

only reconstruction shown in Fig. 4-3. The dominant feature of the structure is a large spike at the locations of the edges in the rectangle function.

As a final example, consider once again the sum of two rectangle functions shown in Fig. 4-4. Using the same argument for the stationary phase approximation that was presented above, the Fresnel zone transform of Eq. (4.2-6) is approximately equal to

$$G(f) \sim 2b\ exp(-i\pi a x_3^2)\ exp\{-i2\pi f x_3\} \quad \times$$

$$\frac{sin[\pi b(ax_3+f)]}{\pi b(ax_3+f)} cos\left[2\pi \frac{(x_2-x_1)}{2}(f+ax_3)\right], \tag{4.3-8}$$

where $x_3 = (x_1 + x_2)/2$. The phase part of this expression is

$$exp\{i\theta(f)\} \sim exp(-i\pi a x_3^2)\ exp\{-i2\pi f x_3\}\ sgn[f+ax_3] \quad \times$$

$$\left\{-1 + 2rect(fb) \otimes \frac{b}{2} comb\left(\frac{f-\frac{1}{2b}+ax_3}{2/b}\right)\right\} \quad \times$$

$$\left\{-1+2rect\left(2\frac{(x_2-x_1)}{2}f\right) \otimes \frac{(x_2-x_1)}{2} comb\left(\frac{f+ax_3}{2/(x_2-x_1)}\right)\right\} \quad . \tag{4.3-9}$$

Taking the inverse Fresnel-zone transform of Eq. (4.3-9) gives

$$\left\{exp(-i\pi a x_3^2)\ exp\{+i\pi a x^2\}\ \delta(x-x_3)\right\} \otimes \frac{-exp(-i2\pi a x_3 x)}{i\pi x} \otimes$$

$$\left\{-\delta(x) + sinc\left(\frac{x}{b}\right)\frac{2}{b} comb\left(\frac{2x}{b}\right) exp(-i2\pi a x_3 x)\ exp\{i\pi x/b\}\right\} \quad \otimes$$

$$\left\{-\delta(x) + sinc\left(\frac{x}{x_2 - x_1}\right) \frac{(x_2 - x_1)}{2}\, comb\left(\frac{2x}{x_2 - x_1}\right) exp(-i2\pi a x_3 x)\right\} . \qquad (4.3\text{-}10)$$

The magnitude of Eq. (4.3-10) is plotted in Fig. 4-7. As in the previous

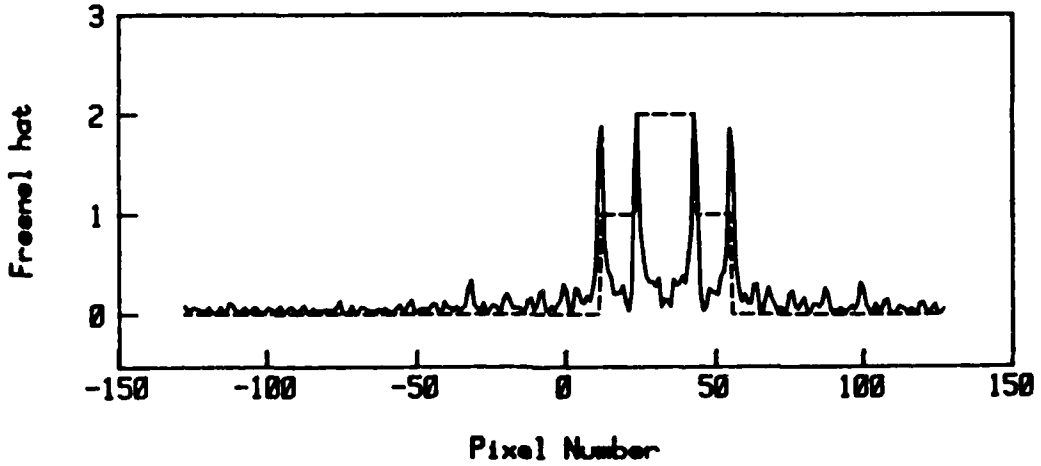

Fig. 4-7 Magnitude of the Fresnel zone transform phase-only reconstruction of the sum of rectangle functions (solid line) and the original function (dashed line).

examples, the dominant features in this reconstruction are the large spikes found at the location of the edges in the original function.

The phase-only reconstructions from Fourier transform data are real-valued quantities. Setting the magnitude equal to unity maintains the property that the real part of the Fourier transform is even and the imaginary part of the Fourier transform is odd. A Fresnel zone transform does not have this property, so setting the magnitude equal to unity will in general lead to a complex-valued reconstruction. This investigation has been limited to real-valued, non-negative images, so looking at the magnitude of the reconstruction is quite reasonable for both Fourier and Fresnel transforms.

It has been shown for both Fourier transforms and Fresnel-zone transforms located near the Fourier transform plane, that the phase of the

transform preserves the information about the edges in the original image. As one moves far away from the Fourier transform plane, the parameter α (and thus, the number of Fresnel zones) increases. Section 3.2 discusses the effects of a large number of Fresnel zones, and it is shown that for a real-valued, non-negative image, the phase of the Fresnel-zone transform behaves as a complex Gaussian, or

$$exp\{i\theta(f)\} \sim exp(+i\pi f^2/\alpha) \qquad (4.3\text{-}11)$$

In this case there is no information about the image contained in the phase of the Fresnel-zone transform. This fact accounts for the degradation in the quality of the phase-only reconstructions (for a set number of iterations) from Fresnel-zone transform phase-only information as the number of Fresnel zones increases.

Chapter Five

Effects of Noise on Image Reconstruction

5.1. Introduction

The formulation and techniques used in image reconstruction from partial Fresnel zone information are based upon properties of coherent optical imaging. In coherent imaging, both the magnitude and phase of a signal can be altered in a predetermined way by the processing system, or changed in an unknown manner by random fluctuations and noise. In this chapter we will develop a model for, and examine the effects of coherently added Gaussian noise on image reconstruction from partial Fresnel zone information. Sections 5.2 and 5.3 will investigate the effects of signal independent additive noise such as thermal noise and amplifier noise, while Sections 5.4 and 5.5 will examine the effects of signal dependent multiplicative noise such as shot noise, or film grain noise.

Consider a scalar component of the electromagnetic field (dropping the explicit time dependence) in which both the magnitude and phase are known. This signal, w_s, can be represented in complex rectangular form as

$$w_s = x_s + iy_s , \tag{5.1-1}$$

or in polar form as

$$w_s = |w_s| \exp\{i\theta_s\}, \tag{5.1-2}$$

where

$$|w_s| = |w_s w_s^*|^{\frac{1}{2}}, \tag{5.1-3}$$

and

$$|w_s| \cos(\theta_s) = x_s, \tag{5.1-4a}$$

$$|w_s| \sin(\theta_s) = y_s. \tag{5.1-4b}$$

The complex signal, w_s, is shown graphically in Fig. 5-1.

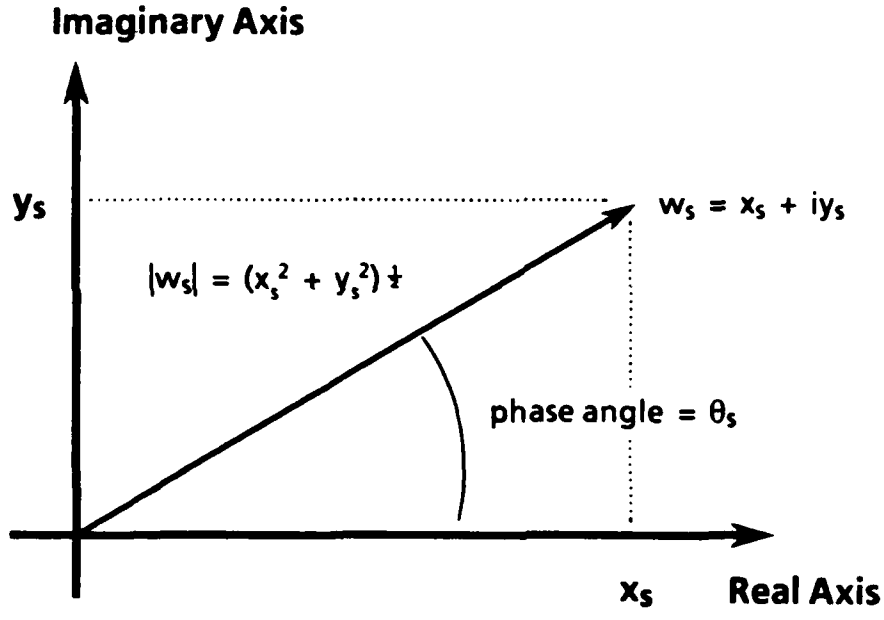

Fig. 5-1. The true signal, $w_s = x_s + iy_s$, with the polar representation, $w_s = |w_s|\exp\{i\theta_s\}$.

When the noise, n, is added to the signal, w_s, we obtain a noisy signal, w_n, defined by

$$w_n = w_s + n, \tag{5.1-5}$$

where the noise signal has been defined in a general form as

$$n = n_x + i n_y . \tag{5.1-6}$$

The detailed form of the probability density function for n will be discussed in more detail in Sect. 5.2. Writing the real and imaginary parts explicitly, we obtain

$$w_n = (x_s + n_x) + i(y_s + n_y), \tag{5.1-7}$$

where we can now make use of new random variables x_n and y_n to give

$$w_n = x_n + i y_n . \tag{5.1-8}$$

The reconstructions are now carried out using either the magnitude or phase of w_n as the known information. Since n_x and n_y are random variables, w_n is a random variable, and both the magnitude and phase of w_n are random variables. One calculation of interest will be to determine the probability density functions for the magnitude and phase of w_n.

Adding noise to both the real and imaginary parts of the signal before calculating either the magnitude or phase of the resultant noisy signal has several advantages. By adding the noise before calculating the magnitude, we are assured that the resultant noisy data, $|w_n|$, is a quantity greater than or equal to zero. If noise were added directly to the true magnitude data one would have to use a noise model which assures the non-negativity of the noisy data. A Gaussian probability density function will not work in this case. Since the phase of the signal is calculated using the ratio of the imaginary part of the signal to the real part of the signal,

any measurement which records these quantities will produce a noisy estimate of each of these values. By using this coherently additive noise model we are able to examine the effects of noise on reconstructing an image both from magnitude-only data and from phase-only data, where the simulated noisy data is the result of a single noise model.

5.2. Coherent, Additive, Signal-independent Noise

5.2.1. Graphical Representation

In image reconstruction experiments, either the magnitude, $|w_s|$, or the phase, $\exp\{i\theta_s\}$, of the Fresnel zone transform is used. In this model, a noise signal, n, will be added to the true signal, w_s, before the magnitude and phase are calculated. The noise signal will be represented as:

$$n = x + iy , \tag{5.2-1}$$

where x and y are independent, uncorrelated, Gaussian distributed, random variables with zero mean and variance σ^2. The joint probability density function $f_{xy}(x, y)$, for x and y is given by

$$f_{xy}(x,y) = \frac{1}{2\pi\sigma^2} exp\left\{\frac{-(x^2+y^2)}{2\sigma^2}\right\} , \tag{5.2-2}$$

where σ^2 is the variance of the noise, and σ is the standard deviation of the noise.

One realization of the noise model discussed above is shown in Fig. 5-2. The resultant signal, w_n, is obtained by adding a noise vector, n, to the true signal, w_s. Different realizations of the noise result in the final signal lying in a "noise cloud" about the true signal. For the case shown in Fig. 5-2 the standard deviation of the noise is much less than the magnitude of the true signal, or $\sigma << |w_s|$. This is the case for a large signal to noise ratio. As expected for the case of a large signal to noise ratio, the measured magnitude and phase will most likely be very close to the true unknown data. The variance of the measured signal will be small compared to the magnitude of the signal.

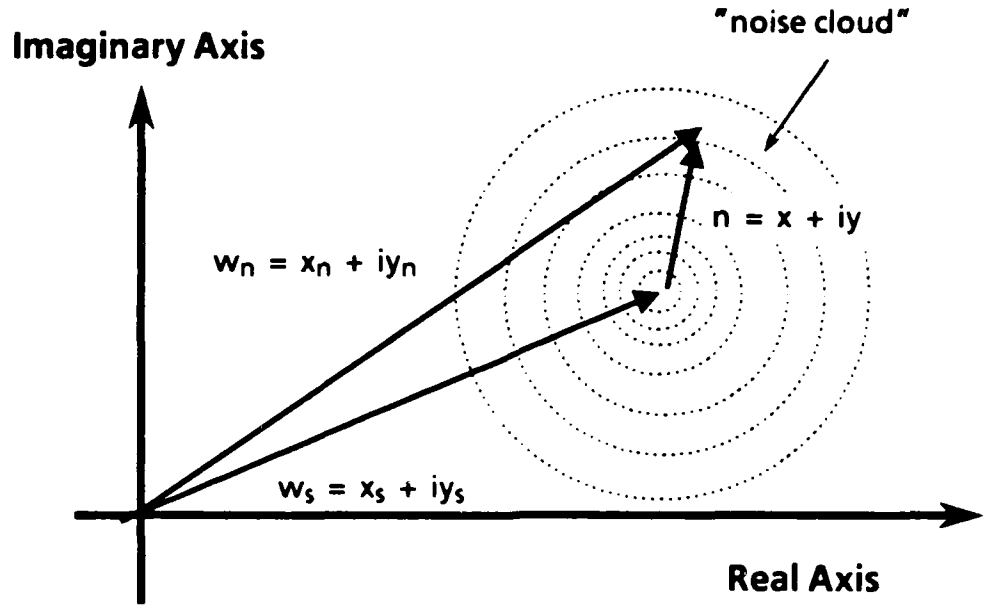

Fig. 5-2. Noisy signal, w_n, results from adding noise vector, n, to the true signal, w_s. For the case shown here the standard deviation of the noise is much less than the magnitude of the true signal, resulting in a small "noise cloud".

The case of a small signal to noise ratio is shown in Fig. 5-3. In this instance, $\sigma >> |w_s|$, and the measured data may differ significantly from the true signal. The variance of the measured signal will depend strongly on the variance of the noise, and not on the magnitude of the true signal. The true signal is buried in the noise. For the special case when $|w_s| = 0.$, the probability density function for the magnitude and phase are the well known Rayleigh and uniform distributions respectively. These distributions will be shown to be the limiting cases as $|w_s|$ tends to zero.

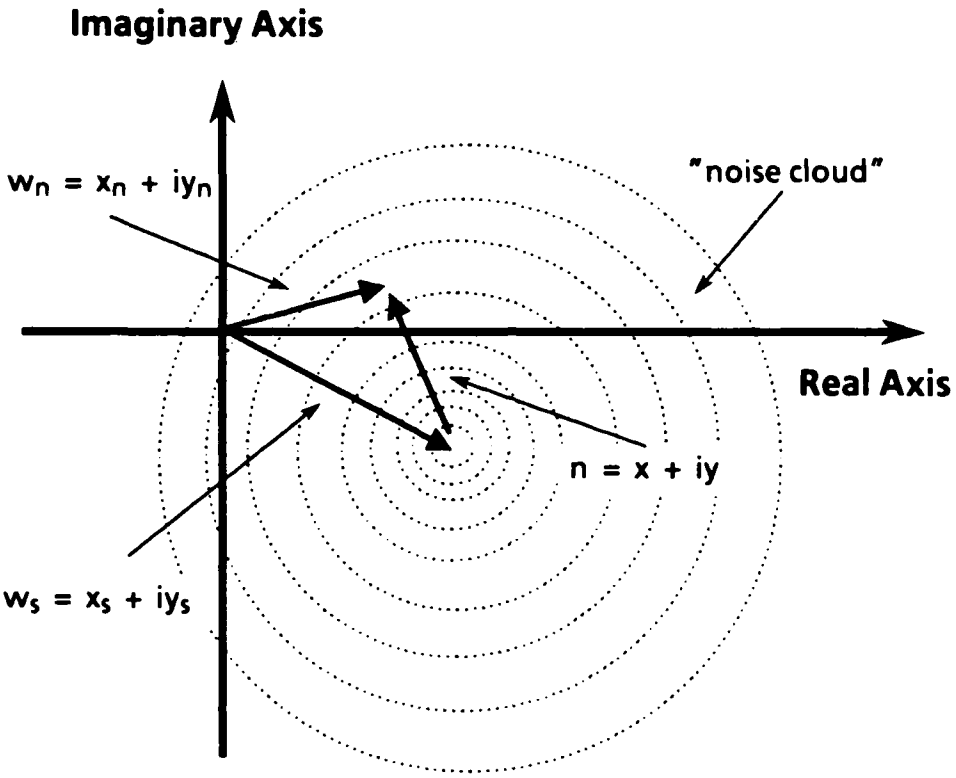

Fig. 5-3. Noisy signal, w_n, results from adding noise vector, n, to the true signal, w_s. For the case shown here the standard deviation of the noise is much greater than the magnitude of the true signal, resulting in a large "noise cloud".

This signal independent noise model has the property that the variance of the measured data will be inversely proportional to the ratio $|w_s|:\sigma$. Although both the magnitude and phase will depend on the ratio $|w_s|:\sigma$, the resultant value of $|w_n|$ will be independent of the phase angle of w_s, and the measured phase will depend upon the phase angle of w_s only as a bias term. It will also be shown that the probability density function for the measured magnitude is non-zero only for magnitudes greater than or

equal to zero, and that the probability density function for the phase angle is symmetric about the true phase angle.

5.2.2. Analytic Calculation

There is a certain type of rotational invariance in the distributions of $|w_n|$ and θ_n. Although the resultant value for w_n depends strongly on the relative sizes of $|w_s|$ and σ, the density function for $|w_n|$ is independent of θ_s, and the density function for θ_n is centered about θ_s. To simplify the analytic calculation of the desired density functions, we will consider a signal for which θ_s is zero. Let

$$w_s = s. \tag{5.2-3}$$

Consider the probability density function $f_{xy}(x, y)$ defined in Eq. (5.2-2). This density function represents the "noise cloud" shown in Figs. 5-2 and 5-3. For the given signal, $w_s = s$, this noise cloud will be centered about the point ($x_n = s$, $y_n = 0$). In effect this probability density function for the noise undergoes a coordinate transformation such that

$$x = b\cos\theta - s \quad , \tag{5.2-4a}$$

and

$$y = b\sin\theta \quad . \tag{5.2-4b}$$

where

$$b = |w_n| \tag{5.2-5}$$

is the resultant magnitude, and

$$\theta = \theta_n \tag{5.2-6}$$

is the resultant phase angle. [For a similar discussion of this type of calculation see; Papoulis, (1965) page 195 Ex.7-8a, page 229 Prob. 7-4, and the discussion leading to Eq. 14-63. also; Goodman, (1985) § 2.9.4]

This coordinate transformation on the probability density function leads to the new probability density function, $f_{b\theta}(b, \theta)$, which is the joint probability density function for the magnitude, b, and the phase angle, θ, and is given by

$$f_{b\theta}(b, \theta) = f_{xy}\Big(x(b, \theta),\, y(b, \theta)\Big)\, |J| \ , \tag{5.2-7}$$

where $|J|$ is the Jacobian of the transformation and is defined as

$$|J| = \begin{vmatrix} \partial x / \partial b & \partial x / \partial \theta \\ \partial y / \partial b & \partial y / \partial \theta \end{vmatrix} \ . \tag{5.2-8}$$

Using Eq. (5.2-4) to evaluate this Jacobian we obtain

$$\begin{vmatrix} cos\theta & -b sin\theta \\ sin\theta & b cos\theta \end{vmatrix} = b \ . \tag{5.2-9}$$

Substituting Eqs. (5.2-4) and (5.2-9) into Eq. (5.2-7), an expression for the joint probability density function is given by:

$$f_{b\theta}(b, \theta) = \frac{b}{2\pi\sigma^2}\, exp\Big\{ -\left[(b\cos\theta - s)^2 + (b \sin\theta)^2 \right] / 2\sigma^2 \Big\} \ , \tag{5.2-10}$$

$$b \geq 0 \ \text{and}, \ -\pi < \theta \leq \pi \ .$$

5.2.3. Probability Density Function for Magnitude Information

To calculate the density function for the magnitude b, denoted by $f_b(b)$, we must evaluate the integral of $f_{b\theta}(b, \theta)$ from zero to 2π:

$$f_b(b) = \int_0^{2\pi} f_{b\theta}(b, \theta)\, d\theta. \tag{5.2-11}$$

Using Eq. (5.2-10) this integral can be expressed as

$$f_b(b) = \frac{b}{\sigma^2} \exp\left\{ -(b^2 + s^2) / 2\sigma^2 \right\} \frac{1}{2\pi} \int_0^{2\pi} \exp\left\{ sb\cos\theta / \sigma^2 \right\} d\theta. \tag{5.2-12}$$

The probability density function for the magnitude b is given by [see; Abromowitz and Stegun, (1972) Eq. 9.6.16]

$$f_b(b) = \frac{b}{\sigma^2} \exp\left\{ -(b^2 + s^2) / 2\sigma^2 \right\} I_0\left(\frac{bs}{\sigma^2} \right), \quad b \geq 0, \tag{5.2-13}$$

where $I_o()$ is the modified Bessel function of the first kind, defined by the power series [see; Abromowitz and Stegun, (1972) Eq. 9.6.12]

$$I_0(x) = \sum_{n=0}^{\infty} \frac{x^{2n}}{2^{2n}(n!)^2}. \tag{5.2-14}$$

In the limit as the true signal, s, goes to zero, the probability density function for the magnitude reduces to

$$f_b(b) = \frac{b}{\sigma^2} \exp\left\{ -b^2 / 2\sigma^2 \right\}, \tag{5.2-15}$$

which is the well known Rayleigh density function.

In the limiting case of a very large signal to noise ratio (i.e. $s >> \sigma$) the resultant magnitude, b, will be approximately equal to the original signal, s. To examine the behavior of the probability density function for the case of a large signal to noise ratio, rewrite Eq. (5.2-13) as

$$f_b(b) = \frac{1}{\sigma} \exp\left\{-(b-s)^2 / 2\sigma^2\right\} \frac{b}{\sigma} \exp\left\{-sb^2/\sigma^2\right\} I_0\left(\frac{bs}{\sigma^2}\right). \quad (5.2\text{-}16)$$

For $s>>\sigma$ the quantity $(sb)/\sigma^2$ tends to infinity for non-zero b. The asymptotic form of the modified Bessel function is given by

$$I_0(x) \sim \frac{exp(x)}{(2\pi x)^{\frac{1}{2}}} . \quad (5.2\text{-}17)$$

An expression for the large signal to noise ratio limit is obtained by using this asymptotic expression in Eq. (5.2-16), and is given by:

$$f_b(b) = \frac{1}{\sigma (2\pi)^{\frac{1}{2}}} \exp\left\{-(b-s)^2 / 2\sigma^2\right\} (b/s)^{\frac{1}{2}}. \quad (5.2\text{-}18)$$

Since $s>>\sigma$, the exponential term will have appreciable value only when $s \approx b$, and the term $(b/s)^{\frac{1}{2}}$ will be very close to unity. We note that in this case the probability density function becomes a very narrow, almost delta-like, Gaussian distribution with a mean equal to the true value, s, and a variance equal to the variance of the noise.

Figure 5-4 shows a plot of $\sigma f_b(b)$ vs. b/σ for various values of the parameter $k = s/\sigma$. These plots show the smooth transition from a Rayleigh distribution when $k = 0$ to a Gaussian type distribution as k increases. The relatively constant width and height of the distribution functions for various value of k is the result of scaling both the horizontal and vertical axes by the standard deviation of the noise, σ.

Three example histograms and their corresponding theoretical probability density functions are shown in Fig. 5-5. For each each of these examples the known signal has a value of 10.0 (i.e. $s = 10.0$), and the

histograms of 10000 data points with noise variance (σ^2) equal to 1.0, 25.0, and 64.0, are shown in Figs. 5-5(a), (b), and (c), respectively. Each of the histograms represent the result of adding signal independent, Gaussian white noise with the specified variance and zero mean to 10000 pixels of constant value, and then calculating the magnitude of the resultant pixels. Recall that in the Gaussian noise model developed here, the noise has both a real and imaginary parts which are uncorrelated. The plots

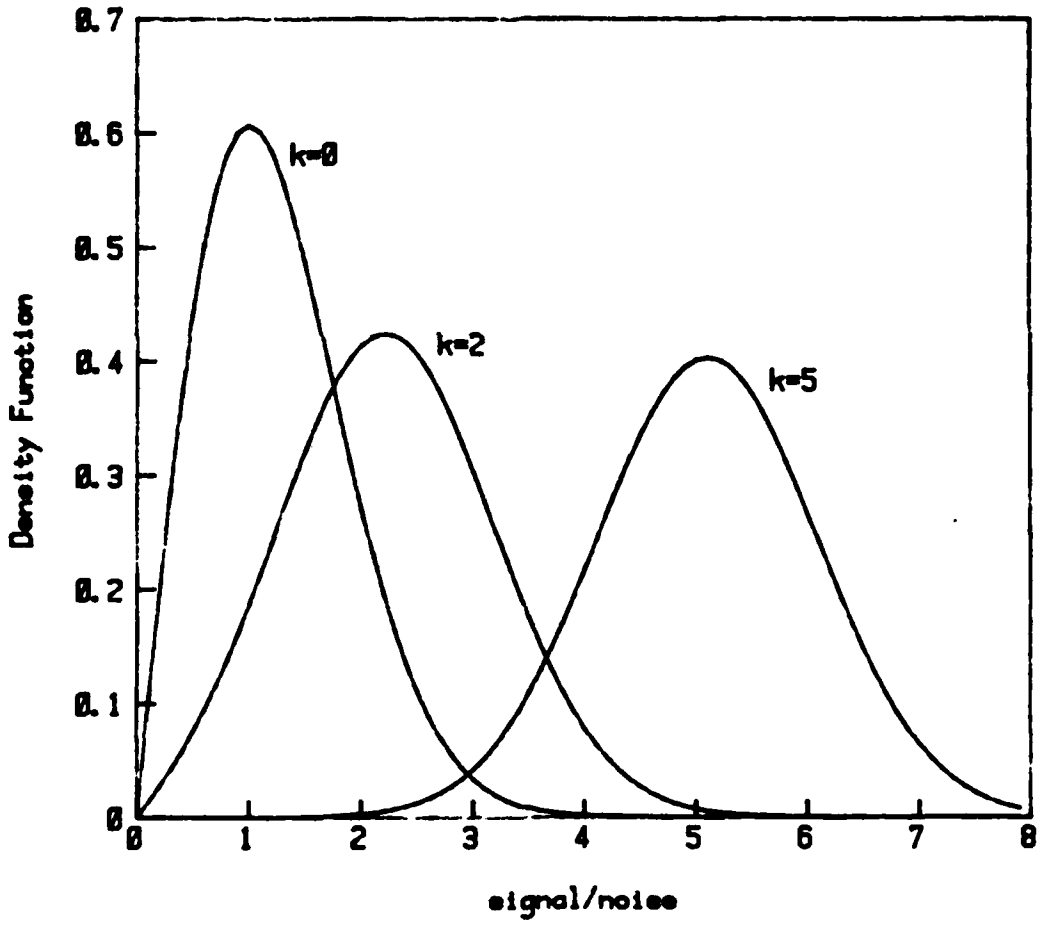

Fig. 5-4. Probability density function of the measured magnitude b resulting from noise with variance σ^2 added to a true signal of magnitude s. The parameter $k = s/\sigma$ is a measure of the signal to noise ratio.

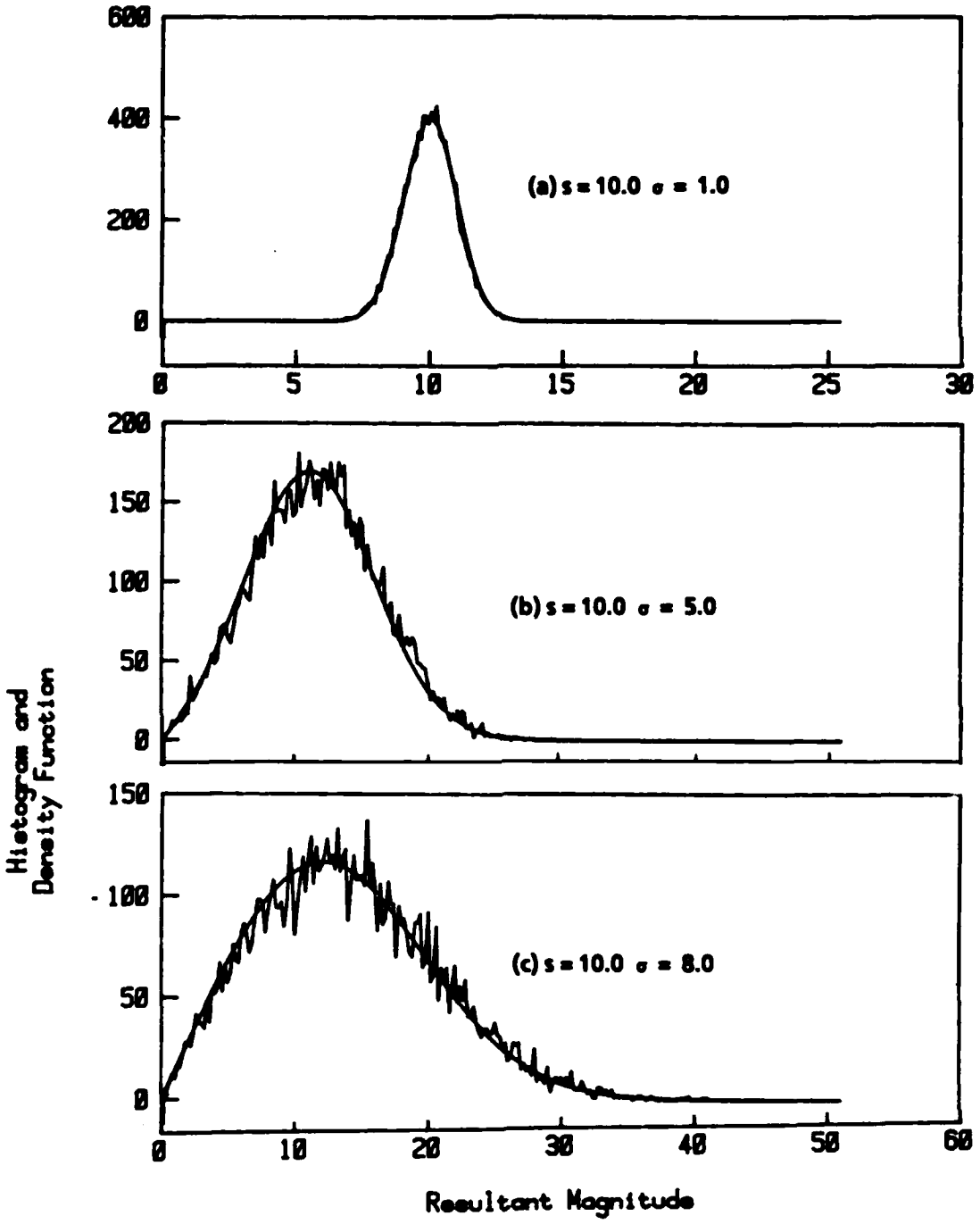

Fig. 5-5 Predicted probability density functions and actual histograms of the measured magnitude, b, for (a) s = 10.0, σ = 1.0 (b) s = 10.0, σ = 5.0, and (c) s = 10.0, σ = 8.0 .

shown in Fig. 5-5 indicate excellent agreement between the theoretically predicted probability density functions and the actual histograms. It should also be noted that the vertical scale is different for all three graphs, and that the horizontal scale in Fig. 5-5(a) has only one-half the range of the horizontal scales used in Figs. 5-5(b) and (c). These different scales were used so that a comparison between the theoretical probability density functions and the histograms could be done visually.

As the ratio of the true signal, s, to the standard deviation of the noise, σ, increases from zero,the probability density function, $f_b(b)$, for the magnitude, b, changes from a wide, low Rayleigh distribution to a very narrow Gaussian.

5.2.4. Probability Density Function for Phase Angle

The density function $f_\theta(\theta)$ is obtained by evaluating the integral

$$f_\theta(\theta) = \int_0^\infty f_{b\theta}(b,\theta)\, db. \tag{5.2-19}$$

Using Eq. (5.2-10) this integral can be expressed as

$$f_\theta(\theta) = \frac{1}{2\pi\sigma^2} exp\left\{-s^2/2\sigma^2\right\} \int_0^\infty b\, exp\left\{-b^2/2\sigma^2 + s\,b\cos\theta/\sigma^2\right\} db. \tag{5.2-20}$$

The probability density function for the phase angle θ is given by [see; Gradshteyn and Ryzhik, (1980) Eq. 3.462.5]

$$f_\theta(\theta) = \frac{exp\{-s^2/2\sigma^2)}{2\pi} + \frac{s\cos\theta}{2\sigma(2\pi)^{\frac{1}{2}}} exp\left\{-(s\sin\theta)^2/2\sigma^2\right\}\left[1 + 2\,erf\left(\frac{s\cos\theta}{\sigma}\right)\right]$$

$$-\pi < \theta \le \pi\,, \tag{5.2-21}$$

where erf() is the error function defined by

$$erf(x) = \frac{1}{(2\pi)^{\frac{1}{2}}} \int_0^x exp(-u^2/2)\, du \,. \qquad (5.2\text{-}22)$$

In the limit as the true signal, s, goes to zero, the probability density function for the phase reduces to

$$f_\theta(\theta) = \frac{1}{2\pi} \qquad -\pi < \theta \leq \pi \,, \qquad (5.2\text{-}23)$$

which is the well known uniform density function.

In the limiting case of a large signal to noise ratio (i.e. $s >> \sigma$), the resultant phase angle, θ, will be approximately equal to the original phase angle, $\theta_s = 0.0$. As the quantity s/σ goes to infinity we obtain an expression for the large signal to noise ratio limit:

$$f_\theta(\theta) = \frac{s\cos\theta}{\sigma(2\pi)^{\frac{1}{2}}} \exp\left\{-(s\sin\theta)^2/2\sigma^2\right\} \qquad (5.2\text{-}24)$$

The exponential will be non-zero only near $\sin(\theta) = 0$. (i.e. $\theta = 0.$). Near $\theta = 0.$, small angle approximations $\cos(\theta) = 1.0$ and $\sin(\theta) = \theta$ can be used. Equation (5.2-24) can now be expressed in terms of a delta function by using the relation

$$\delta(t) = \lim_{N\to\infty} N exp(-N^2 \pi t^2) \,, \qquad (5.2\text{-}25)$$

to give

$$f_\theta(\theta) = \delta(\theta) \qquad -\pi < \theta \leq \pi \,, \qquad (5.2\text{-}26)$$

So for the case of a large signal to noise ratio, the probability density function becomes a delta function located at the true phase angle.

Figure 5-6 shows a plot of $f_\theta(\theta)$ vs. θ for various values of the parameter

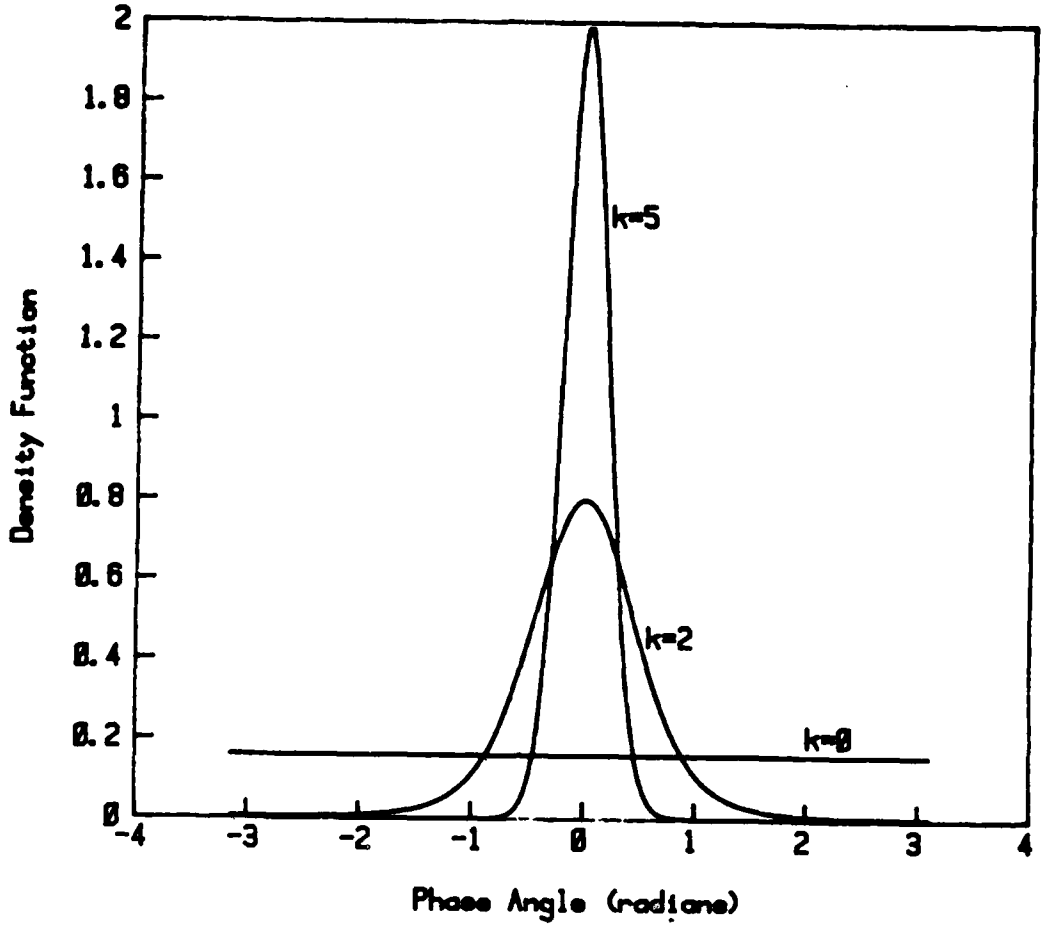

Fig. 5-6 Probability density function of the measured phase angle θ resulting from noise with a variance σ^2 being added to a true signal with a magnitude equal to s, and a phase angle equal to zero. The parameter $k = s/\sigma$ is a measure of the signal to noise ratio.

$k = s/\sigma$. These plots show the smooth transition from a uniform distribution when k = 0., to a Gaussian type distribution, and finally to a delta function as k tends to infinity.

Three example histograms and their corresponding theoretical probability density functions are shown in Fig. 5-7. For each each of these examples the known signal has a value of 10.0 (i.e. s = 10.0), and the histograms of 10000 data points, with noise variance (σ^2) equal to 1.0, 25.0, and 64.0, are shown in Figs. 5-7(a), (b), and (c), respectively. Each of

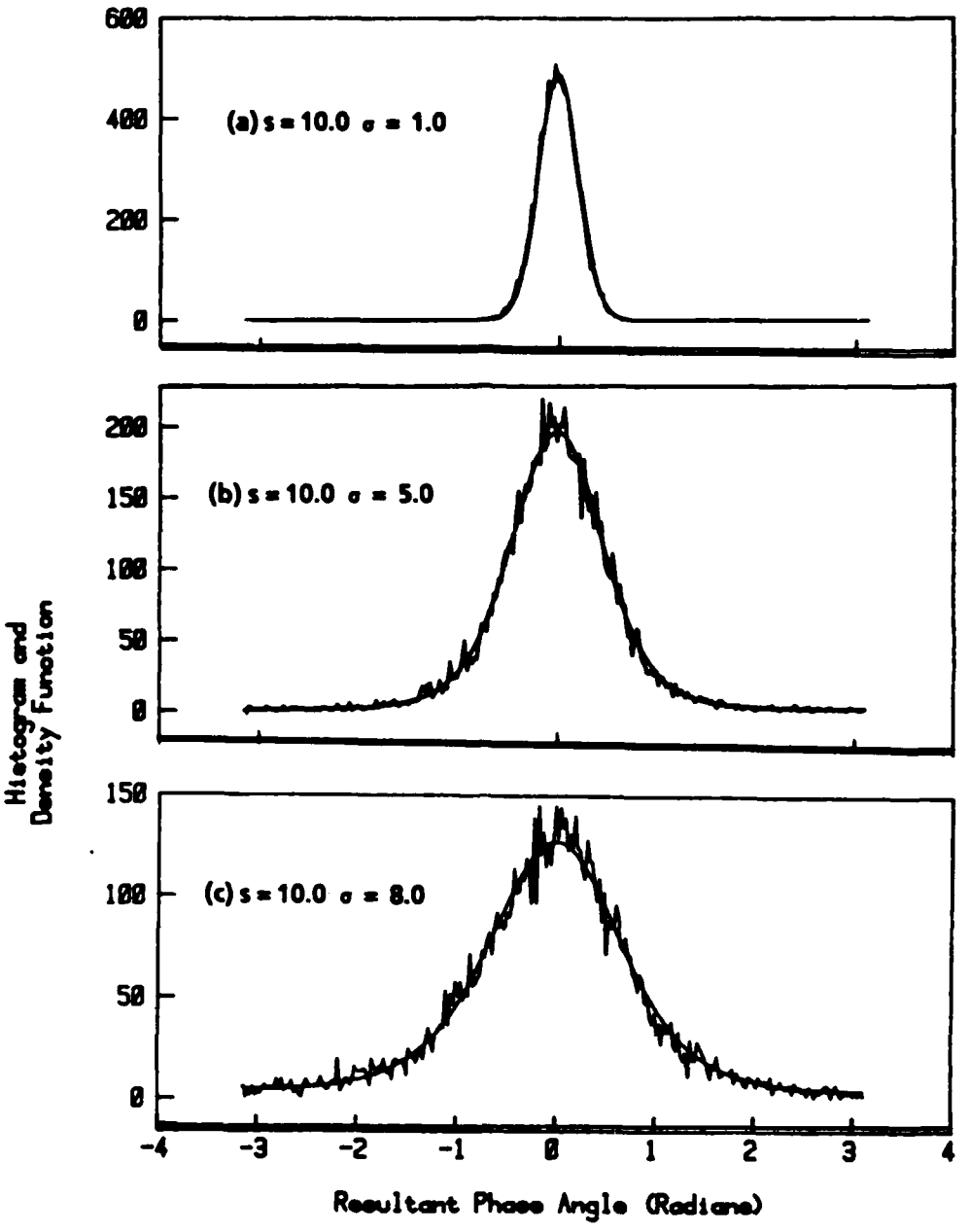

Fig. 5-7 Predicted probability density functions and actual histograms of the measured phase angle, θ, for (a) $s = 10.0, \sigma = 1.0$ (b) $s = 10.0, \sigma = 5.0$, and (c) $s = 10.0, \sigma = 8.0$.

the histograms represent the result of adding signal independent, Gaussian white noise with the specified variance and zero mean to 10000 pixels of constant value, and then calculating the phase angle of the resultant pixels. The plots shown in Fig. 5-7 indicate excellent agreement between the theoretically predicted probability density functions and the actual histograms.

As the ratio of the true signal, s, to the standard deviation of the noise, σ, increases from zero,the probability density function, $f_\theta(\theta)$, for the phase angle, θ, changes from a uniform distribution, to a narrow Gaussian, and finally to a delta function.

5.3 Effects of Additive Noise on Image Reconstruction

5.3.1. Magnitude-only Reconstruction

The noise model developed in Sect. 5.2 was applied to various Fresnel zone transforms before calculating the magnitude data. By attempting to reconstruct an image from this noisy data, effects of noise and the stability of the reconstruction process in the presence of noise can be understood.

For this model of signal independent noise it is difficult to define a signal to noise ratio for a given noise variance and Fresnel zone transform. As mentioned in Chapt. 2, as the Fresnel zone transform moves further away from the Fourier transform plane and the number of Fresnel zones increases, the magnitude data tends to spread out while the phase information takes on a very definite circular structure. In Sect. 5.2 it was shown that the probability density function, and thus the expected value and variance, of the measured signal depends on the ratio of the magnitude of the true signal to the standard deviation of the noise. For signal independent noise, the variance of the noise will be the same over the entire Fresnel zone transform, but the magnitude of the true signal will vary from pixel to pixel, thus the signal to noise ratio will vary from pixel to pixel.

The values of the maximum, mean, and variance of the magnitude information for several different Fresnel zones is shown in table 5.1. Although this data represents the Fresnel zone transforms from only one image, the general trends of a decrease in the maximum value and variance, accompanied by an increase in the mean value has been observed for other images that were examined. It should also be noted

# of Fresnel Zones	Maximum (x10^5)	Mean (x10^3)	Variance (x10^8)
00.0	64.5	3.96	8.54
00.5	37.0	4.24	8.52
03.0	5.57	6.10	8.33
05.0	3.78	7.63	8.12
07.0	2.80	9.16	7.86
10.0	2.13	11.5	7.38
16.0	1.45	16.1	6.12

Table 5-1. Values for the maximum, mean, and variance of the magnitude of the Fresnel zone transform for several different Fresnel zones

that the minimum value of the magnitude data is generally less than 10, and is quite often equal to zero. From this table we can see that the known magnitude data has quite a large dynamic range, and thus for any particular Fresnel zone transform, the signal to noise ratio will vary significantly over the transform plane.

To investigate the effects of noise on reconstructing from Fresnel zone magnitude-only data, various amounts of noise were added to the Fresnel zone transform at several different Fresnel zones. Both a visual inspection of the reconstructed images and an analytic measure of the error in the reconstruction were done.

The measure of the absolute error in the transform plane, $E_M^{(i)}$, is given by

$$E_M^{(i)} = \frac{1}{N^2} \sum_{m=0}^{N-1} \sum_{n=0}^{N-1} \left| |G(m,n)| - |G_i(m,n)| \right| , \qquad (5.3\text{-}1)$$

where i is the iteration number, $|G(m,n)|$ is the measured magnitude data, and $|G_i(m,n)|$ is the magnitude data calculated from the Fresnel zone transform of the guess for the image after i iterations. This error is a direct measure of how well the iteration is progressing in terms of being consistent with the known magnitude information.

The measure of the relative squared error in the image plane, $E_I^{(i)}$, is given by

$$E_I^{(i)} = \frac{\sum_{m=0}^{N-1}\sum_{n=0}^{N-1} \left| g_i(m,n) - g_i'(m,n) \right|^2}{\sum_{m=0}^{N-1}\sum_{n=0}^{N-1} \left| g_i(m,n) \right|^2} \qquad (5.3\text{-}2)$$

where i is the iteration number, $g_i(m,n)$ is the calculated guess for the image after i iterations and before the image plane constraints have been imposed, and $g_i'(m,n)$ is the result of applying the image plane constraints on $g_i(m,n)$. Although this error is very difficult to relate to the known transform magnitude information, this error does give an indication as to how much the guess for the image is having to be modified to fulfill the image plane constraints.

For the case when there is no noise in the measured data, it is possible to fulfill all the constraints imposed in both the image and transform domains, so that these errors can go to zero. When noise is added to the measured data, the magnitude information imposed in the transform domain may no longer be compatible with the constraints of a real valued, non-negative object. The absolute error in the transform domain

and the relative squared error in the image plane could not both go to zero in this case.

Figure 5-8 is a plot of the absolute error, $E_M^{(i)}$, for the first 75 iterations at 7.0 Fresnel zones for various amounts of noise. We see in these plots that the error tends to change the most in the first several iterations and then decreases very slowly. Note also that the rate of change of the error from iteration 2 until approximately iteration 25 is directly proportional to the amount of noise in the data. For approximately the first 25 iterations, the more noise there is in the measured data, the greater decrease there is in the absolute error between the measured noisy data and the calculated transform magnitude. Although Fig. 5-8 contains the error plots for only one realization of the noise at 7.0 Fresnel zones, the general structure and shape of the error curves are very similar both for different realizations of the noise and for data recorded at different locations in the Fresnel zone.

One of the observations that is made in examining the plots shown in Fig. 5-8 is that the error tends to stagnate on a level which is approximately equal to one-half the value of the standard deviation of the signal independent noise. Figure 5-9 is a plot of the value of this stagnation error verses the standard deviation of the noise for several different Fresnel zones. The value of the error at the stagnation level is calculated as the average value of the error between iteration 50 and iteration 75. From this plot we can see that the error level is approximately equal to one-half the value of the standard deviation of the noise, independent of the Fresnel zone at which the data was measured.

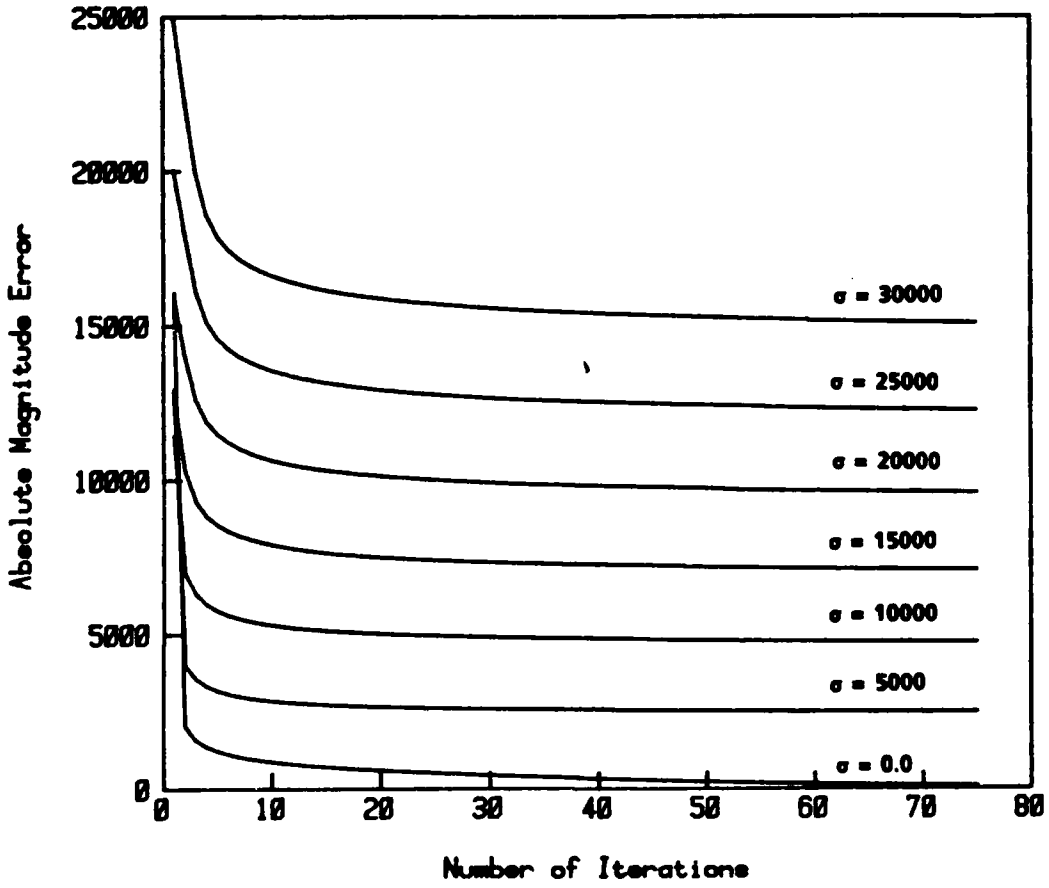

Fig. 5-8 Absolute error between current transform magnitude and measured transform magnitude for magnitude-only reconstruction at 7.0 Fresnel zones. Errors are shown for cases when the standard deviation of the noise is equal to 0, 5000, 10000, 15000, 20000, 25000, and 30000.

Figure 5-10 is a plot of the relative squared error, $E_I^{(i)}$, for the first 75 iterations at 7.0 Fresnel zones for various amounts of noise. We see in these plots that the error tends to change the most in the first several iterations and then decreases very slowly. Note also that the rate of change of the error for the first few iterations is directly proportional to the amount of noise in the data. For approximately the first 25 iterations, the more noise there is in the measured data, the greater decrease there is in the relative squared error in the image plane.

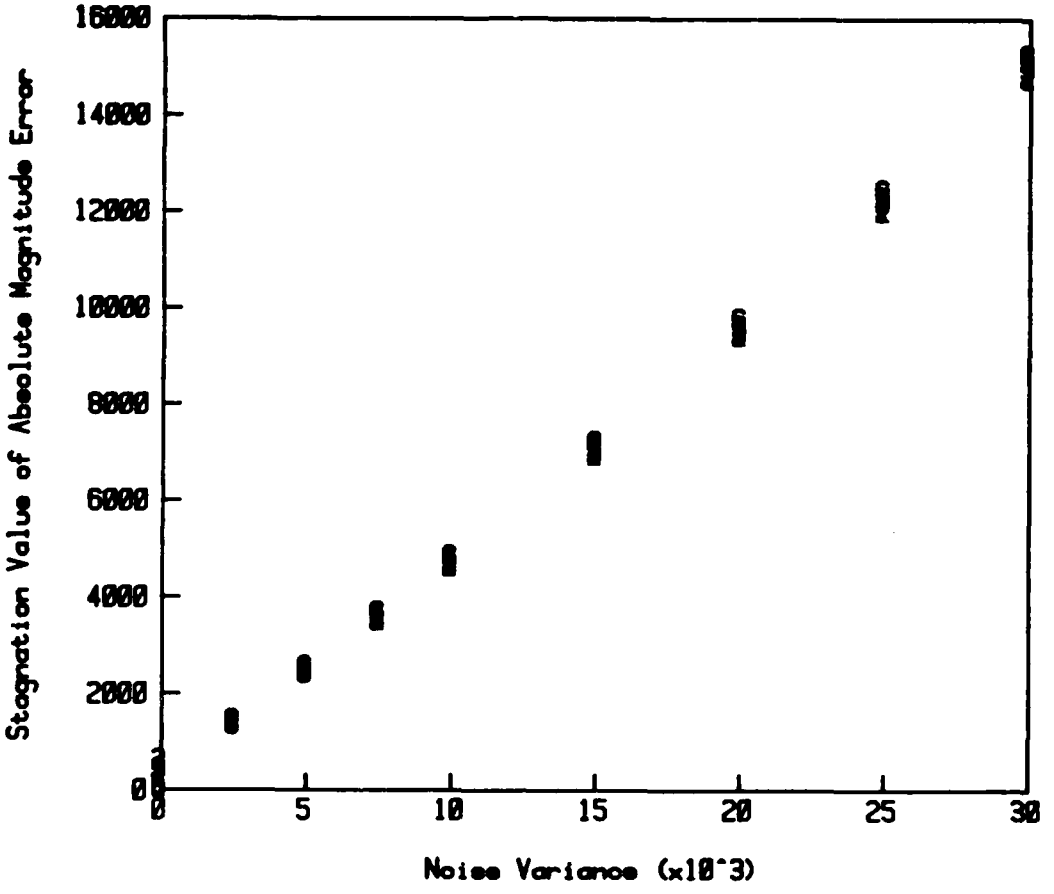

Fig. 5-9 Average value of the absolute error in the magnitude-only reconstruction for iterations 50 through 75 for various amounts of noise at several different Fresnel zone locations. The plotted symbols 1-6 are for Fresnel zones equal to 0.0, 0.5, 3.0, 5.0, 7.0, and 10.0 respectively.

As shown in Fig. 5-10, the error tends to stagnate at a level which is directly proportional to the value of the standard deviation of the signal independent noise. Figure 5-11 is a plot of the value of this steady error verses the standard deviation of the noise for several different Fresnel zones. The value of the error at the stagnation level is calculated as the average value of the error between iteration 50 and iteration 75. From this plot we can see that the stagnation error level for a given noise

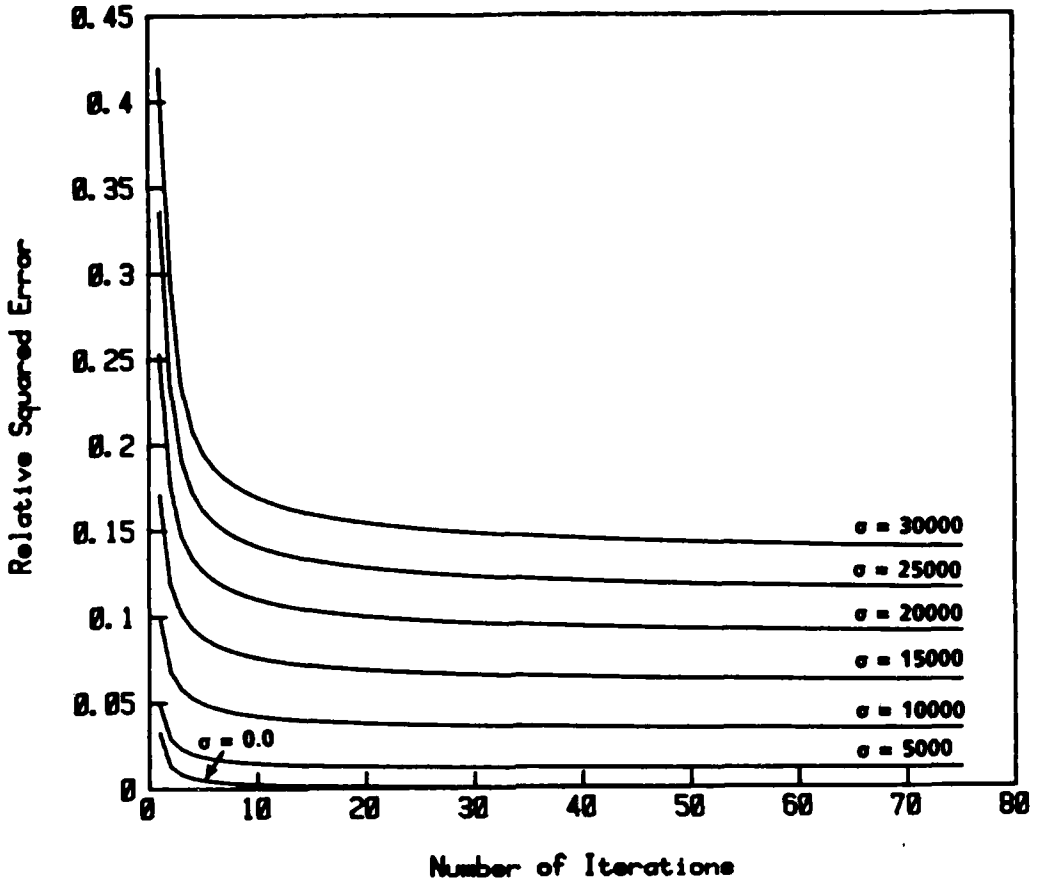

Fig. 5-10 Relative squared error in the image plane for 75 iterations at 7.0 Fresnel zones for magnitude-only reconstructions. Errors are shown for the cases when the standard deviation of the noise, σ, is equal to 0, 5000, 10000, 15000, 20000, 25000, and 30000.

variance is independent of the Fresnel zone at which the data was measured.

To see how this absolute error in the reconstruction relates to the quality of the reconstructed image, consider the sample of images shown in Figs. 5-12 through 5-14. Figure 5-12 is an example of a reconstruction at 3.0 Fresnel zones after 15 and 75 iterations from data corrupted by noise with standard deviations of 0, 2500, 10000, and 25000. From these

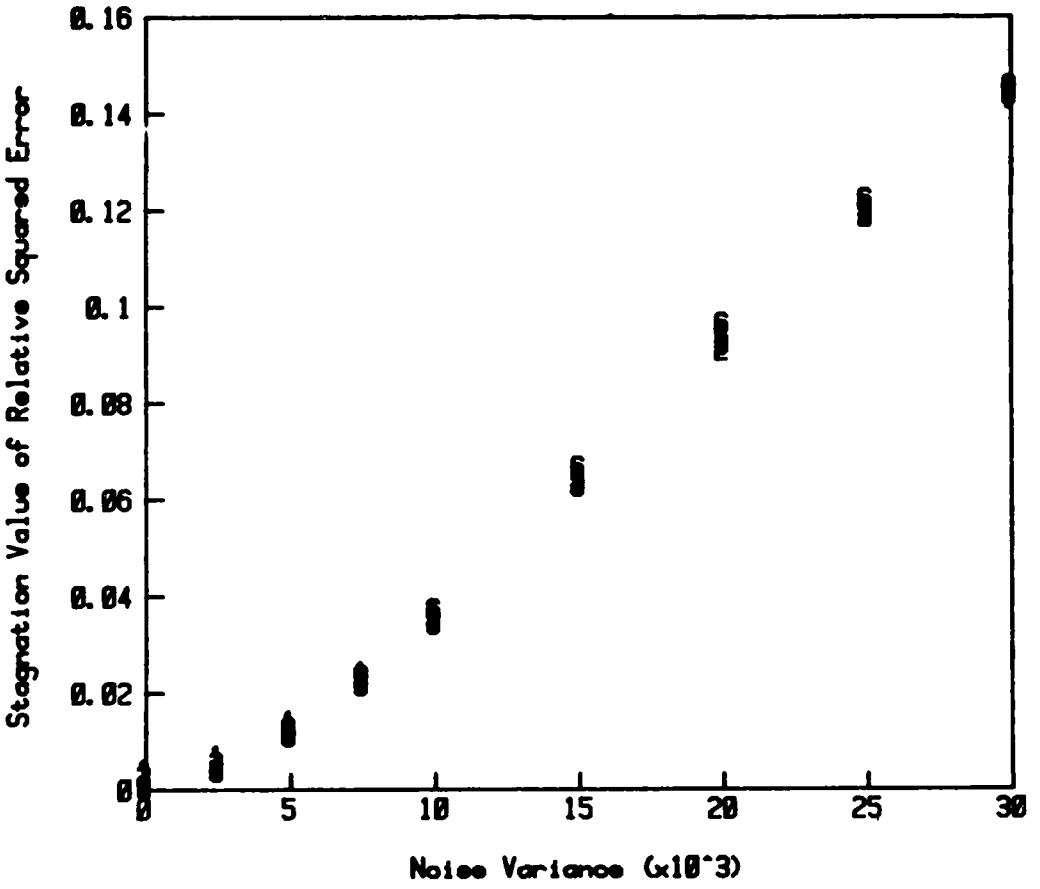

Fig. 5-11 Average value of the relative squared error in the magnitude-only reconstruction for iterations 50 through 75 for various amounts of noise at several different Fresnel zone locations. The plotted symbols 1-6 are for Fresnel zones 0.0, 0.5, 3.0, 5.0, 7.0, and 10.0 respectively.

reconstructed images we see that the quality of the reconstruction changes less and less from iteration 15 to iteration 75 as the amount of noise is increased. For noise values equal to 0 and 2500 there is a visible increase in the quality of the reconstruction, for noise with a standard deviation of 10000 there is no visible change in this barely recognizable image, and for noise with a standard deviation of 25000 the image is not recognizable for any number of iterations.

Figures 5-13 and 5-14 are examples of the same set of reconstructed images as discussed for Fig. 5-12, but the reconstructions for Fig. 5-13 were done at 7.0 Fresnel zones, and the reconstructions for Fig. 5-14 were done at 10.0 Fresnel zones. From these images we observe that there is still a general increase in the quality of the reconstructed image as the number of Fresnel zones increases, even in the presence of small amounts of noise, but the presence of large amounts of noise yields a reconstruction which is not recognizable.

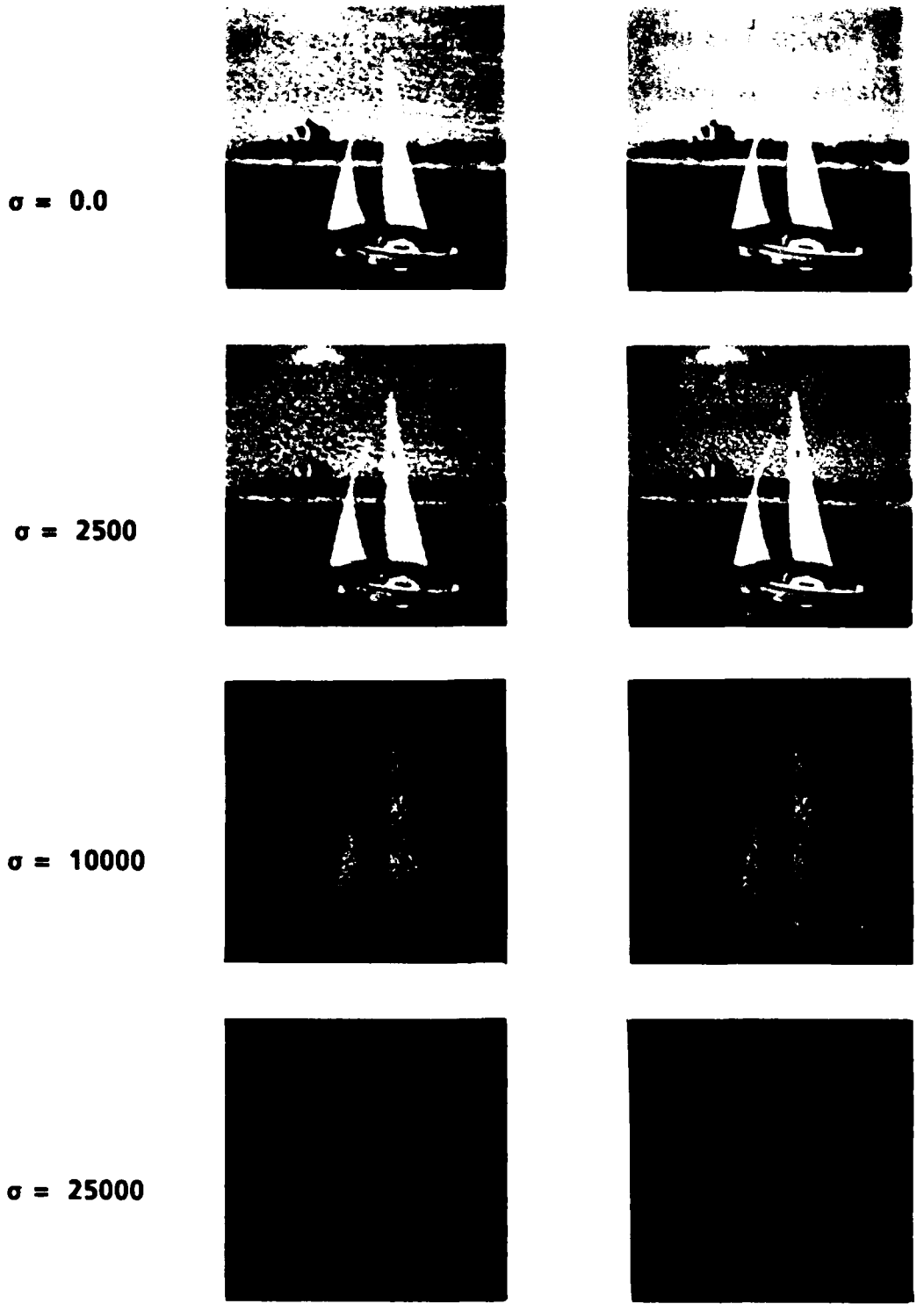

Fig. 5-12 Magnitude-only reconstructions from noisy data at 3.0 Fresnel zones. The reconstructions are shown after 15 iterations (left) and 75 iterations (right) for various amounts of noise as indicated.

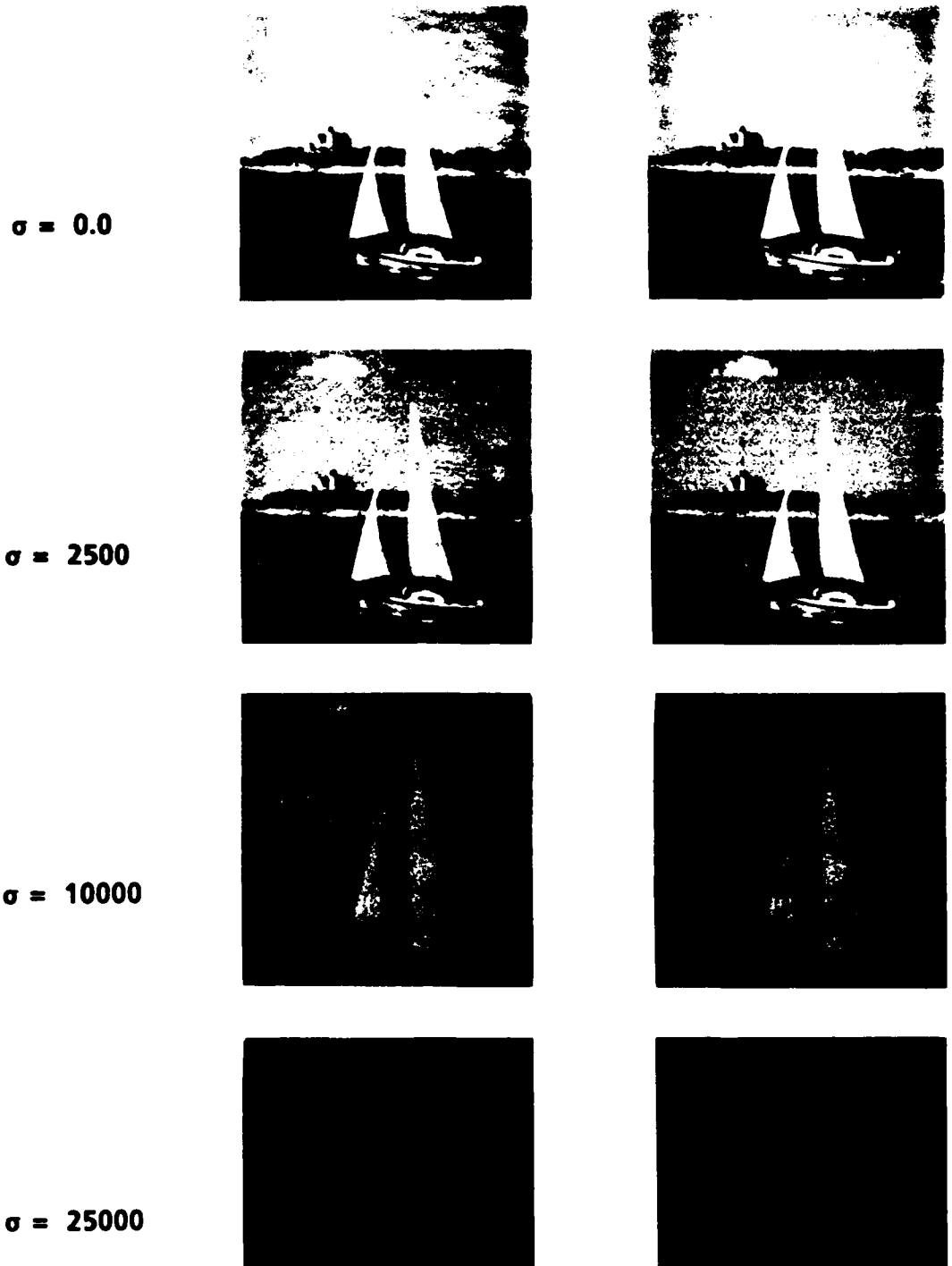

Fig. 5-13 Magnitude-only reconstructions from noisy data at 7.0 Fresnel zones. The reconstructions are shown after 15 iterations (left) and 75 iterations (right) for various amounts of noise as indicated.

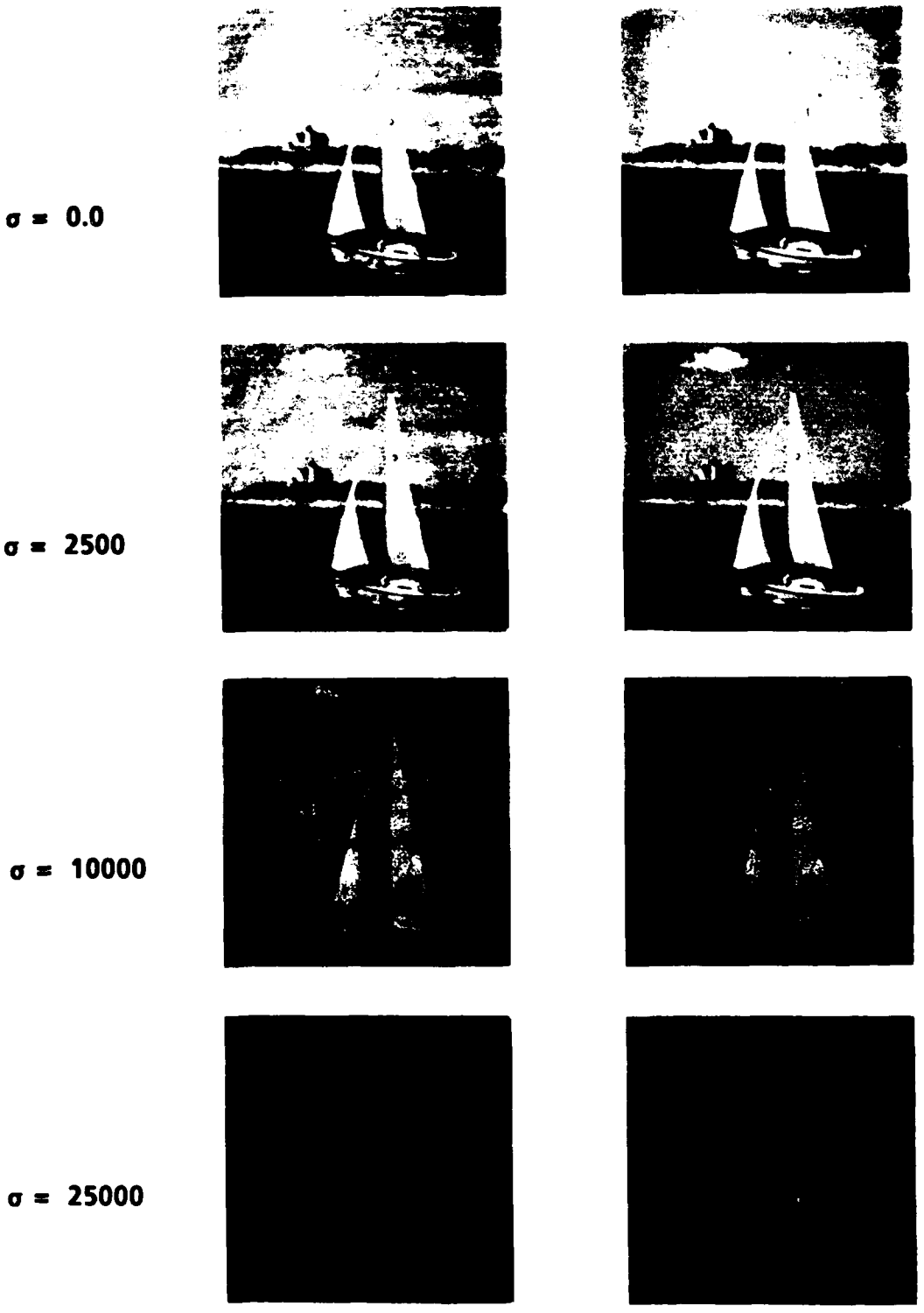

Fig. 5-14 Magnitude-only reconstructions from noisy data at 10.0 Fresnel zones. The reconstructions are shown after 15 iterations (left) and 75 iterations (right) for various amounts of noise as indicated.

5.3.2 Phase-only Reconstruction

The noise model developed in Sect. 5.2 was also applied to various Fresnel zone transforms before calculating the phase angle data, and then attempting to reconstruct an image from this noisy data.

As discussed earlier in Sect. 5.3.1, it is difficult to define a signal to noise ratio for a given noise variance and Fresnel zone transform. In Sect. 5.2 it was shown that the probability density function, and thus the expected value and variance of the measured phase angle data depends on the ratio of the magnitude of the true signal to the standard deviation of the noise. In phase-only reconstruction it is assumed that this magnitude information is not known. In addition, the calculation of the phase information in the Fresnel zone transform may require the measurement of several intensity distributions or interference patterns, followed by the numerical calculation of the phase angle at each pixel, Although the measurement of the phase-only information is often a complicated one, the noise model chosen has the property that the stronger the signal at a given pixel, the less corrupted the phase information is at that pixel for a given amount of noise.

To investigate the effects of noise on reconstructing an image from Fresnel zone phase-only data, various amounts of noise were added to the Fresnel zone transform at several different Fresnel zones. Both a visual inspection of the reconstructed images and an analytic measure of the error in the reconstruction were done.

A measure of the analytic error in the transform domain, $E_P(i)$, is defined as by

$$E_P^{(i)} = \frac{1}{N^2} \sum_{m=0}^{N-1} \sum_{n=0}^{N-1} \left| \exp\{i\,\theta(m,n)\} - \exp\{i\,\theta_i(m,n)\} \right| , \qquad (5.3\text{-}3)$$

where $\exp\{i\theta(m,n)\}$ is the known phase information, and $\exp\{i\theta_i(m,n)\}$ is the phase of the Fresnel zone transform of the guess for the image after i iterations. The relative squared error in the image plane, defined in Eq. (5.3-2), was used as an analytic measure of the error in the image plane during the reconstruction process.

A plot of the absolute phase error, $E_P^{(i)}$, is shown in Fig. 5-15. Although the presence of only a small amount of noise results in a large increase in the absolute phase error, there is not a large degradation in the visual quality of the reconstructed image. It is interesting to note that when noise is present in the known data, the absolute phase error has a minimum after 3 or 4 iterations, then increases to a steady state value which is slightly greater than the minimum value located near iteration number 3.

A plot of the stagnation value of the absolute phase error verses the standard deviation of the noise is shown in Fig. 5-16. The stagnation value of the absolute phase error is equal to the average value of the error for iterations 15 through 20. From Fig. 5-16 we see that even a small amount of noise results in a large increase in the absolute phase error, and that the phase error is slightly less at locations which are farther away from the Fourier transform plane.

Figure 5-17 is a plot of the relative squared error, $E_I^{(i)}$, for the first 20 iterations at 7.0 Fresnel zones for various amounts of noise. We see from

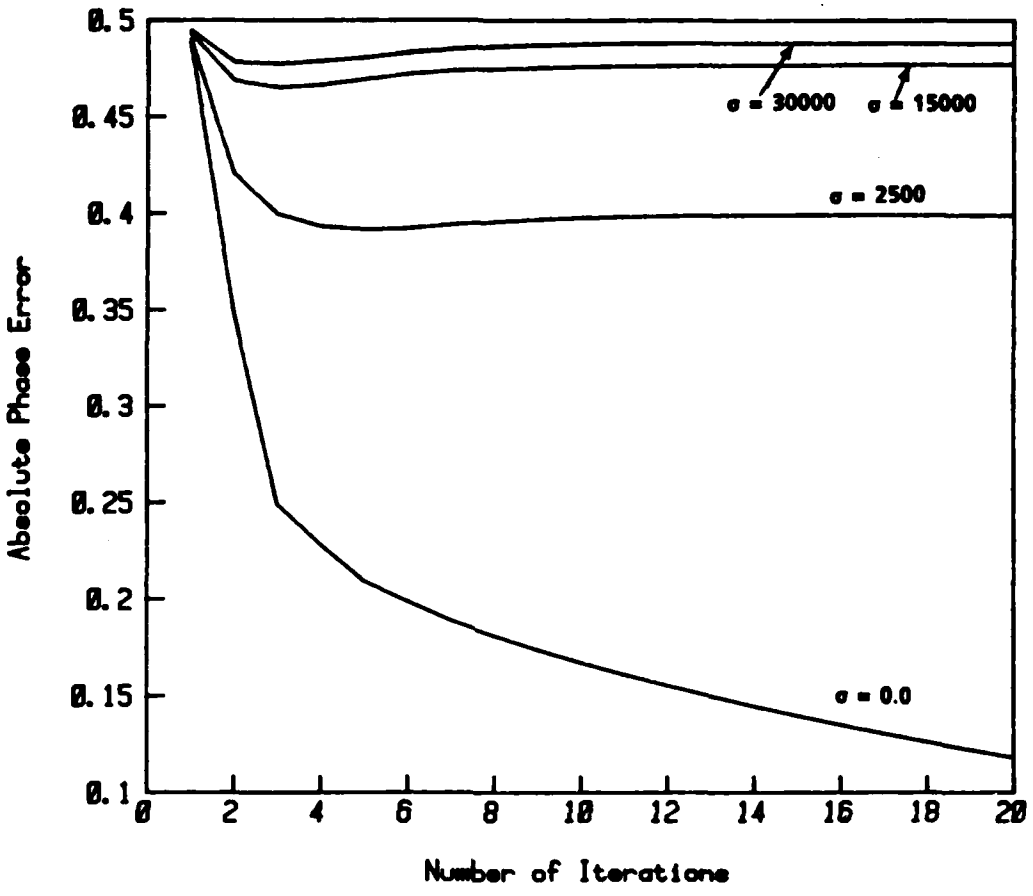

Fig. 5-15 Absolute phase error in the transform plane for 20 iterations at 7.0 Fresnel zones from phase-only data. Errors are shown for cases where the standard deviation of the noise, σ, is equal to 0, 2500, 15000, and 30000.

these plots that the error tends to change the most in the first few iterations and then decrease very slowly. The relative squared error is not very sensitive to the presence of small amounts of noise.

Figure 5-18 is a plot of the average value of the relative squared error from iteration number 15 to iteration number 20 verses the standard deviation of the noise for several different Fresnel zones. From this plot we see that the stagnation value of the relative squared error increases

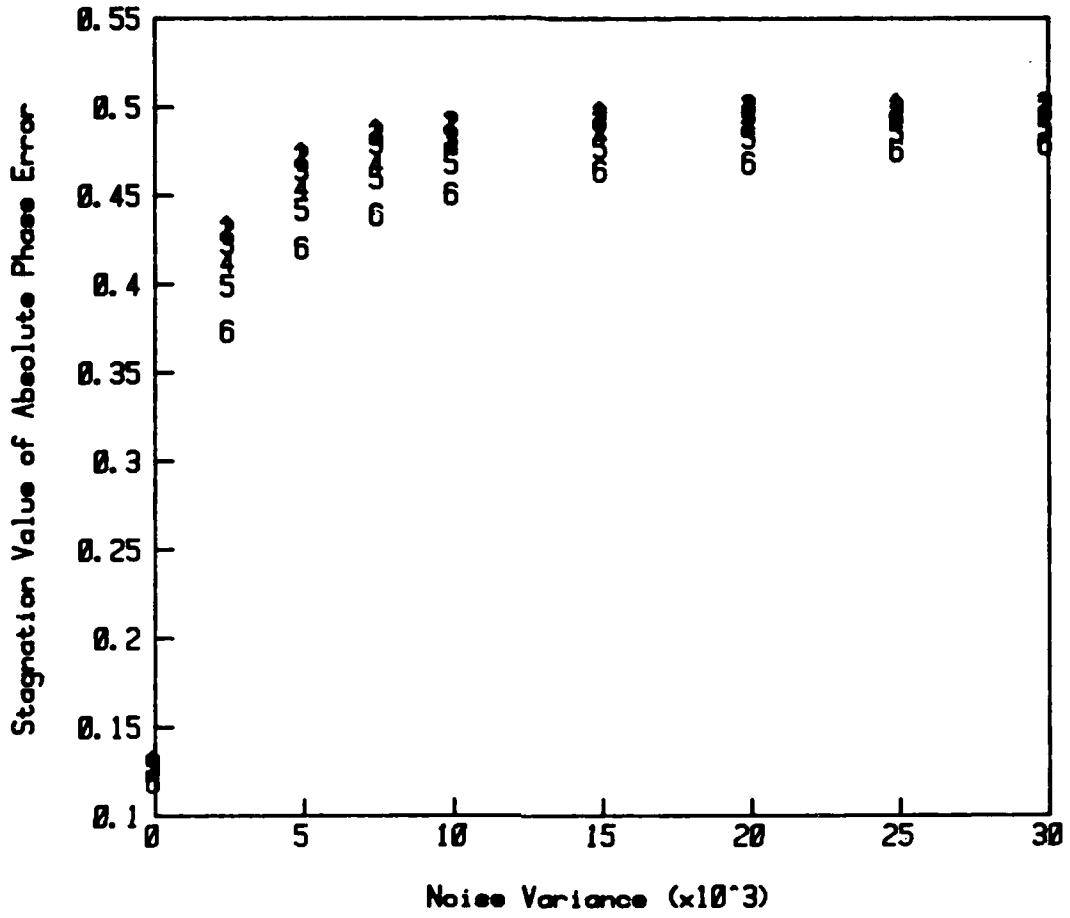

Fig. 5-16 Average value of the absolute phase error in the image plane for iterations 15 through 20 at Fresnel zones equal to 0.0, 0.5, 3.0, 5.0, 7.0, and 10.0 (indicated by the symbols 1-6 respectively). Errors are plotted for cases where the standard deviation of the noise, σ, is equal to 0, 2500, 5000, 7500, 10000, 15000, 20000, 25000, and 30000.

both as the amount of noise increases, and as the number of Fresnel zones increases.

To see how this error in the reconstruction relates to the quality of the reconstructed image, consider the sample of images shown in Figs. 5-19 through 5-21. Figure 5-19 is an example of a reconstruction at 3.0 Fresnel zones after 3 and 20 iterations from data corrupted by noise with

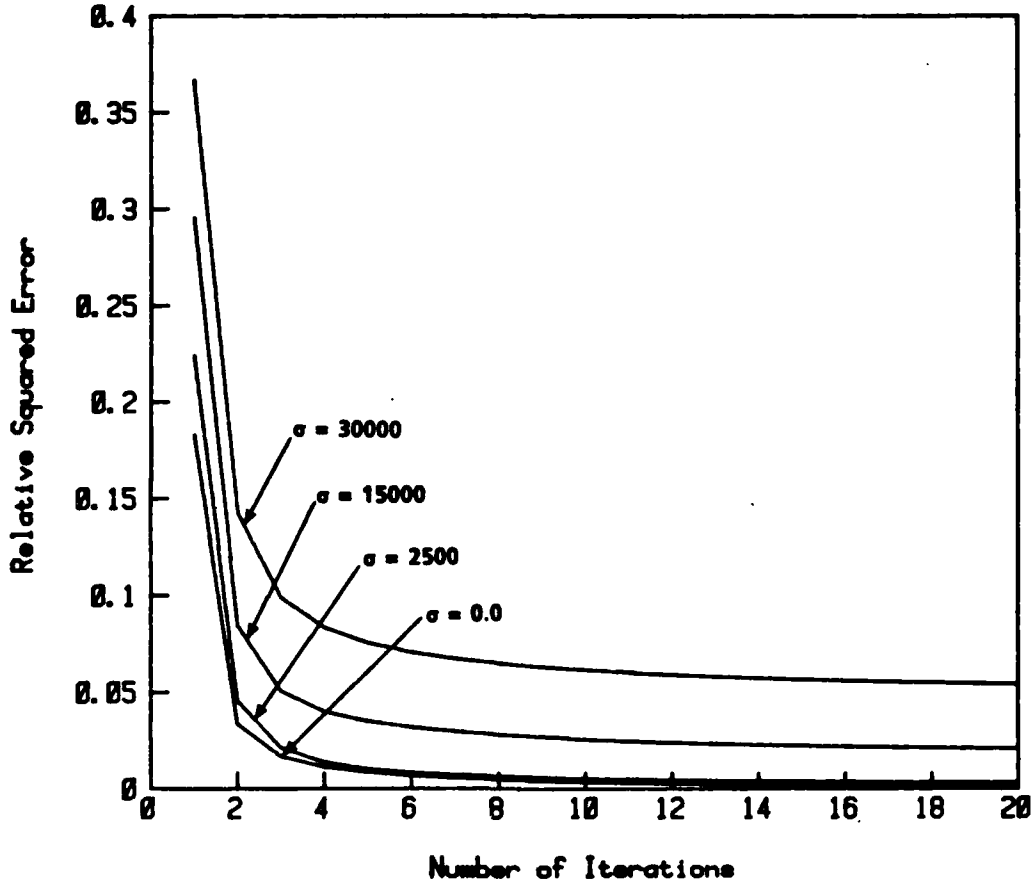

Fig. 5-17 Relative squared error in the image plane for 75 iterations at 7.0 Fresnel zones from phase-only data. Errors are shown for cases where the standard deviation of the noise, σ, is equal to 0, 2500, 15000, and 30000.

deviations of 0, 2500, 15000, and 30000. From these reconstructed images we see that the quality of the reconstruction changes both as the number of iterations increases, and as the amount of noise is increased. Generally, in the first few iterations the fine detail and sharp edges show up with a higher contrast than there is in iteration numbers 10 through 20. The reconstruction procedure is forfeiting some of the high contrast detail in an attempt to remove the low frequency noise ripples. This smoothing of

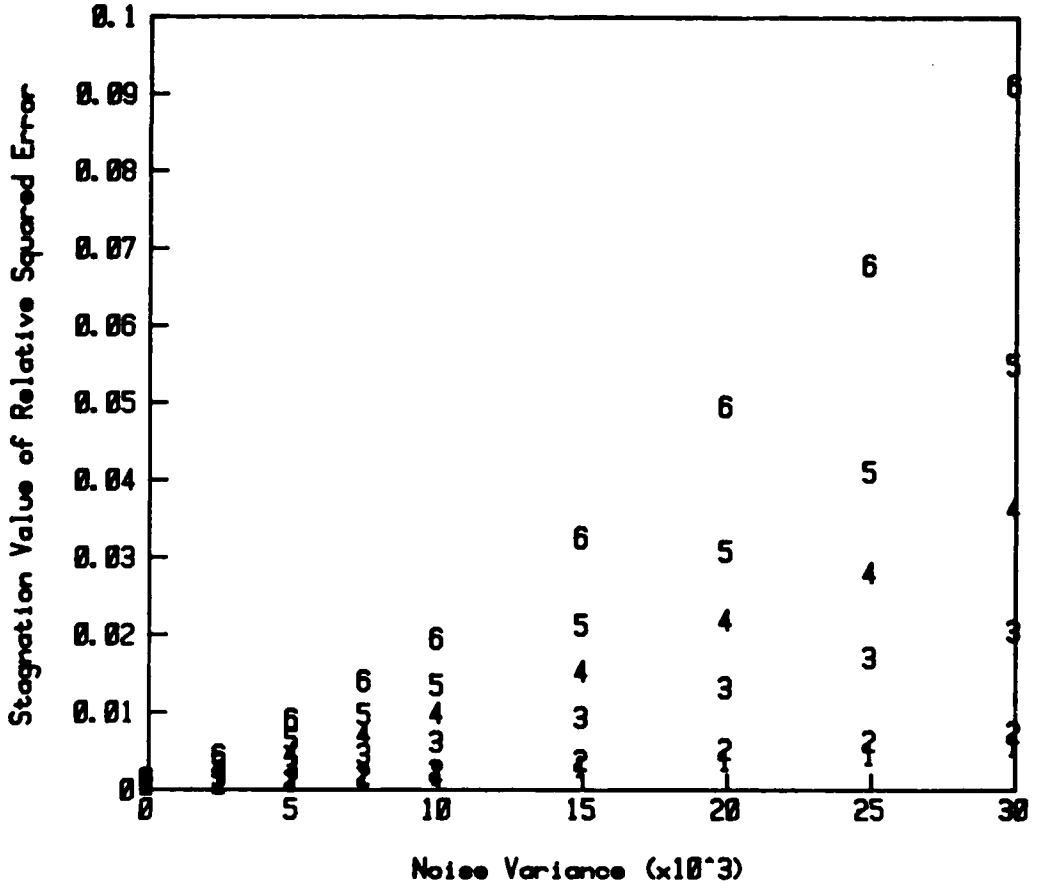

Fig. 5-18 Stagnation level of the relative squared error in phase-only reconstruction for several amounts of noise at different Fresnel zone locations. The plotted symbols 1-6 are for Fresnel zones equal to 0.0, 0.5, 3.0, 5.0, 7.0, and10.0 respectively.

the high contrast detail to satisfy the image plane constraints results in a slight increase in the absolute phase error that is shown in Fig. 5-15. The end result is a blurry but easily recognized image. Even in the presence of large amount of noise, reconstruction from phase-only information yields a surprisingly good reconstructed image.

Figures 5-20 and 5-21 show the same set of images discussed for Fig. 5-19, but the reconstructions for Fig. 5-20 were done at 7.0 Fresnel zones,

and the reconstructions for Fig. 5-21 were done at 10.0 Fresnel zones. From these images we observe that as the number of Fresnel zones increases the reconstruction algorithm is very stable, and indeed is insensitive to the presence of even large amount of noise.

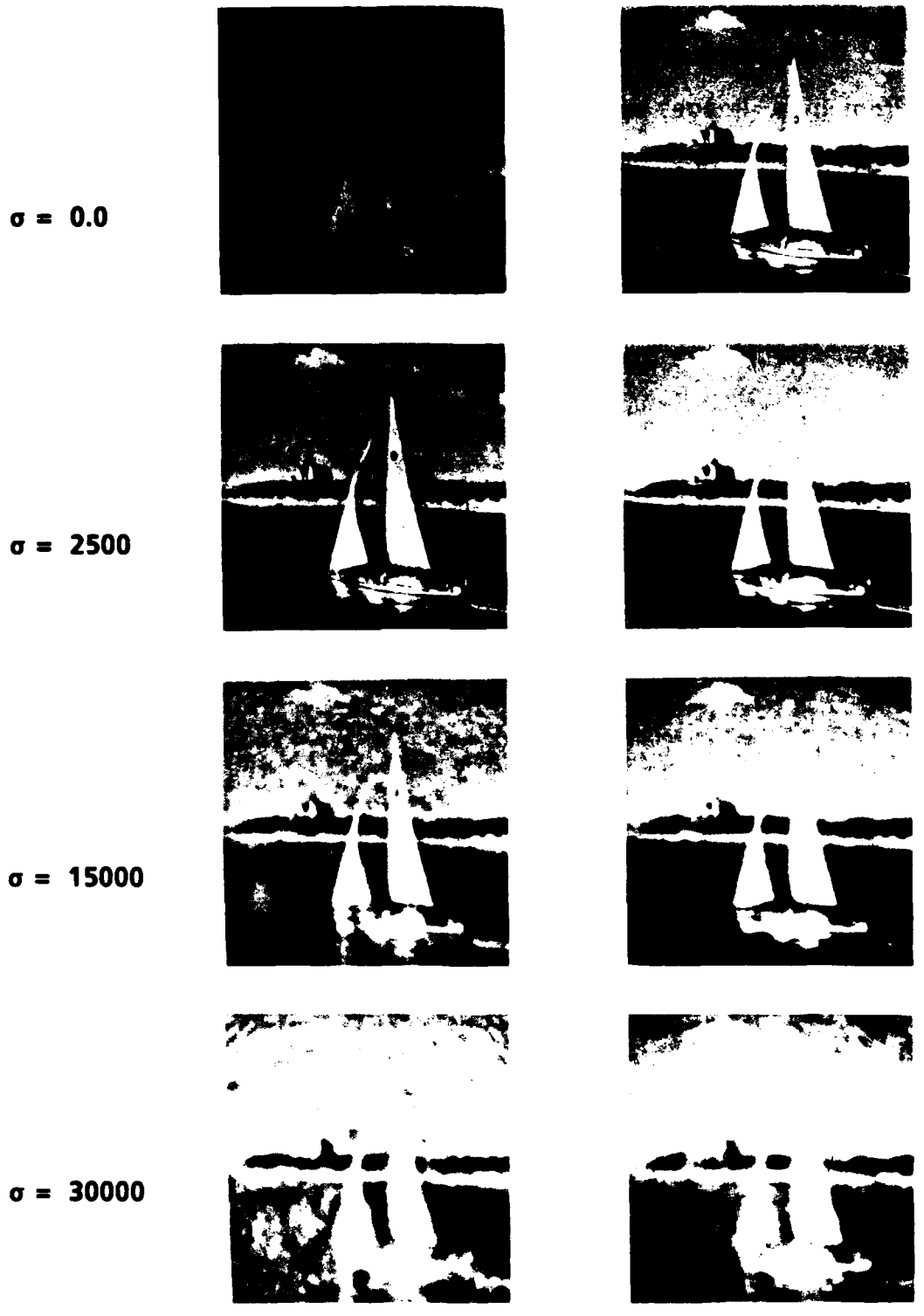

Fig. 5-19 Phase-only reconstructions from noisy data at 3.0 Fresnel zones. The reconstructions are shown after 3 iteration (left) and 20 iterations (right) for various amounts of noise as indicated.

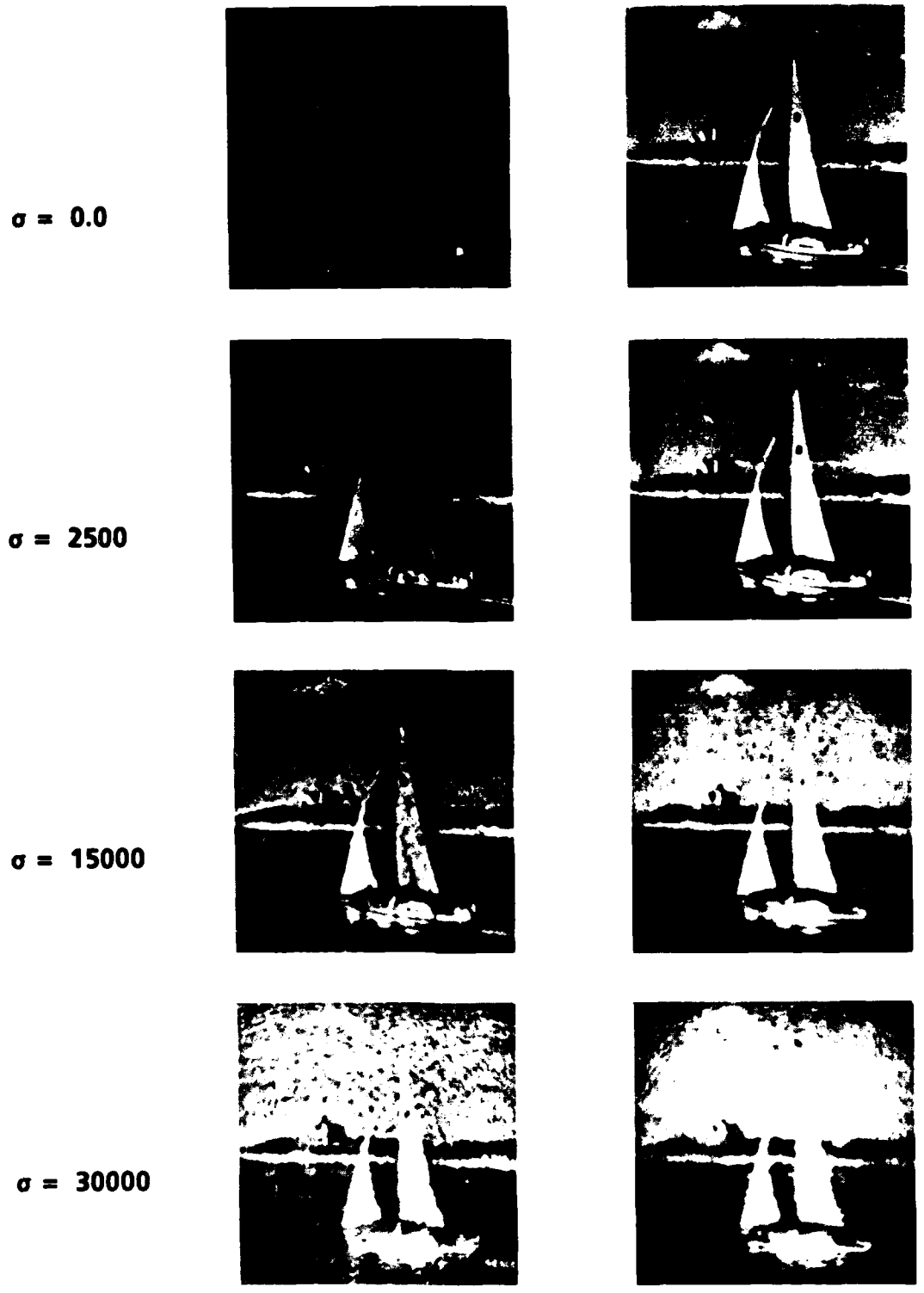

Fig. 5-20 Phase-only reconstructions from noisy data at 7.0 Fresnel zones. The reconstructions are shown after 3 iterations (left) and 20 iterations (right) for various amounts of noise as indicated.

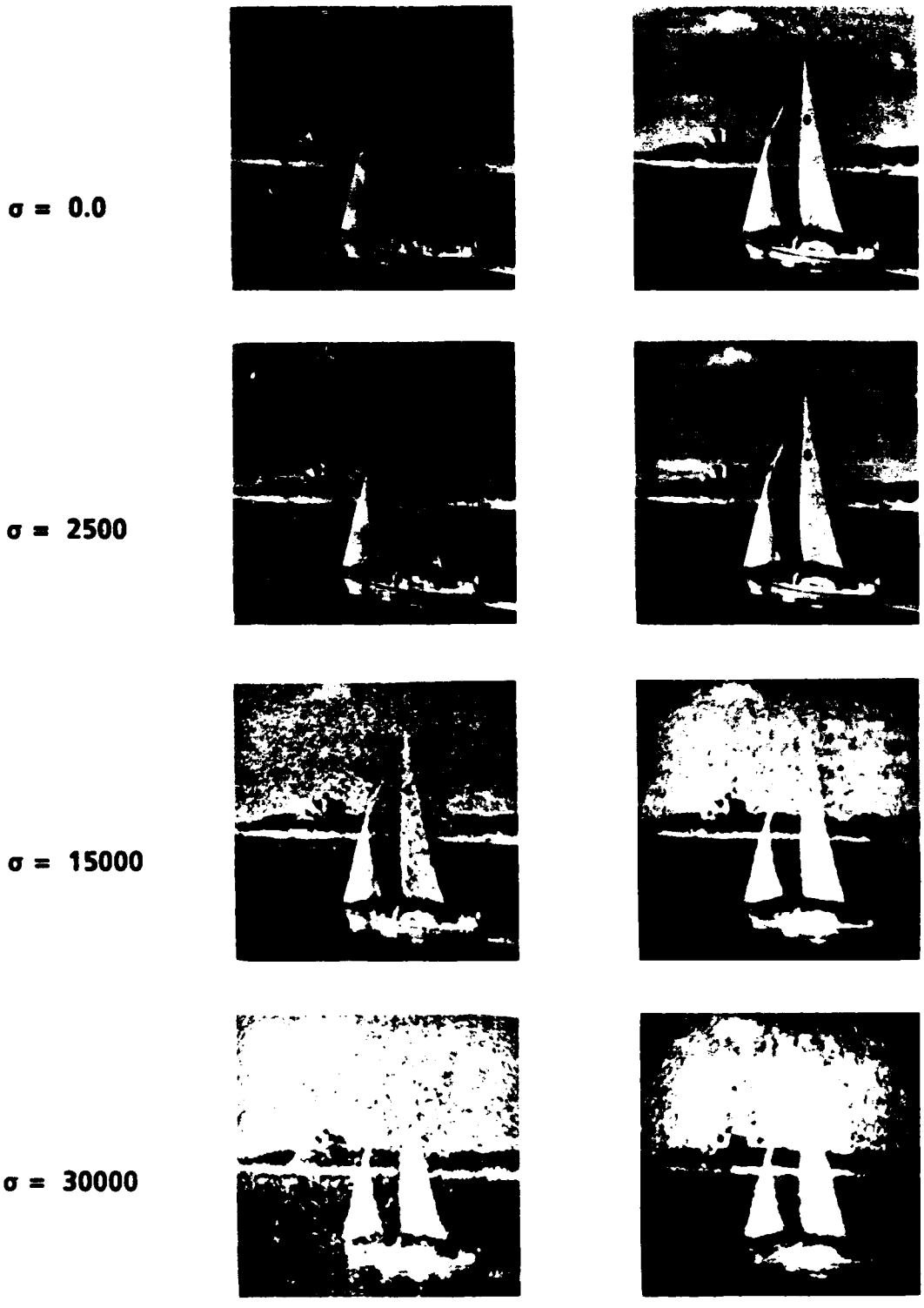

Fig. 5-21 Phase-only reconstructions from noisy data at 10.0 Fresnel zones. The reconstructions are shown after 3 iterations (left) and 20 iterations (right) for various amounts of noise as indicated.

5.4 Coherent, Multiplicative, Signal-dependent Noise

5.4.1. Noise Model

In Sect. 5.2 a model for coherently additive, signal independent, uncorrelated Gaussian noise was developed. In this model, the variance of the noise was independent of the magnitude of the signal at each pixel, and the variance of the noise was a constant over the entire Fresnel zone transform. For the case of signal dependent, or multiplicative, noise, the variance of the noise will depend upon the magnitude of the signal, and thus the variance of the noise will vary across the Fresnel zone transform.

In this multiplicative noise model, a noise signal is multiplied by the magnitude of the true signal, and then added coherently to the true signal. The additive noise signal will be represented as

$$n = \Gamma |w_s| (x + iy) , \qquad (5.4\text{-}1)$$

where x and y are independent, uncorrelated, Gaussian distributed, random variable with zero mean and unit variance, $|w_s|$ is the magnitude of the true signal, and Γ is a scaling factor used to control the signal to noise ratio.

Recording devices such as film or photo-detectors respond to the intensity of the signal, $|w_s|^2$, and the film grain noise or shot noise present in the detection system will have a standard deviation which is proportional to the square root of the detected intensity. Since x and y come from a distribution with unit variance, multiplying by $|w_s|$ will give a noise value with a standard deviation equal to the square root of the intensity. Multiplying the noise by the variable Γ will provide a means of choosing the signal to noise ratio. If the signal intensity is $|w_s|^2$ and the

variance of the noise is $\Gamma^2|w_s|^2$,then the signal to noise ratio will be defined as

$$\frac{S}{N} = \frac{1}{\Gamma^2} \tag{5.4-2}$$

The graphical model and analytic derivations presented in Sect. 5.2 for the case of signal independent additive noise are still valid for the case of signal dependent multiplicative noise. The only difference is that for signal independent noise, the standard deviation of the noise, σ, is an independent variable, and now for the case of signal dependent noise, the standard deviation of the noise is given by:

$$\sigma = \Gamma|w_s| \,, \tag{5.4-3}$$

where Γ is used to vary the amount of noise. The standard deviation of the noise varies from pixel to pixel in the Fresnel zone transform and is equal to the product of Γ and the magnitude of the signal at the given pixel.

The joint probability density function for the magnitude and phase will be

$$f_{b\theta}(b,\theta) = \frac{b}{2\pi(\Gamma s)^2} \exp\left\{ -\left[(b\cos\theta - s)^2 + (b\sin\theta)^2\right] / 2(\Gamma s)^2 \right\} \,, \tag{5.4-4}$$

$$b \geq 0 \text{ and, } -\pi < \theta \leq \pi \,.$$

The probability density function for the measured magnitude, b, is given by

$$f_b(b) = \frac{b}{(\Gamma s)^2} \exp\left\{ -(b^2 + s^2) / 2(\Gamma s)^2 \right\} I_0\left(\frac{b}{s\Gamma^2}\right), \quad b \geq 0 \,, \tag{5.4-5}$$

and the probability density function for the measured phase angle, θ, is given by

$$f_\theta(\theta) = \frac{exp\{-1/2\Gamma^2)}{2\pi} + \frac{cos\theta}{2\Gamma(2\pi)^{\frac{1}{2}}} exp\left\{-(sin\theta)^2/2\Gamma^2\right\}\left[1 + 2\,erf\left(\frac{cos\theta}{\Gamma}\right)\right] \qquad (5.4\text{-}6)$$

$$-\pi < \theta \leq \pi ,$$

The plots for the probability density functions of the magnitude and phase are the same as the plots shown in Figs. 5-4 and 5-6 with the understanding that $\sigma = s\Gamma$ and the parameter $k = s/\sigma$ is to be replaced by $k = 1/\Gamma$.

5.5 Effects of Multiplicative Noise on Image Reconstruction

5.5.1. Magnitude-only Reconstruction

For the model discussed in Sect. 5.4, a signal to noise ratio (S/N) denoted by

$$S/N = 1/\Gamma^2 \ , \tag{5.5-1}$$

where Γ is defined in Eq. (5.4-1) as a method of controlling the signal to noise ratio, has been used. To investigate the effects of noise on reconstructing an image from Fresnel zone magnitude-only data, various amounts of noise were added to the Fresnel zone transform at several different locations. Both a visual inspection of the reconstructed images and an analytic measure of the error in the reconstruction were done.

A measure of how well the reconstruction is progressing in terms of being consistent with the known magnitude information is the absolute error in the transform plane, $E_M^{(i)}$, defined in Eq.(5.3-1). Figure 5-22 is a plot of the absolute error, $E_M^{(i)}$, for the first 75 iterations at 7.0 Fresnel zones for various amounts of noise. We can see from these plots that the error drops sharply in the first two iterations, and then stagnates at a value which is proportional to the amount of noise present in the data. For the case when no noise is present, the error continues to decrease steadily toward zero.

The value at which the error levels off depends upon both the number of Fresnel zones and the signal to noise ratio. Figure 5-23 is a plot of the average value of the absolute error for iterations 50 through 75 for various amounts of noise at several different Fresnel zone locations. The plotted symbols 1-6 correspond to the number of Fresnel zones being

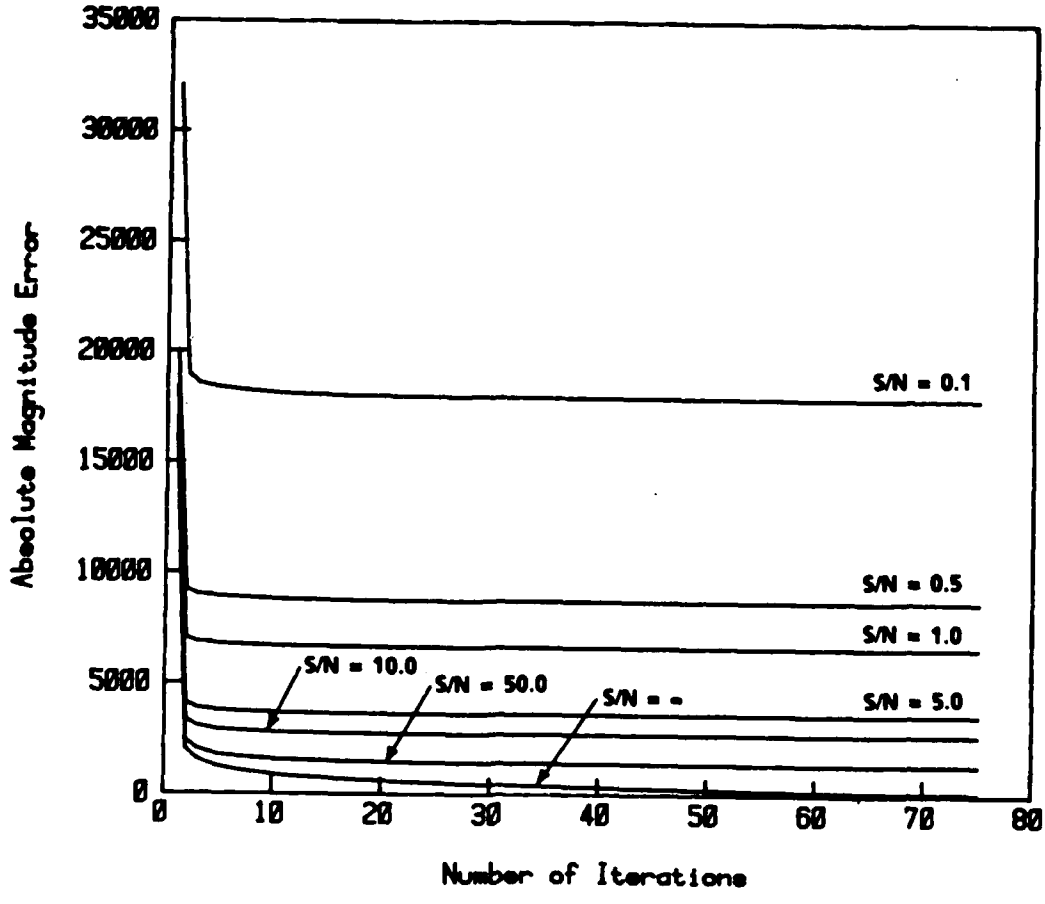

Fig. 5-22 Absolute error between current transform magnitude and measured transform magnitude for magnitude-only reconstruction at 7.0 Fresnel zones. Errors are shown for cases when the signal to noise ratio is equal to ∞, 50.0, 10.0, 5.0, 1.0, 0.5, and 0.1.

equal to 0.0, 0.5, 3.0, 5.0, 7.0, and 10.0 respectively. These errors are plotted for various values of the parameter Γ corresponding to signal to noise ratios of ∞, 50.0, 10.0, 5.0, 1.0, 0.5,and 0.1. From this plot we see that the error level depends both on the signal to noise ratio and on the number of Fresnel zones. The error level increases both with the amount of noise (i.e. a decrease in S/N) and with the number of Fresnel zones.

The error levels plotted in Fig. 5-23 are close to the value of $\Gamma/2$ times the average value of the true transform magnitude data. The average standard deviation of the noise in this signal dependent noise model is Γ times the average value of the transform magnitude data. This error level corresponds very well with the case of signal independent noise, where the error level was found to be approximately equal to $\sigma/2$.

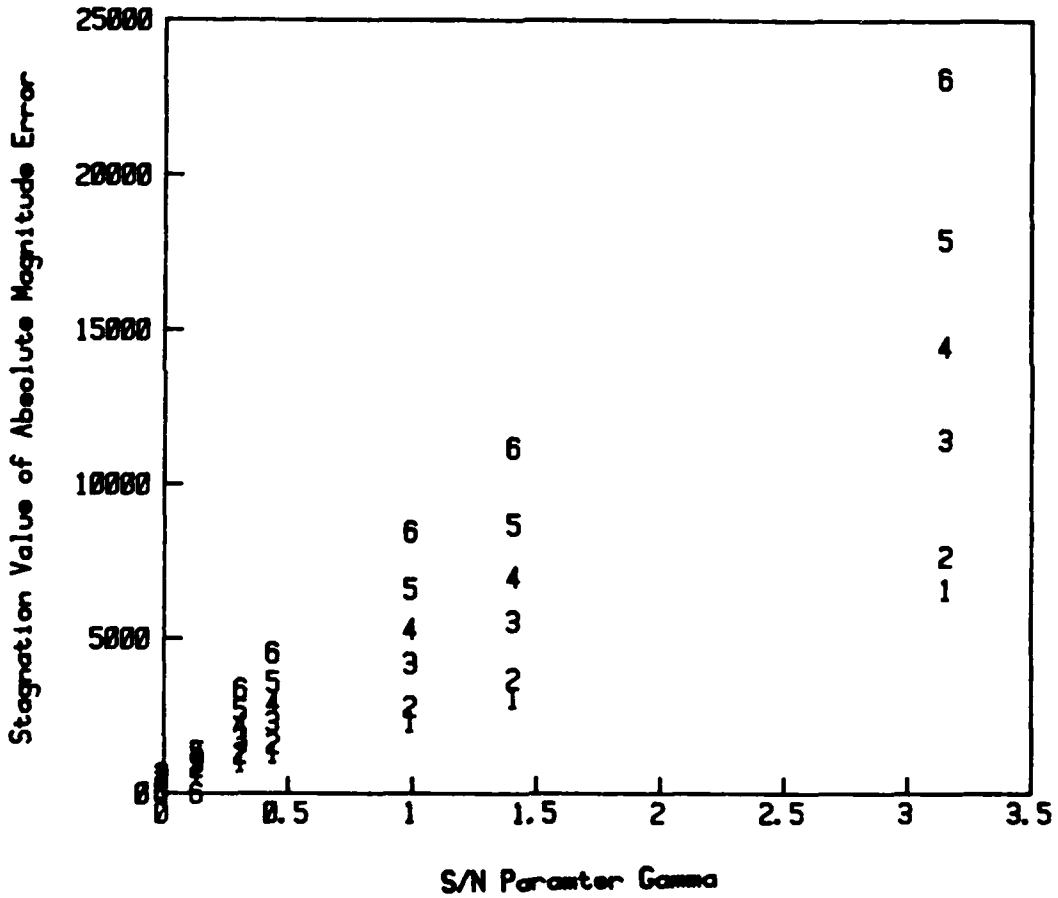

Fig. 5-23 Average values of the absolute error in the magnitude-only reconstruction for iterations 50 through 75 at Fresnel zones equal to 0.0, 0.5, 3.0, 5.0, 7.0, and 10.0 (shown by the characters 1-6 respectivley). Errors are shown for the cases when the signal to noise ratio is equal to ∞, 50.0, 10.0, 3.0, 1.0, 0.5, and 0.1.

For completeness and for comparison with the case of signal independent noise, a plot of the relative squared error in the image plane is shown in Fig. 5-24. The basic structure in these plots; where the error decreases most in the first several iterations, and then levels off to a value which is proportional to the signal to noise ratio, is common to both other realizations of the noise, and to reconstructions at different Fresnel zone locations.

A plot of the stagnation value of the relative squared error in the image plane is shown in Fig. 5-25. For a noise parameter, Γ, which is less than or equal to one (i.e. S/N $\geqq 1.0$) the relative squared error is independent of the number of Fresnel zones. For large amounts of noise (i.e. $\Gamma > 1.$), the error depends both on the number of Fresnel zones and on the signal to noise ratio. The plots shown in Fig, 5-25 represent only one realization for the noise. Different choices for the noise yield error plots which are very similar to Fig, 5-25 for small noise levels, but for large amount of noise the stagnation value of the noise can change by approximately ± 0.1.

To see how the analytic error relates to the visual quality of the reconstructed image, consider the sample of images shown in Figs. 5-26 through 5-28. Figure 5-26 is an example of a reconstruction at 3.0 Fresnel zones after 15 and 75 iterations from data with a signal to noise ratio of ∞, 50.0, 5.0, and 0.1. From these reconstructed images we see that the reconstruction does not change noticeably from iteration 15 to iteration 75, which is consistent with the error plots shown in Figs. 5-22 and 5-24. With a signal to noise ratio of 50.0, the reconstructed image is only slightly

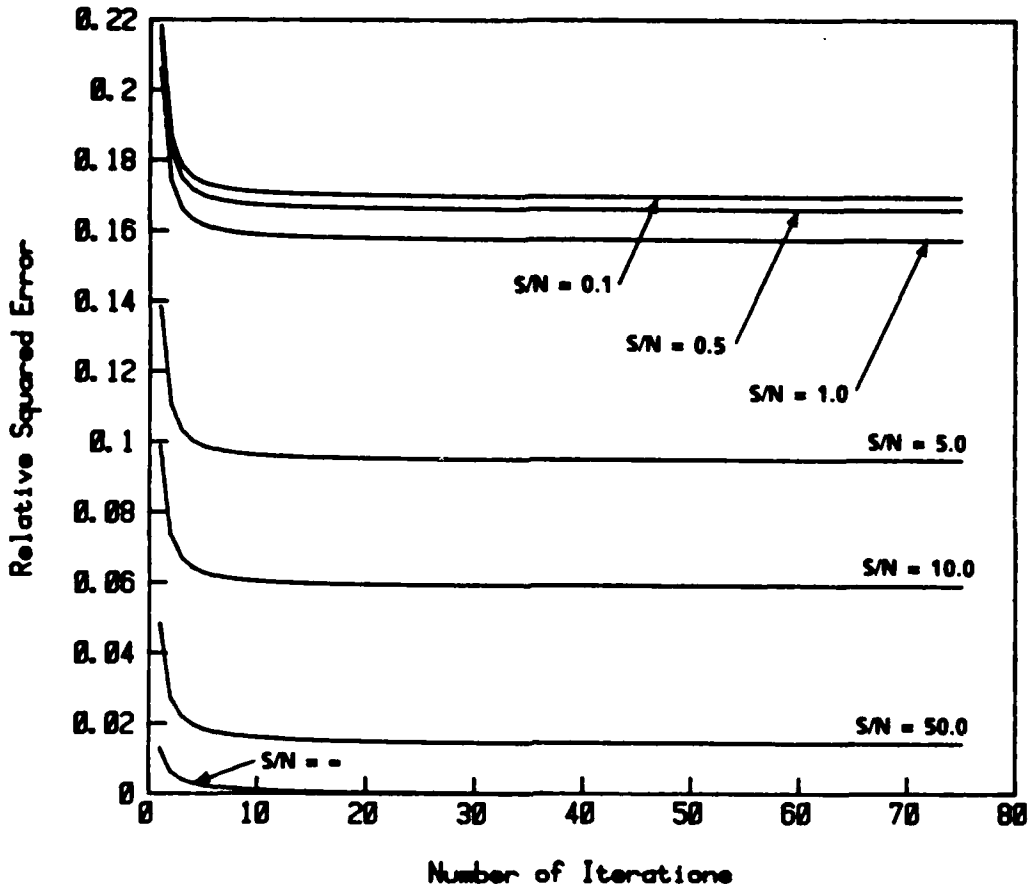

Fig. 5-24 Relative squared error in the image plane for 75 iterations at 7.0 Fresnel zones for magnitude-only reconstuctions. Errors are shown for the cases when the signal to noise ratio is equal to ∞, 50.0, 10.0, 3.0, 1.0, 0.5, and 0.1.

degraded. With a signal to noise ratio of 5.0, the reconstructed image is barely recognizable. With a signal to noise ratio of 0.1, the image is essentially unrecognizable.

Figures 5-27 and 5-28 are the same set of reconstructed images as discussed for Fig. 5-26, but the reconstructions for Fig. 5-27 were done at 7.0 Fresnel zones, and the reconstructions in Fig. 5-28 were done at 10.0 Fresnel zones.

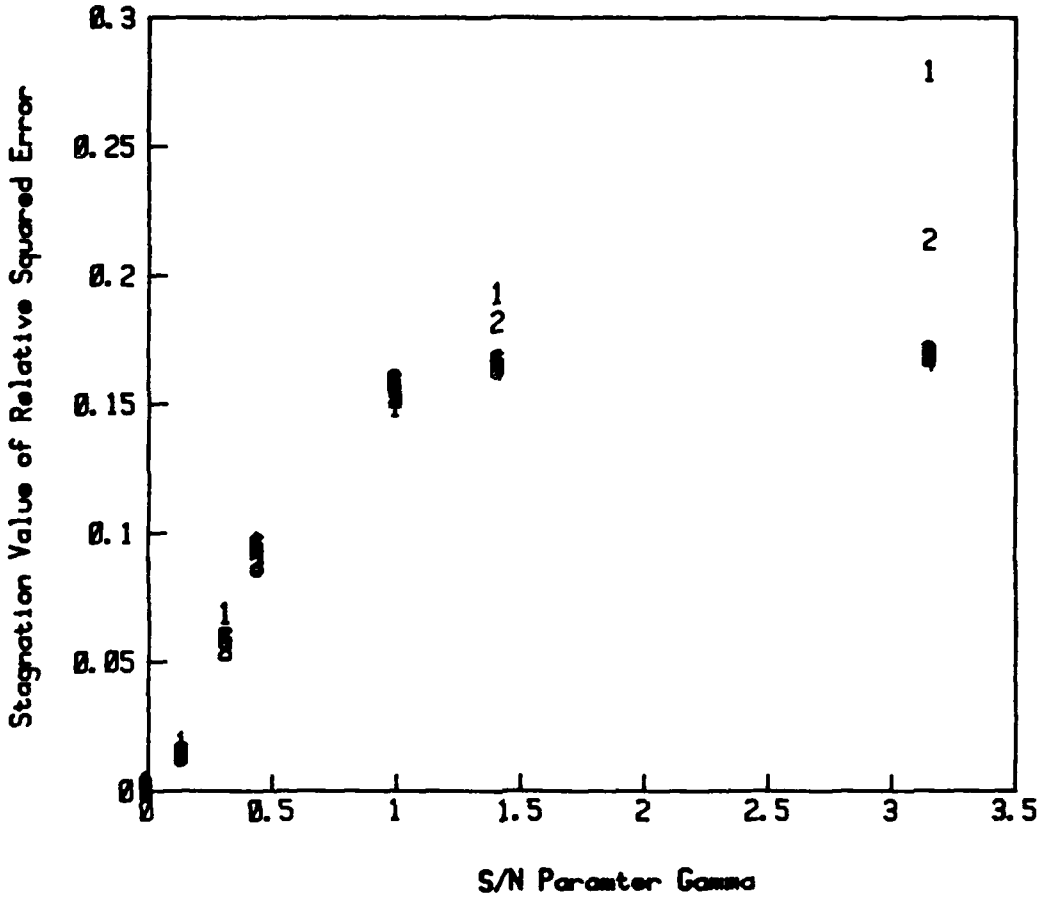

Fig. 5-25 Average values of the relative squared error in the image plane for iterations 50 through 75 at Fresnel zones equal to 0.0, 0.5, 3.0, 5.0, 7.0, and 10.0 (shown by the characters 1-6 respectivley). Errors are shown for the cases when the signal to noise ratio is equal to ∞, 50.0, 10.0, 3.0, 1.0, 0.5, and 0.1.

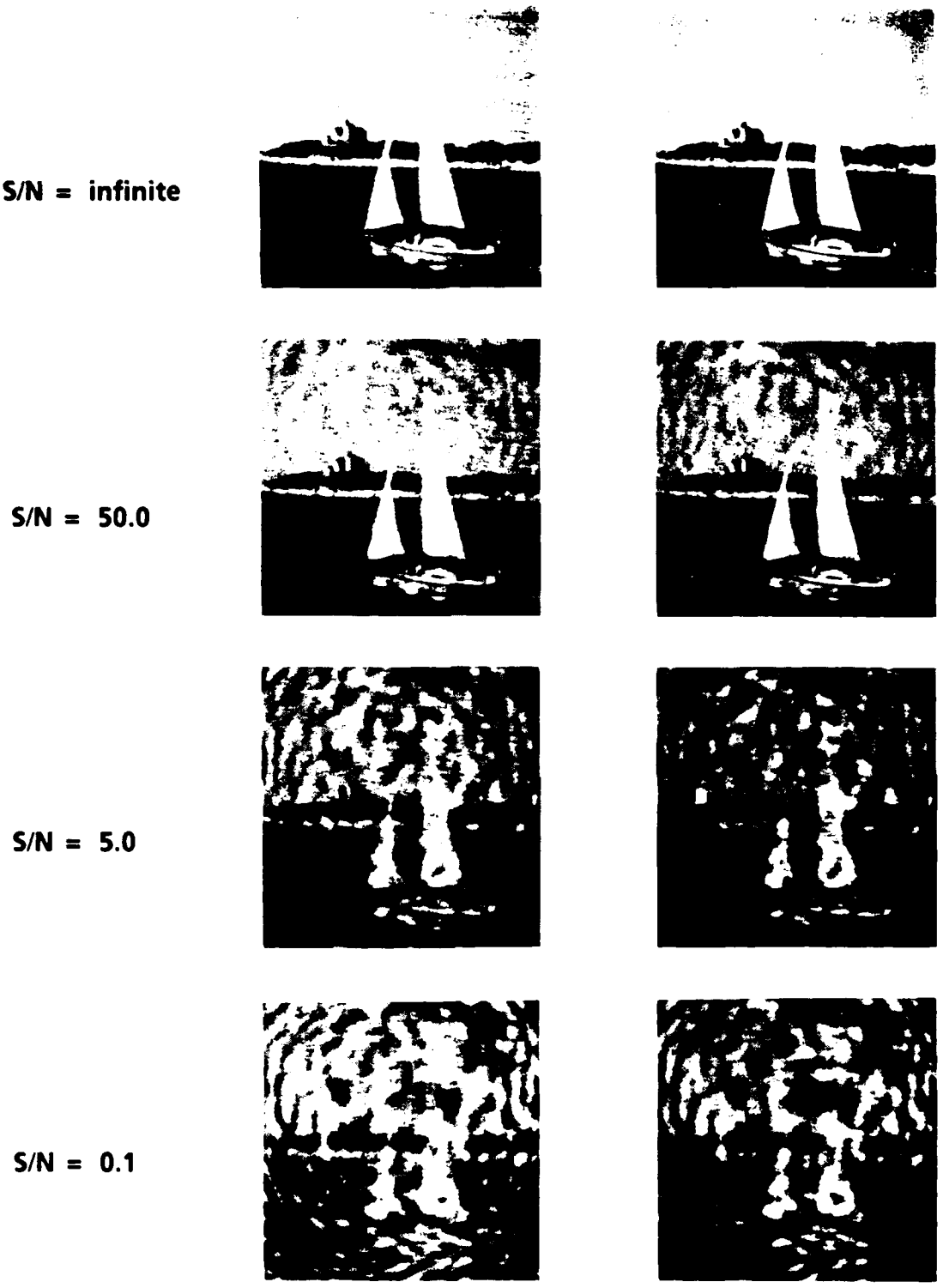

Fig. 5-26 Magnitude-only reconstructions from noisy data at 3.0 Fresnel zones. The reconstructions are shown after 15 iterations (left) and 75 iterations (right) for various signal to noise ratios (S/N) as indicated.

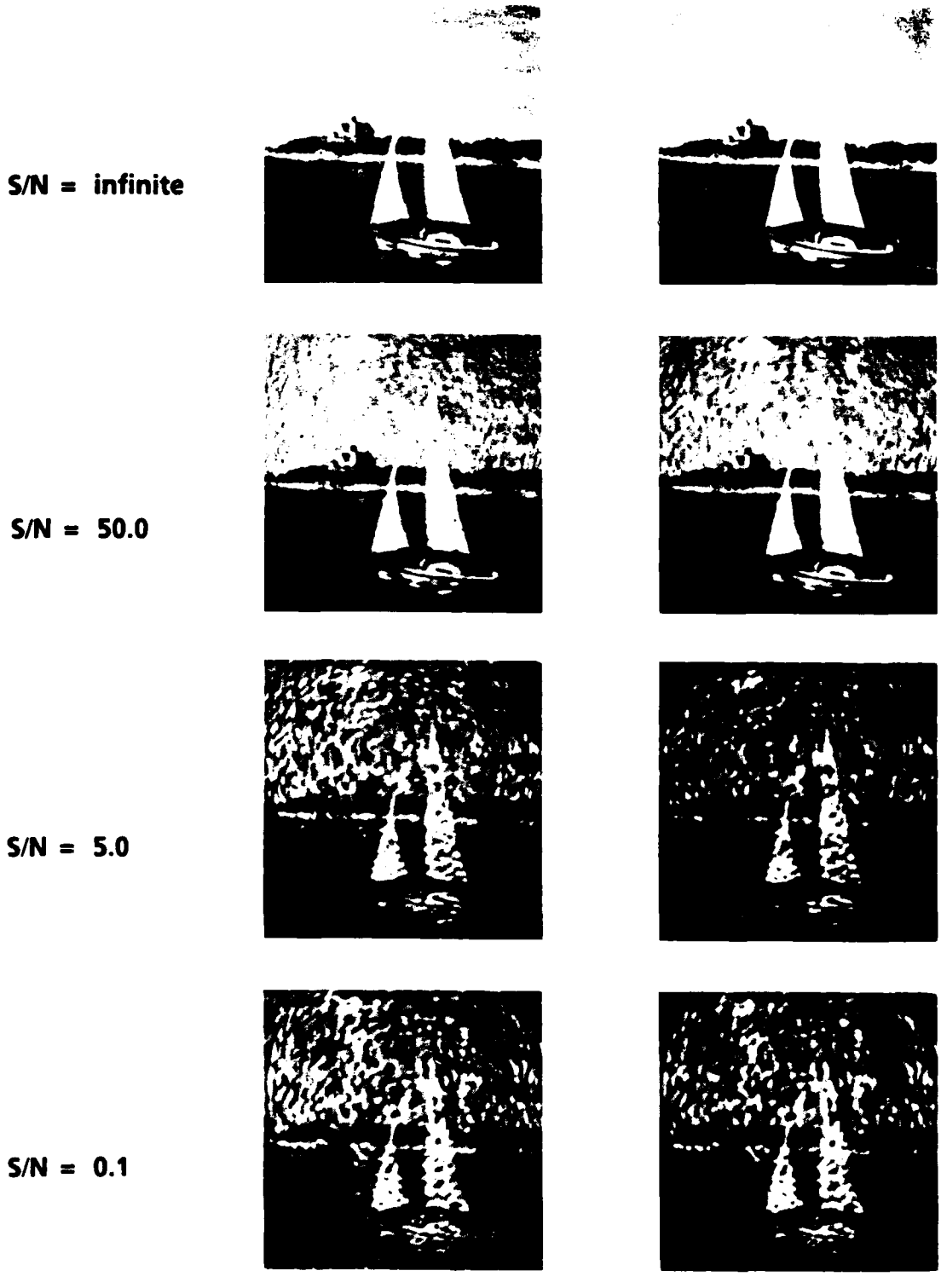

Fig. 5-27 Magnitude-only reconstructions from noisy data at 7.0 Fresnel zones. The reconstructions are shown after 15 iterations (left) and 75 iterations (right) for various signal to noise ratios (S/N) as indicated.

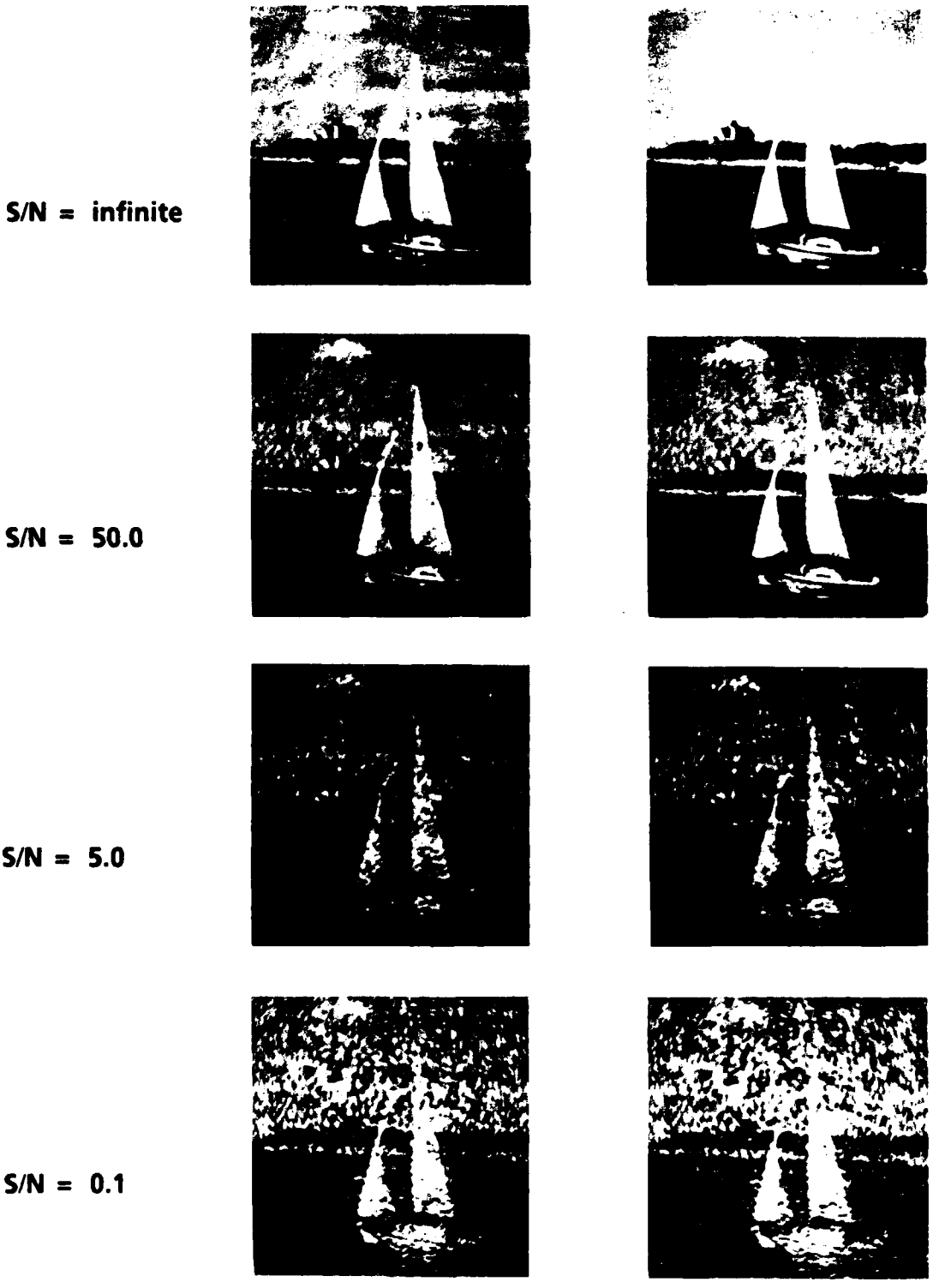

Figure 5-28 Magnitude-only reconstructions from noisy data at 10.0 Fresnel zones. The reconstructions are shown after 15 iterations (left) and 75 iterations (right) for various signal to noise ratios (S/N) as indicated.

5.5.2. Phase-only Reconstruction

To investigate the effects of noise on reconstructing an image from Fresnel zone phase-only data, various amounts of noise were added to the Fresnel zone transform at several different locations. Both a visual inspection of the reconstructed images and an analytic measure of the error in the reconstruction were done.

The absolute phase error in the transform plane, $E_P^{(i)}$, defined in Eq. (5.3-3) and the relative squared error in the image plane, $E_I^{(i)}$, defined in Eq. (5.3-2) were used as analytic measures of the errors during the reconstruction procedure.

Figure 5-29 is a plot of the absolute phase error, $E_P^{(i)}$, for the first 20 iterations at 7.0 Fresnel zones for various signal to noise ratios. The error at the first iteration is approximately .5, and is independent of the amount of noise. The decrease in the error during the first few iterations is indirectly proportional to the amount of noise that is present, when no noise is present the error continues to decrease even after 20 iterations. For the cases with large amounts of noise the error decreases slightly after the first few iterations and then stagnates at a constant value.

A plot of the stagnation values of the absolute phase error for several different Fresnel zones is shown in Fig. 5-30. From this plot we see that for small amounts of noise, the error level is directly proportional to the number of Fresnel zones. When the signal to noise ratio is less than or equal to one (i.e. $\Gamma \geqq 1$.) the error level is independent of the number of Fresnel zones, and in all cases is very close to 0.5. The error in

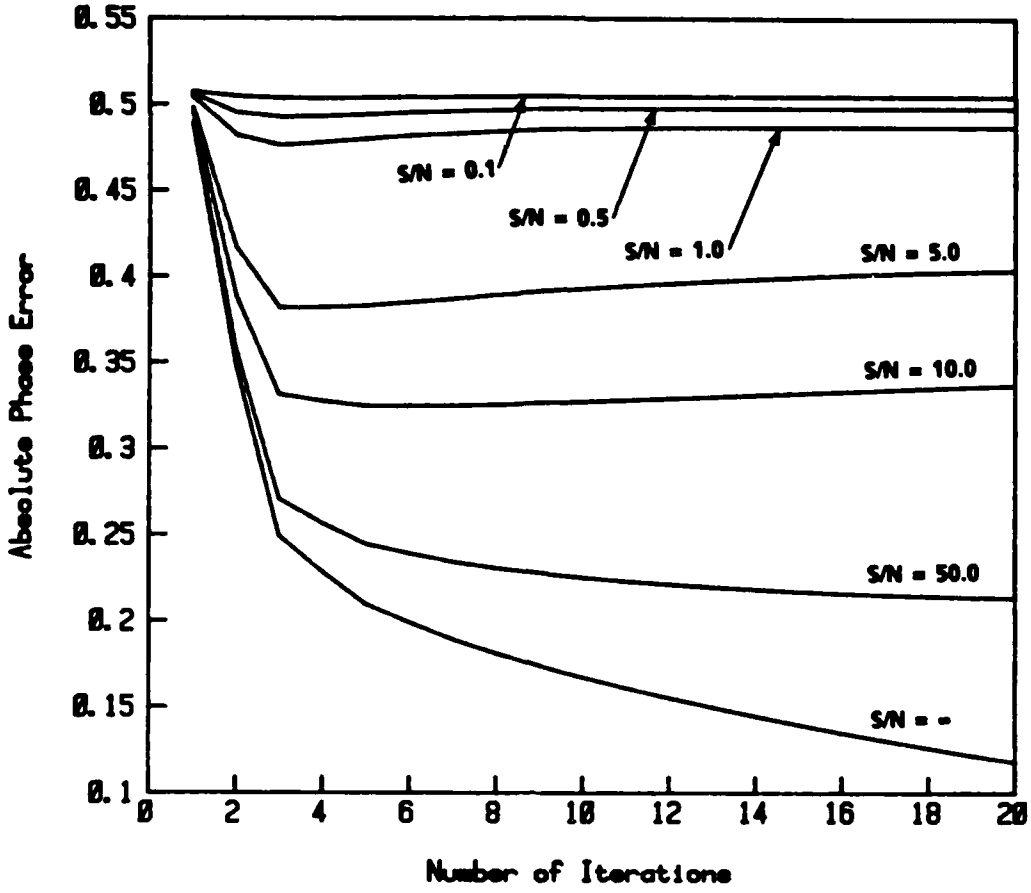

Fig. 5-29 Absolute phase error in the transform plane for 20 iterations at 7.0 Fresnel zones from phase-only data. Errors are shown for cases where the standard deviation of the noise, σ, is equal to 0, 2500, 15000, and 30000.

reconstructing from Fourier transform phase-only data is consistently lower than the error in reconstructing from Fresnel zone phase-only data.

Figure 5-31 is a plot of the relative squared error, $E_I^{(i)}$, for the first 20 iterations at 7.0 Fresnel zones for various signal to noise ratios. In the presence of noise the error decreases for the first few iterations, and then stagnates at a level which is indirectly proportional to the signal to noise ratio.

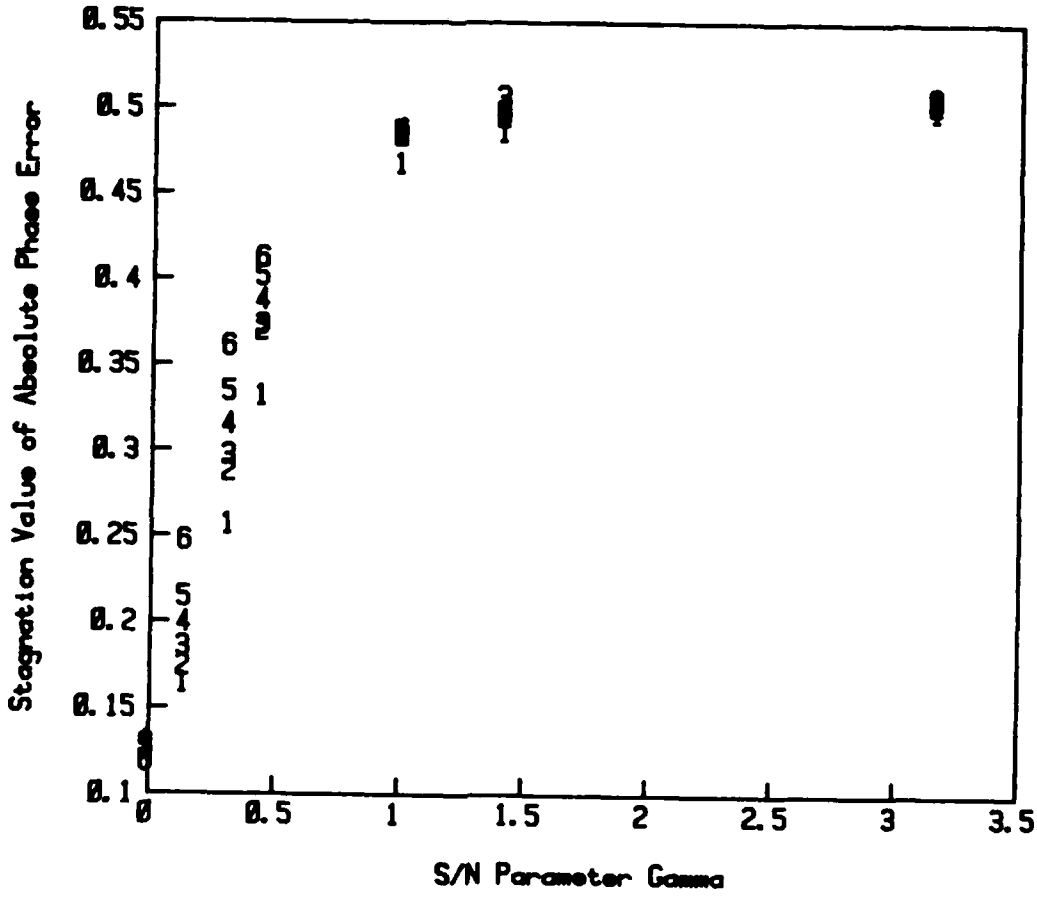

Fig. 5-30 Average values of the absolute phase error for iterations 15 through 20 at Fresnel zones equal to 0.0, 0.5, 3.0, 5.0, 7.0, and 10.0 (shown by the characters 1-6 respectivley). Errors are shown for the cases when the signal to noise ratio is equal to ∞, 50.0, 10.0, 3.0, 1.0, 0.5, and 0.1.

A plot of the stagnation values of the relative squared error for several different Fresnel zones is shown in Fig. 5-32. For the cases when the signal to noise parameter, Γ, is greater than or equal to .5, the error is slightly less in the Fourier transform plane. When the parameter Γ is less than .5, the stagnation level of the error is independent of the number of Fresnel zones.

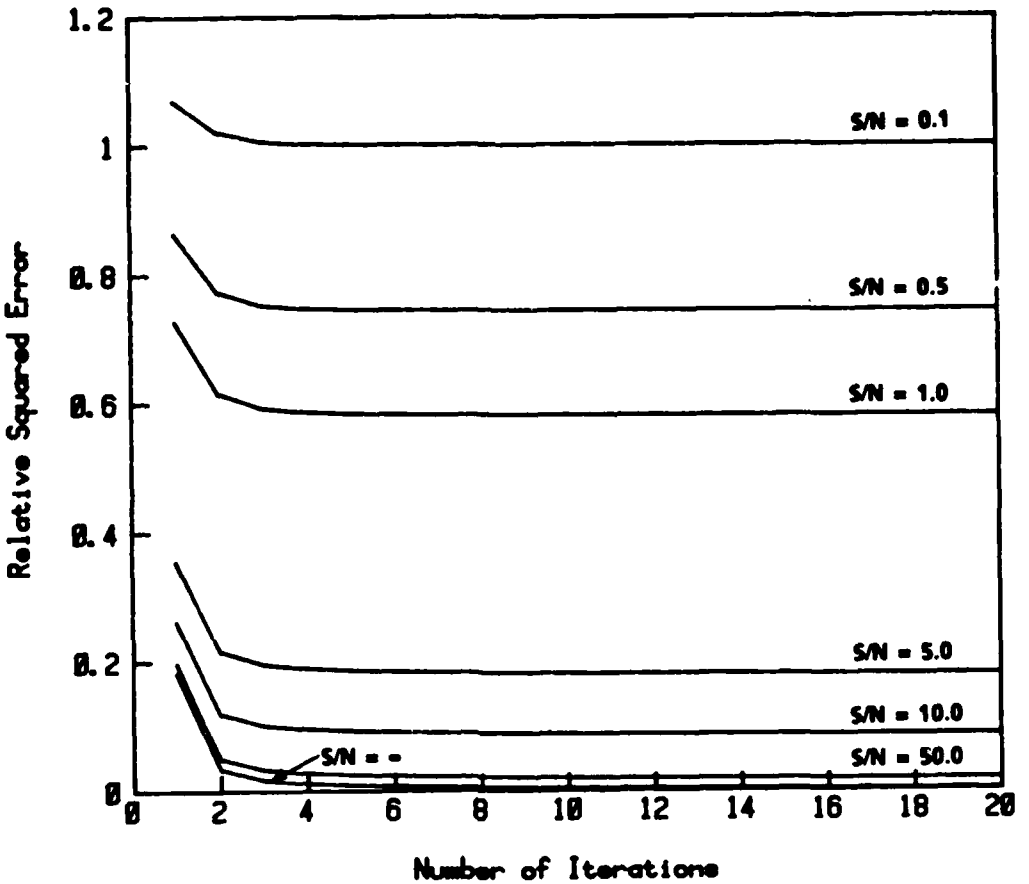

Fig. 5-31 Relative squared error in the image plane for 20 iterations at 7.0 Fresnel zones for phase-only reconstructions. Errors are shown for the cases when the signal to noise ratio is equal to ∞, 50.0, 5.0, and 0.1.

To see how this error in the reconstruction relates to the quality of the reconstructed image, consider the sample of images shown in Figs. 5-33 through 5-35. Figure 5-33 is an example of a reconstruction at 3.0 Fresnel zones after 3 and 20 iterations from data corrupted by noise with signal to noise ratio of ∞, 50.0, 5.0, and 0.1.. From these reconstructed images we see that the quality of the reconstruction changes both as the number of iterations increases, and as the amount of noise is increased. Generally, in

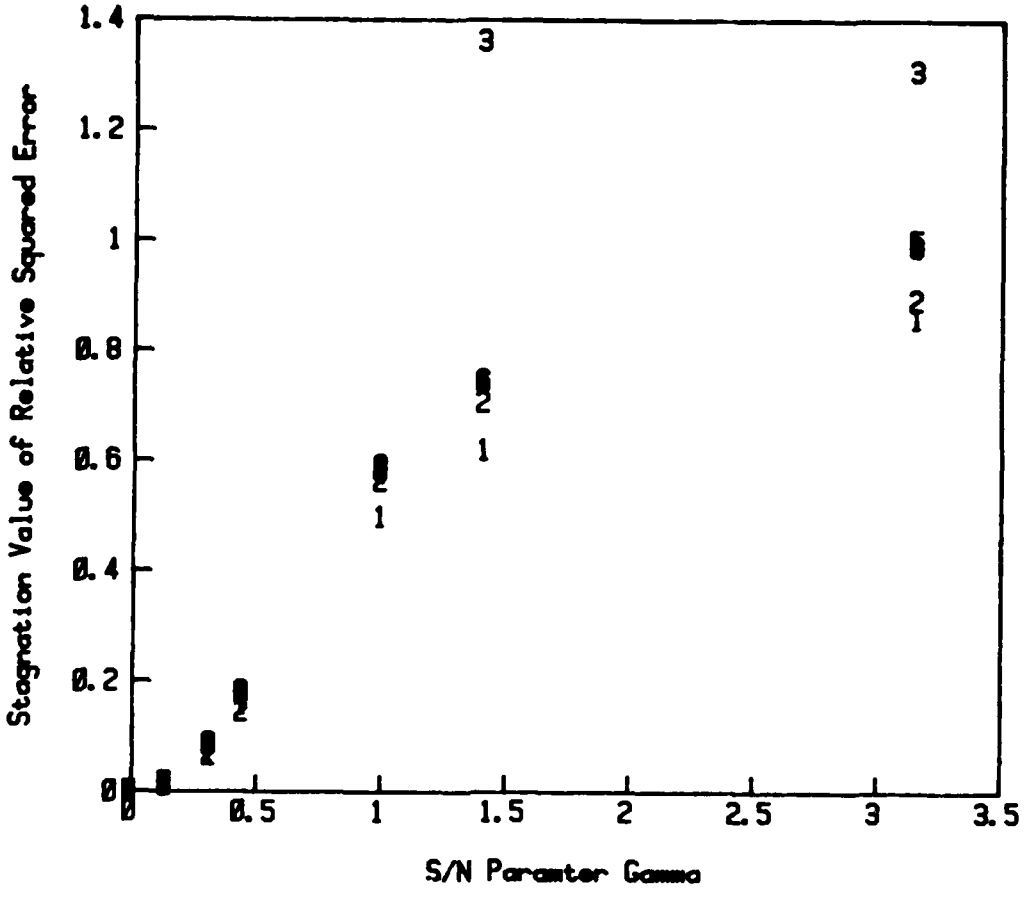

Fig. 5-32 Average value of the relative squared error in the image plane for iterations 15 through 20 at Fresnel zones equal to 0.0, 0.5, 3.0, 5.0, 7.0, and 10.0 (indicated by the characters 1-6 respectively). Errors are plotted for the cases when the siganl to noise ratio is equal to ∞, 50.0, 5.0, and 0.1.

the first few iterations the fine detail and sharp edges show up with a higher contrast than there is in iteration numbers 10 through 20. The reconstruction procedure is forfeiting some of the high contrast detail in an attempt to remove the low frequency noise ripples.

Figures 5-34 and 5-35 are the same set of images discussed for Fig. 5-33, but the reconstructions for Fig. 5-34 were done at 7.0 Fresnel zones, and

the reconstructions for Fig. 5-35 were done at 10.0 Fresnel zones. From these images we observe that as the number of Fresnel zones increases the reconstruction algorithm is very stable,and indeed is very insensitive to the presence of even large amount of noise.

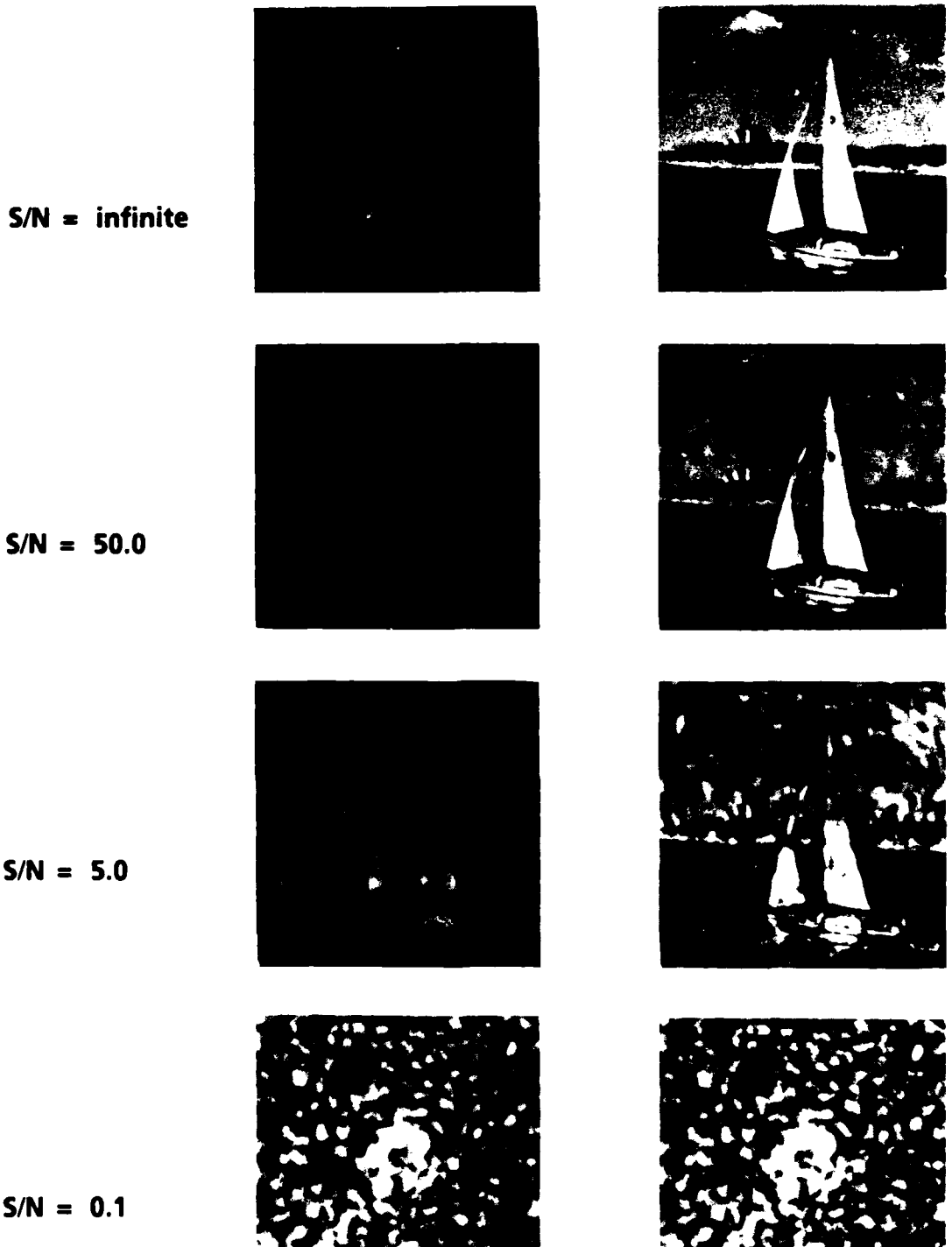

Fig. 5-33 Phase-only reconstructions from noisy data at 3.0 Fresnel zones. The reconstructions are shown after 3 iteration (left) and 20 iterations (right) for various signal to noise ratios as indicated.

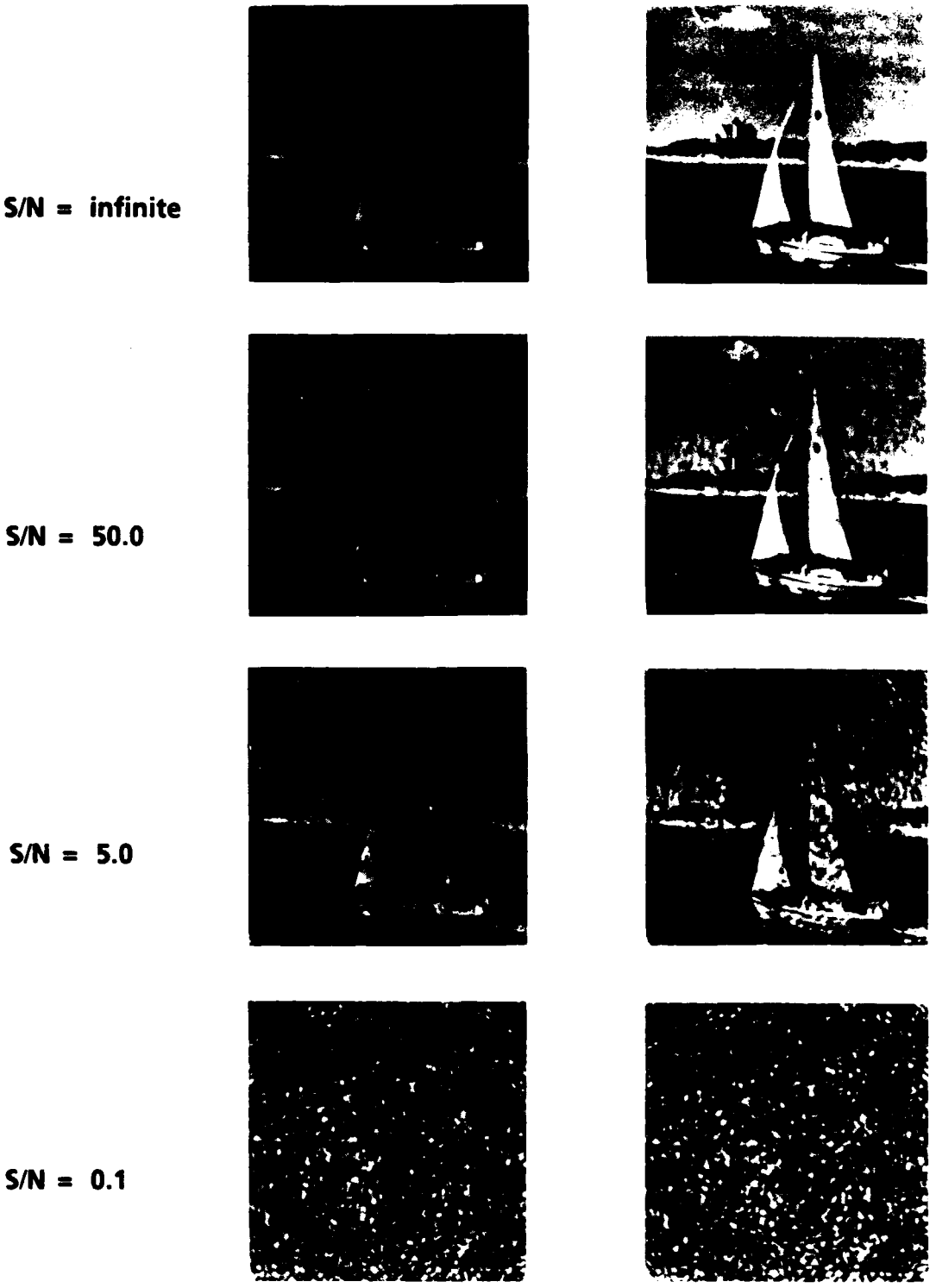

Fig. 5-34 Phase-only reconstructions from noisy data at 7.0 Fresnel zones. The reconstructions are shown after 3 iterations (left) and 20 iterations (right) for various signal to noise ratios as indicated.

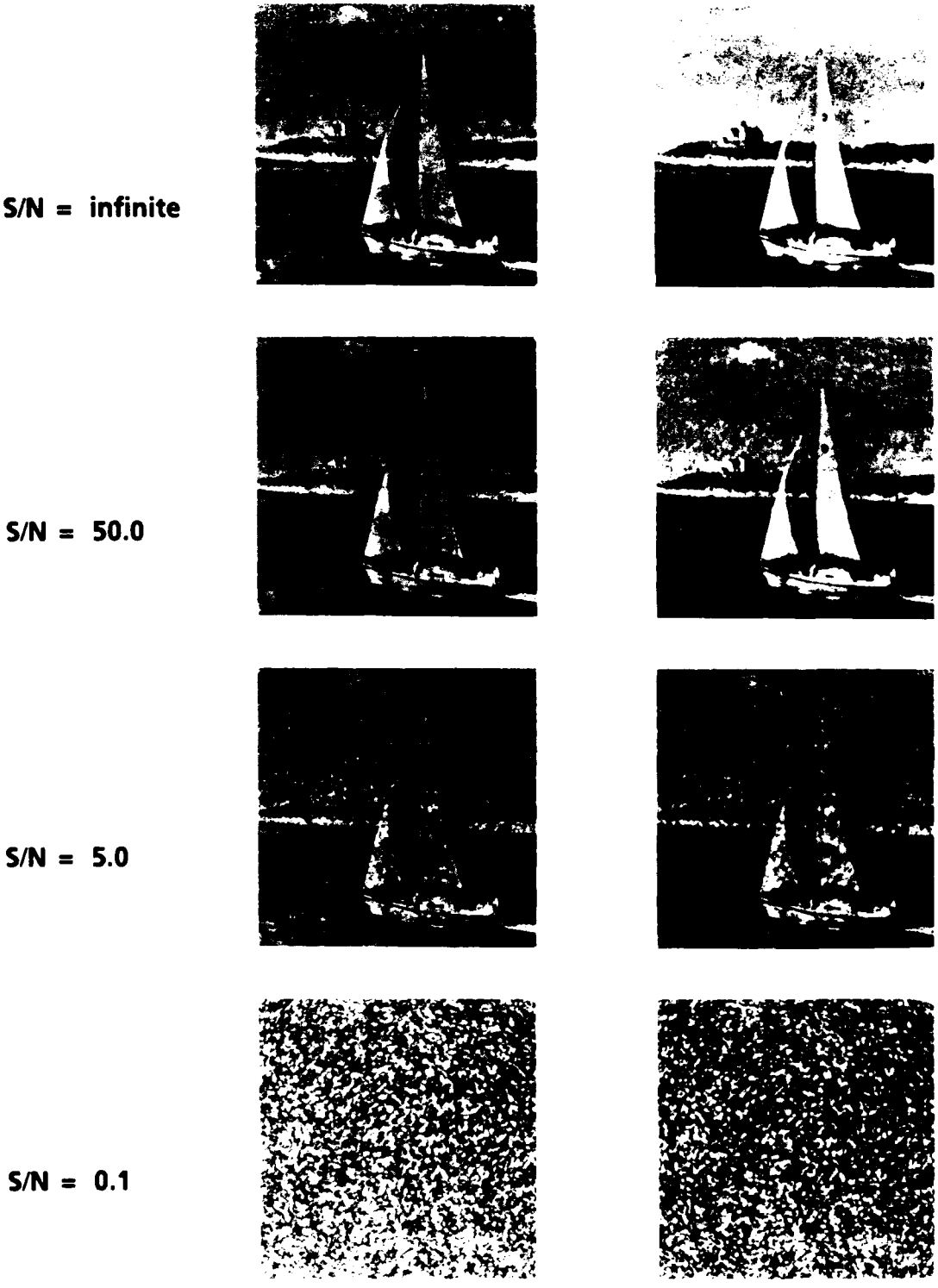

Fig. 5-35 Phase-only reconstructions from noisy data at 10.0 Fresnel zones. The reconstructions are shown after 3 iterations (left) and 20 iterations (right) for various signal to noise ratios as indicated.

Chapter Six

Effects of an Error in the Number of Fresnel Zones

6.1 Introduction

Up to this point, the reconstruction algorithms have assumed that the number of Fresnel zones, Z_F, is a known quantity. The number of Fresnel zones is connected to the distance out of the Fourier transform plane by the relation

$$Z_F = \left(1 - \frac{d_1}{F}\right) \frac{1}{2\lambda F} \left(\frac{NT}{2}\right)^2 , \qquad (6.1\text{-}1)$$

where d_1 is the distance behind the lens (see Fig. 2-1), F is the focal length of the lens, λ is the wavelength, N is the number of sample points, and T is the sampling interval. From this equation we can see that if the distance d_1 is given incorrectly, the result is an error in the parameter Z_F. An error similar to this was also discussed by Childs and Misell [1973] for the case of an error in the amount of defocus in image deconvolution, where it was discovered that "the use of the correct defocus value is extremely important."

An incorrect value of d_1 could be the result of experimental error, where the distance is either measured incorrectly, or can not be measured accurately. In these cases, one should be able to estimate a value for Z_F, but would like to know the effects of having to use an estimated value.

Section 6.2 will examine the effects upon the reconstructed images of this type of error in the reconstruction process.

A different problem exists when the given information, either magnitude-only or phase-only data, is from an unknown location in the Fresnel zone region. This may be the case when the distance d_1 is simply unavailable for measurement. An alternate possibility is that the data has been purposely encrypted by a method similar to the technique suggested by VanderLught [1985]. Section 6.3 will describe a method of searching through the Fresnel zone region, and thus reconstruct an image from partial data at an unknown location in the Fresnel region.

6.2 Use of Incorrect Number of Fresnel Zones

As discussed in Chapter 2, the reconstruction algorithms require the use of a complex Gaussian phase term, $\exp\{-i\pi\alpha_1(x^2 + y^2)\}$. This complex Gaussian is not needed for an inverse Fresnel zone transform if the object is known to be real and non-negative, but this term is crucial to the calculation of the forward Fresnel zone transform of an image. This section will investigate the effects of using an estimate for the number of Fresnel zones, that is, the value of Z_F used in the reconstruction algorithm is nearly equal to the value of Z_F which gave rise to the given partial information.

Figure 6-1 is the original 256 X 256 X 8-bit image. The corresponding

Fig. 6-1. The original digitized image, 256 X 256 X 8-bits.

magnitudes of the Fresnel zone transforms at 7.3, 7.7, and 8.1 Fresnel zones are shown in Figs. 6-2(a), (b), and (c) respectively. The phases of the Fresnel zone transforms at 7.3, 7.7, and 8.1 Fresnel zones are shown in

(a) Z_F = 7.3

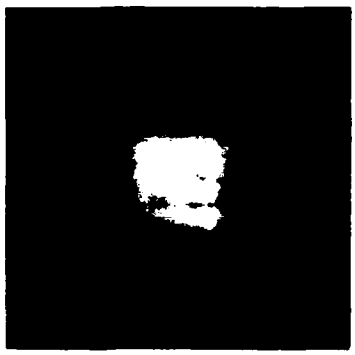

(b) Z_F = 7.7

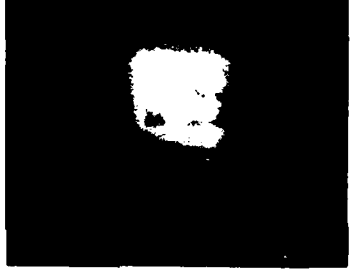

(c) Z_F = 8.1

Fig. 6-2. Magnitude of the Fresnel zone transforms at (a)7.3, (b)7.7, and (c)8.1 Fresnel zones

Figs. 6-3(a), (b), and (c) respectively. The Fresnel zone values of 7.3 and 8.1 correspond to differences of approximately 5% from the central value of 7.7 Fresnel zones. From Figs. 2-4 and 2-9 it is seen that for a given image, both the phase and magnitude of the Fresnel zone transform depend upon the number of Fresnel zones. The change in the phase and magnitude as one moves through the Fresnel zone region is a smooth and gradual transition. While there is a visually discernable difference in the Fresnel zone transforms from locations far apart in the Fresnel zone region, the change is slight for locations near one another in the Fresnel zone region. Note that the magnitudes and phases shown in Figs. 6-2 and 6-3 differ only slightly for the different values of the number of Fresnel zones.

6.2.2 Phase-only Reconstruction

To examine the sensitivity of the reconstruction algorithm, three reconstructions using phase-only data from 7.7 Fresnel zones were performed. The parameter Z_F was set equal to 7.3, 7.7 and 8.1 for each of the attempted reconstructions. The values of 7.3 and 8.1 correspond to the case when data was actually obtained at 7.7 Fresnel zones, but the data is incorrectly assumed to be the result of a Fresnel zone transform which differs by 5% from the correct value. Figures 6-4(a), (b), and (c) are the results of these phase-only reconstructions after 10 iterations. Note that there is still a recognizable image reconstructed but the quality of the reconstruction is below that which is obtained when the correct number of Fresnel zones is used.

(a) $Z_F = 7.3$

(b) $Z_F = 7.7$

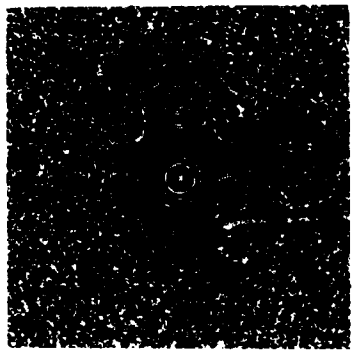

(c) $Z_F = 8.1$

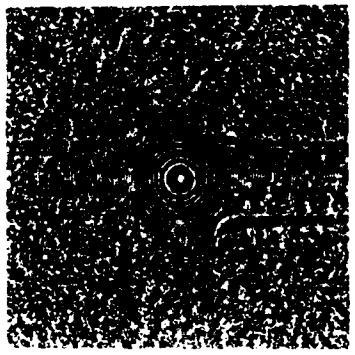

Fig. 6-3. Phase of the Fresnel zone transforms at (a)7.3, (b)7.7, and (c)8.1 Fresnel zones

(a) $Z_F = 7.3$

(b) $Z_F = 7.7$

(c) $Z_F = 8.1$

Fig. 6-4. The phase-only reconstructions after 10 iterations using (a) $Z_F = 7.3$, (b) $Z_F = 7.7$, and (c) $Z_F = 8.1$.

Figure 6-5 is a plot of the errors in the transform plane, E_P, for the 10

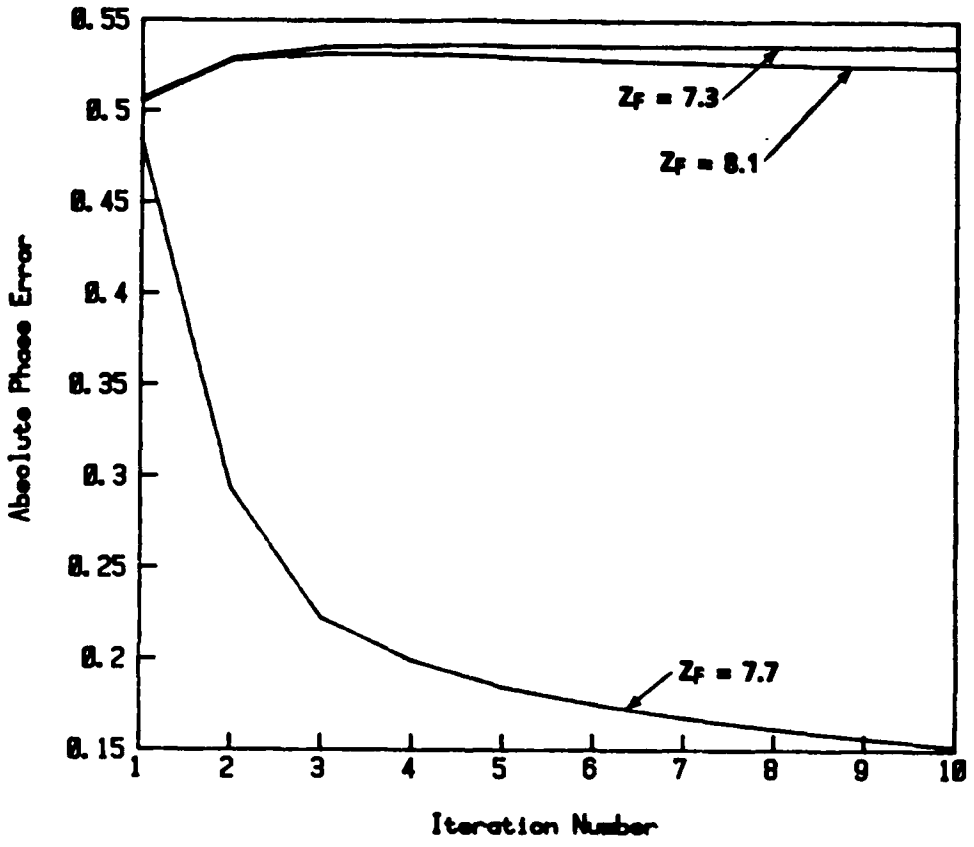

Fig. 6-5. Absolute error in the transform plane, $E_p^{(i)}$ vs. the number of iterations using. The assumed number of Fresnel zones is indicated.

iterations in each reconstruction. Having a 5% error in the number of Fresnel zones is seen to have a significant effect on the absolute phase error in the transform plane. The two iterations using the incorrect value for the number of Fresnel zones show no convergence in the transform error.

Figure 6-6 is a plot of the relative squared errors in the image plane, E_I, for the 10 iterations in each reconstruction. Again, using the incorrect

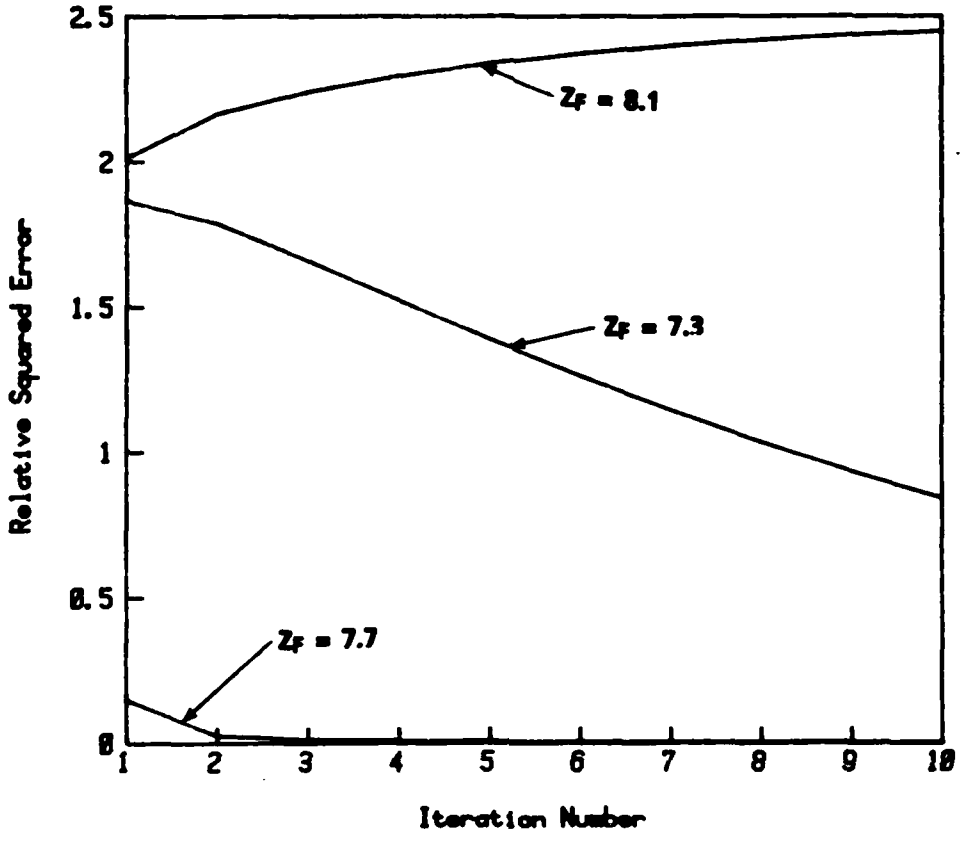

Fig. 6-6. Relative squared errors in the image plane, $E_I^{(i)}$ vs. the number of iterations The assumed number of Fresnel zones is indicated.

number of Fresnel zones has a significant effect on the error in the image plane. There is no convergence in the image plane error as the reconstruction algorithm progresses.

6.2.3 Magnitude-only reconstructions

To examine the sensitivity of the magnitude-only reconstruction algorithm, a set reconstructions using magnitude-only data from 7.7 Fresnel zones were done with the parameter Z_F set equal to 7.3, 7.7, and

8.1 in the reconstruction algorithm. This is the same type of reconstruction that was discussed in the previous example of phase-only reconstructions. Figures 6-7(a), (b), and (c) are the results of this magnitude-only reconstruction after 20 iterations. There is still a recognizable image reconstructed but the quality of the reconstruction is noticably degraded from that which is obtained when the correct number of Fresnel zones is used.

Figure 6-8 is a plot of the absolute magnitude error in the transform plane, E_M, for the 20 iterations in each reconstruction. In this case, there appears to be a convergence of the reconstruction algorithm, but the errors are consistently higher when the incorrect number of Fresnel zones is used.

Figure 6-9 is a plot of the relative squared error in the image plane, E_I, for the 20 iterations in each reconstruction. Again, there is a convergence in the error when there is an error in the number of Fresnel zones, but the stagnation level of the error is consistently higher when the incorrect number of Fresnel zones is used.

From these reconstruction experiments it has been shown that the reconstruction algorithm is sensitive to a 5% error in the value for the number of Fresnel zones, but that the reconstruction algorithm is not unstable with this type of error. In reconstructing from phase-only data, there is a marked degradation in the reconstructed image as the algorithm progresses. The reconstructed image during the first few iterations is fairly insensitive to an error in the number of Fresnel zones, but as the reconstruction algorithm continues, the quality of the

reconstructed image is sacrificed in an attempt to minimize the overall error in both the image and transform planes. In reconstructing from magnitude-only data, there is a definite degradation in the quality of the reconstructed images and the stagnation levels of the errors are larger when there is an error in the number of Fresnel zones. The effects for very large errors are discussed below in Sect. 6-3.

(a) Z_F = 7.3

(b) Z_F = 7.7

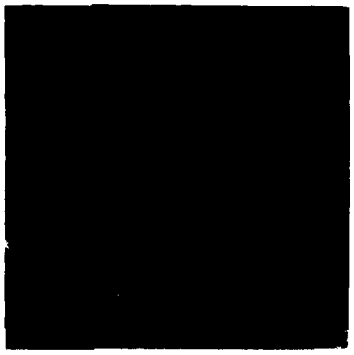

(c) Z_F = 8.1

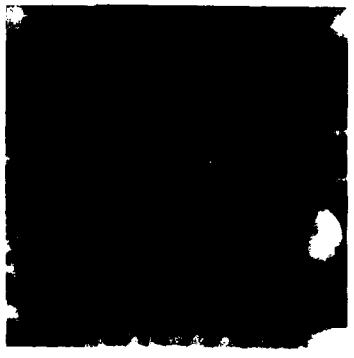

Fig. 6-7. The magnitude-only reconstructions after 20 iterations using (a) $Z_F = 7.3$, (b)$Z_F = 7.7$, and (c)$Z_F = 8.1$.

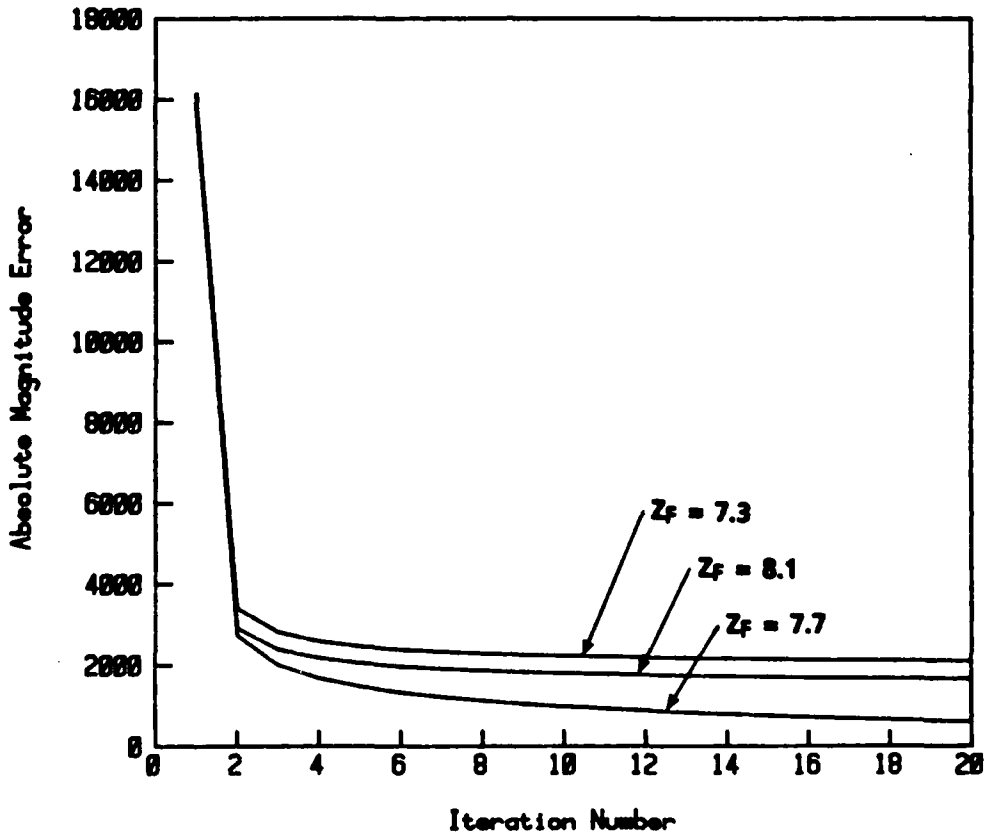

Fig. 6-8. Absolute error in the transform plane, $E_M^{(i)}$ vs. the number of iterations. The assumed number of Fresnel zones is indicated.

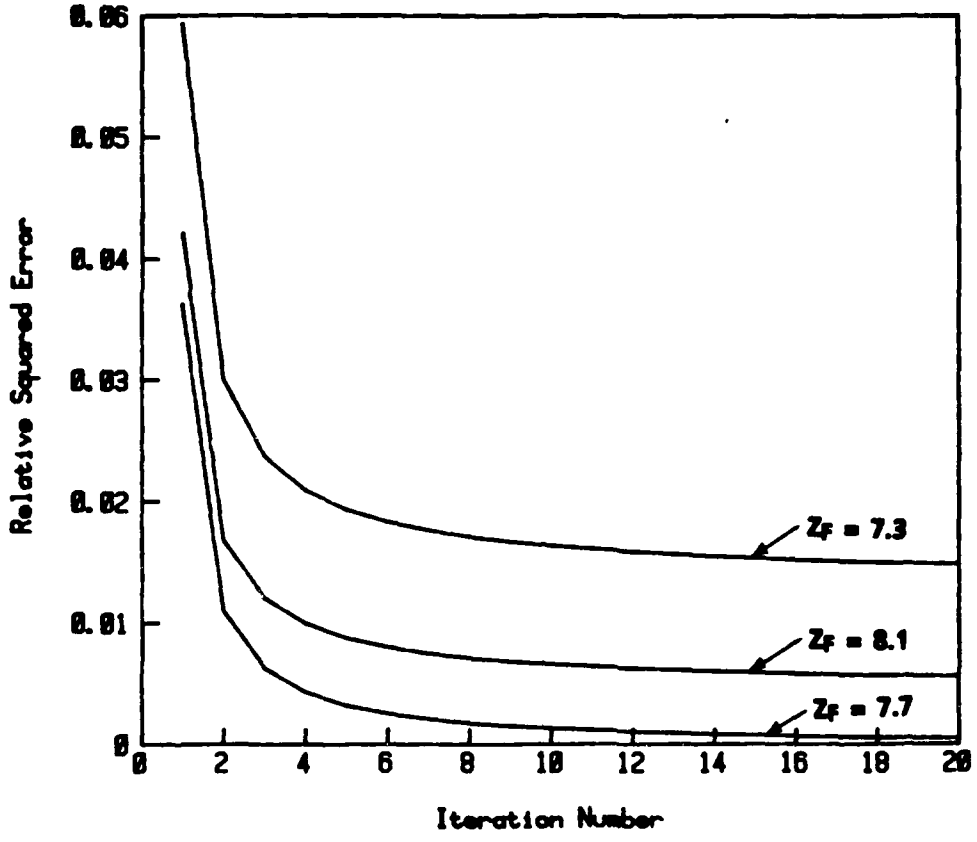

Fig. 6-9. Relative squared errors in the image plane, $E_I^{(i)}$ vs. the number of iterations. The assumed number of Fresnel zones is indicated.

6.3 Searching Through the Fresnel Region

As discussed above, if the number of Fresnel zones is known only approximately, the reconstruction algorithm is stable, but yields a reconstructed image which degrades slowly and steadily depending upon how close to the correct value of Z_F the algorithm is using. If no information about the number of Fresnel zones is available, a guess must be used.

6.3.2 Searching using Magnitude-only data

Figure 6-10 shows the magnitude data of a Fresnel zones transform

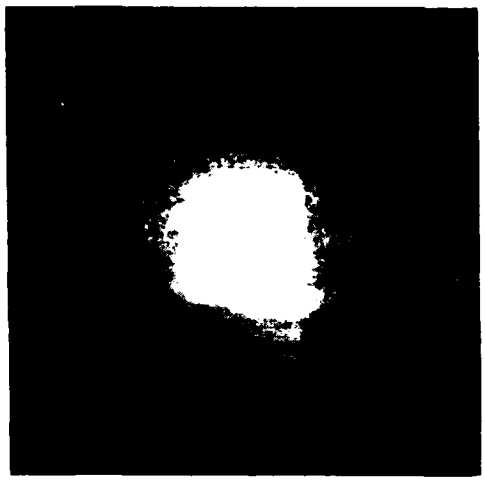

Fig. 6-10. Magnitude of a Fresnel zone transform at an unknown location in the Fresnel zone region.

from an unknown location in the Fresnel zone region. It is assumed that because of sampling considerations, the number of Fresnel zones is less than or equal to 12.0.

The first stage of the search for the correct number of Fresnel zones involves trying to reconstruct from various locations in the Fresnel zone region. For a set of values $0.5 \leqq Z_F \leqq 12.0$ with an increment of 0.5, the magnitude-only reconstruction algorithm was run through two complete cycles for each value of Z_F. Both the absolute magnitude error, E_M, and the relative squared error, E_I, were tabulated for the attempted reconstructions. Figure 6-11 is a plot of the absolute error in the

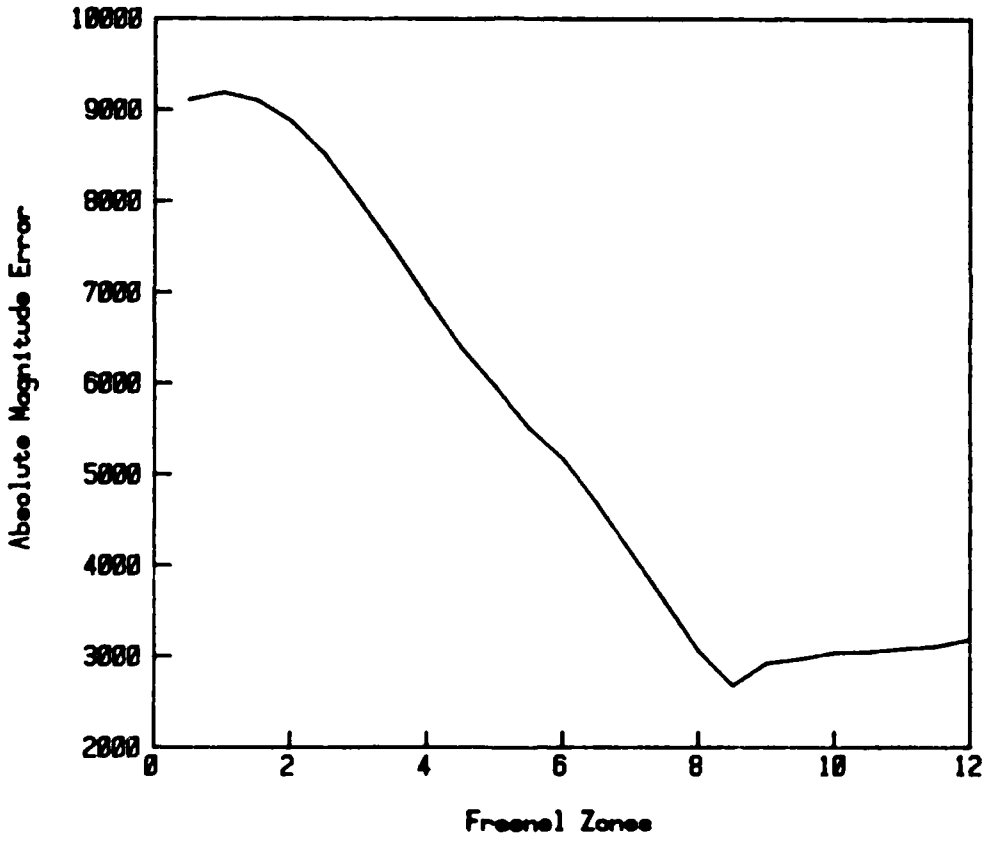

Fig. 6-11. Plot of the absolute magnitude error, $E_M^{(i)}$, vs. guesses for the number of Fresnel zones.

transform plane after the second iteration verses the assumed number of

Fresnel zones. Note that this curve has a distinct minimum in the area around 8.0 to 8.5 Fresnel zones.

To obtain a more accurate estimate for the unknown value of Z_F, a fine scale search is now done for $8.0 \leqq Z_F \leqq 8.5$ with step a size of 0.1. The results of this fine scale search are shown in Fig. 6-12. Again, note that

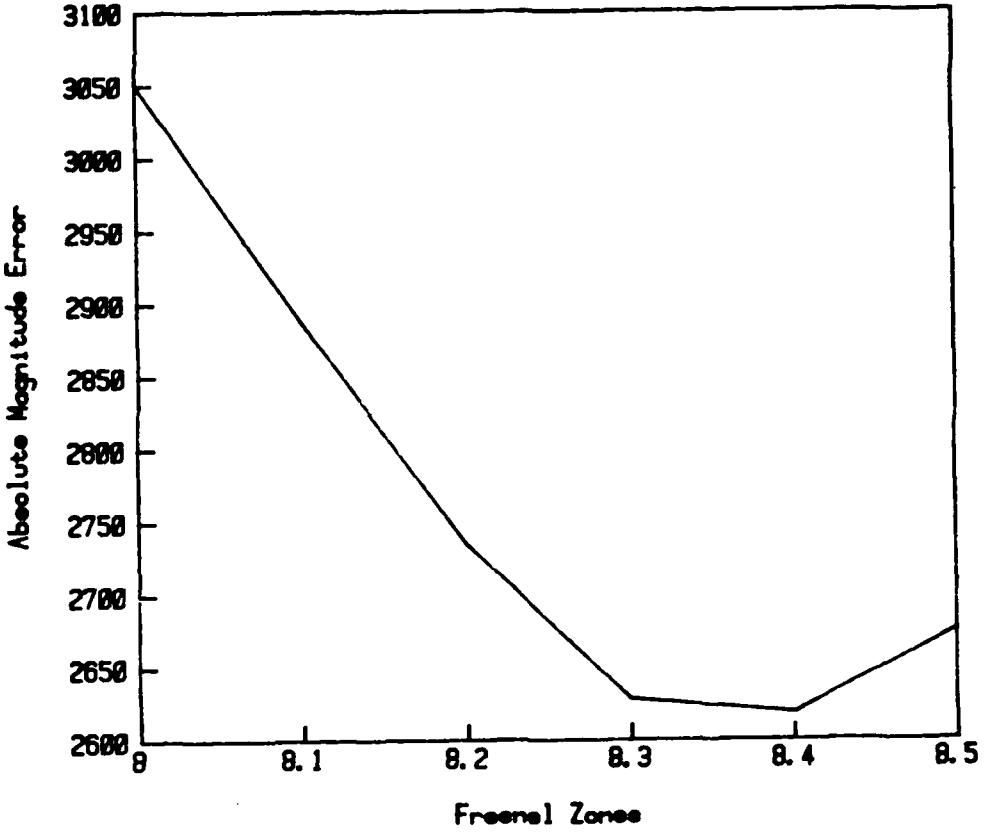

Fig. 6-12. Plot of the absolute magnitude error, $E_M^{(i)}$, vs. fine scale guesses for the number of Fresnel zones.

there is a distinct minimum in the region near 8.3 Fresnel zones.

Using the value of 8.3 for Z_F, a number of iterations were now performed. The reconstructed image after 10 iterations is shown in Fig. 6-

13. This reconstructed image is easily recognized. It is interesting to note

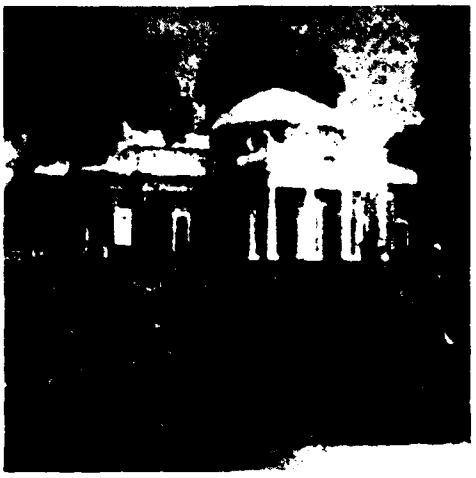

Fig. 6-13. Reconstruction after 10 iterations using $Z_F = 8.3$. The true number of Fresnel zones is 8.32.

that the unknown magnitude data shown in Fig. 6-10 was actually calculated at 8.32 Fresnel zones. This searching technique could be continued to yield a more accurate estimate for the number of Fresnel zones, but it was demonstrated in the previous section that the quality of the reconstruction is dependent upon the estimate for the number of Fresnel zones. The time and effort spent on this searching would depend upon the quality of the reconstruction which is desired.

6.3.3 Searching Using Phase-only data

Figure 6-14 shows the phase data of a Fresnel zone transform from an unknown location in the Fresnel zone region. The same type of searching algorithm that was discussed in the previous section was used with the

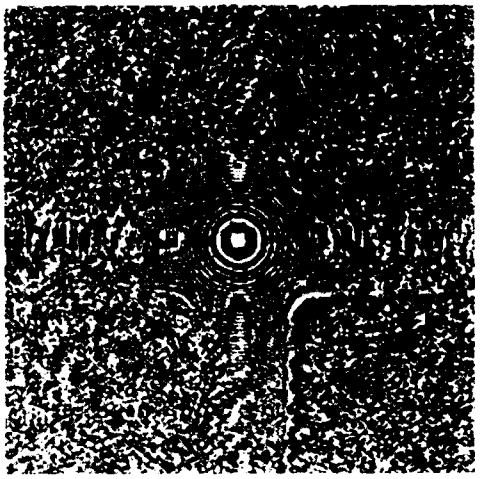

Fig. 6-14. Phase of a Fresnel zone transform at an unknown location in the Fresnel zone region.

same assumption that the number of Fresnel zones is less than or equal to 12.0.

The first stage of the search for the correct number of Fresnel zones requires a finer search through the entire possible range of Fresnel zones. For a set of values $0.25 \leqq Z_F \leqq 12.0$ with an increment of 0.25, the phase-only reconstruction algorithm was run through two complete cycles. For each guess at the number of Fresnel zones, both the absolute phase error, E_P, and the relative squared error, E_I, were tabulated for the for the first two cycles of the reconstruction algorithm. Figure 6-15 is a plot of the absolute phase error in the transform plane after the second iteration verses the assumed number of Fresnel zones. Note that this curve has a much sharper minimum than the curve shown in Fig. 6-11, which is the reason a smaller increment in the number of Fresnel zones is used in the

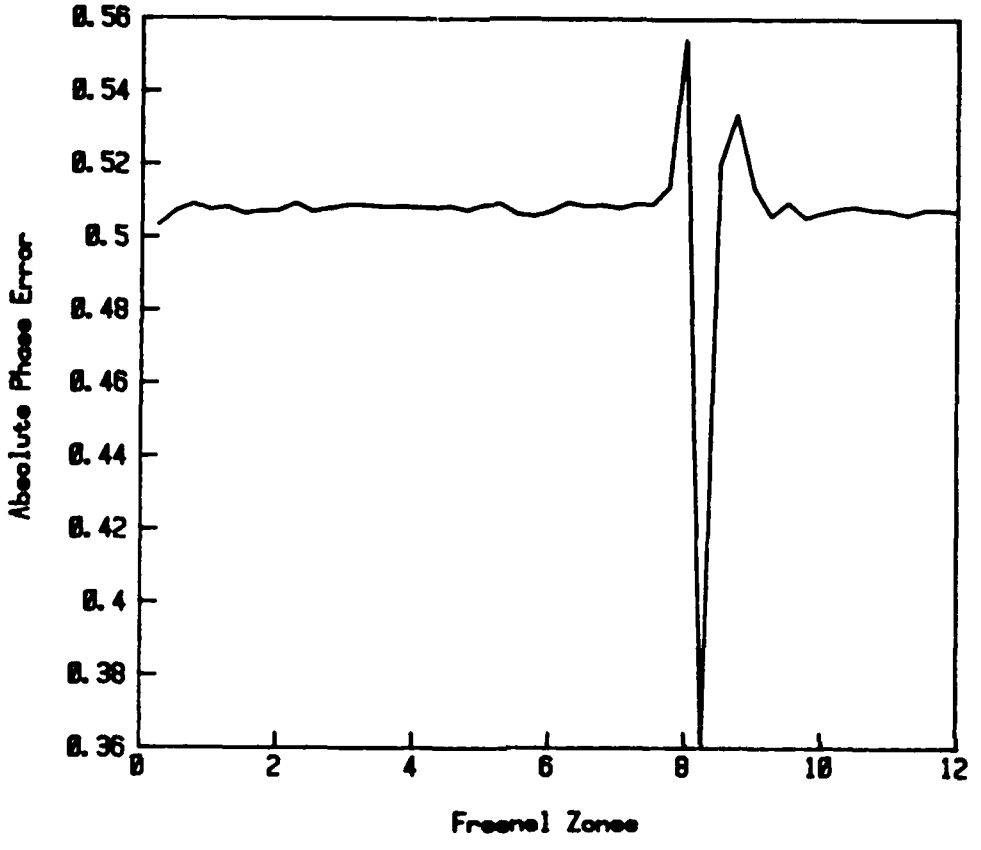

Fig. 6-15. Plot of the absolute phase error, $E_P^{(i)}$, vs. guesses for the number of Fresnel zones.

searching. The very sharp minimum is in the area around 8.0 to 8.5 Fresnel zones.

To obtain a more accurate estimate for the unknown value of Z_F, a fine scale search is now done for $7.8 \leqq Z_F \leqq 8.7$ with step a size of 0.1. The results of this fine scale search are shown in Fig. 6-16. Again, note that there is a distinct minimum when the guess for the Fresnel zones is equal to 8.3.

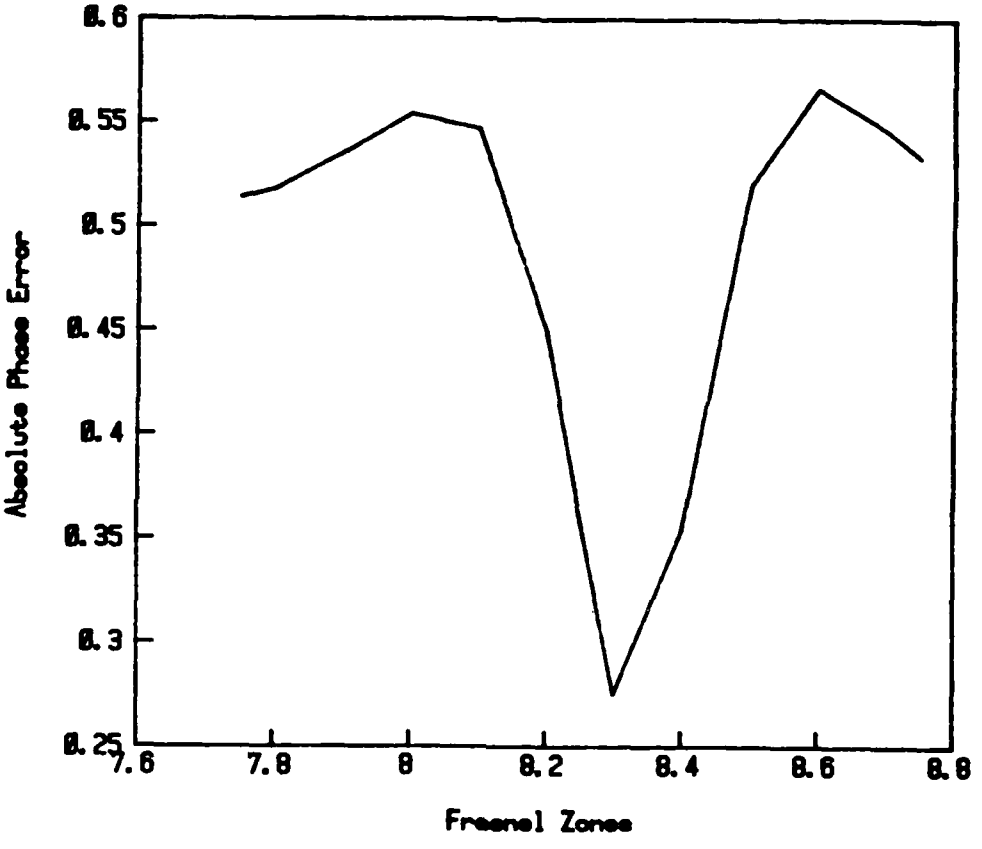

Fig. 6-16. Plot of the absolute phase error, $E_p^{(i)}$, vs. fine scale guesses for the number of Fresnel zones.

Using the value of 8.3 for Z_F, a number of iterations were now performed. The reconstructed image after 10 iterations is shown in Fig. 6-18. This reconstructed image is easily recognized. It is interesting to note that as in the previous example, the given phase data shown in Fig. 6-14 was actually calculated at 8.32 Fresnel zones. An exact value for the correct number of Fresnel zones is not needed to successfully recover a good quality image.

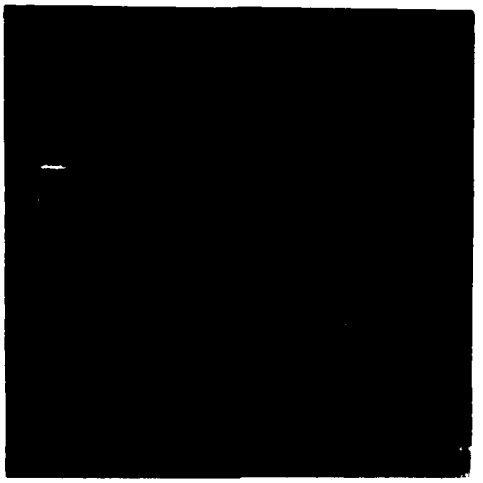

Fig. 6-17. Reconstruction after 5 iterations using $Z_F = 8.3$. The true number of Fresnel zones is 8.32.

6.3.4 Conclusions

In Sect 6.2 it was shown that a 5% error in the number of Fresnel zones produces a definite degradation in the quality of the reconstructions. Both the magnitude-only and phase-only reconstruction algorithms are sensitive to this type of error.

The stability and sensitivity of the reconstruction algorithms allowed for the development of another algorithm which is designed to search through the Fresnel zone region to determine the correct value of Z_F The error metrics used to do the searching are the same measures of error that are used to monitor the progression of the reconstruction algorithms. It is very likely possible to develop improved error metrics and searching techniques for the reconstruction of images from partial data at an unknown location in the Fresnel zone region.

Bibliography

M. Abramowitz and I. A. Stegun,
Handbook of Mathematical Functions with Formulas, Graphs, and Mathematical Tables, M. Abramowitz and I. A. Stegun, eds., (U.S. Government Printing Office, Washington D.C., 1972)

H. A. Arsenault and K. Chalaskinska-Macukow,
"The solution to the phase retrieval problem using the sampling theorem," Opt. Comm. **47**, 380-386 (1983).

J. F. Asmus,
"Digital image processing in art conservation," Byte **12**, 151-165 (1987).

H. P. Baltes, ed.,
Inverse Source Problems in Optics, (Springer-Verlag, Berlin, 1978).

H. P. Baltes, ed.,
Inverse Scattering Problems in Optics, (Springer-Verlag, Berlin, 1980).

R. H. T. Bates,
"Fourier phase problems are uniquely solvable in more than one dimension. I: Underlying theory," Optik **61**, 247-262 (1982).

R. H. T. Bates and M. J. McDonnell,
Image Restoration and Reconstruction, (Oxford University Press, 1986).

M. Born and E. Wolf,
Principles of Optics, (Pergamon Press, New York, 1980).

J. C. Bortz,
"Phase retrieval by optical phase differentiation," Ph. D. Dissertation, University of Rochester, (1983).

R. H. Boucher,
"Convergence of algorithms for phase retrieval from two intensity distributions," in *1980 International Optical Computing Conference*, W.T. Rhodes, ed., Proc. Soc. Photo-Opt. Instrum. Eng. **231**, 130-141 (1980a).

R. H. Boucher,
"Phase retrieval techniques for image and wavefront reconstruction," Ph. D. Dissertation, University of Rochester, (1980b).

B. J. Brames,
"Unique phase retreival with explicit support information," Opt. Lett. **11**, 61-63 (1986).

B. J. Brames,
"Uniqueness and other aspects of the optical phase problem," Ph. D. Dissertation, University of Rochester, (1985).

Yu. M. Bruck and L. G. Sodin,
"On the ambiguity of the image reconstruction problem," Opt. Comm. **30**, 304-308 (1979).

P. A. Childs and D. L. Misell,
"Some aspects of image deconvolution in electron microscopy," J. Phys. D: Appl. Phys. **6**, 1653-1663 (1973).

E. T. Copson,
Asymptotic Expansions, (Cambridge University Press, 1965).

W. J. Dallas,
"Digital computation of image comples amplitude from image- and diffraction-intensity: an alternative to holography," Optik **44**, 45-59 (1975).

W. J. Dallas,
"Digital computation of image complex-amplitude from intensities in two image-space planes," Opt. Comm. **18**. 317-320 (1976).

H. V. Deighton, M. S. Scivier and M.A. Fiddy,
"Solution of the two-dimensional phase-retrieval problem," Opt. Lett. **10**, 250-251 (1985).

A. Erdelyi,
Asymptotic Expansions, (Dover, New York, 1956).

G. B. Feldkamp and J. R. Fienip,
"Noise properties of images reconstructed from Fourier modulus," in *1980 International Optical Computing Conference*, W.T. Rhodes, ed., Proc. Soc. Photo-Opt. Instrum. Eng. **231**, 84-93 (1980).

M. A. Fiddy, G.Ross, M. Nieto-Vesperinas and A. M. Huiser,
"Encoding of information in inverse optical problems," Optica Acta **29**, 23-40 (1982).

M. A. Fiddy, B. J. Brames and J. C. Dainty,
"A sufficient condition for phase retrieval in two dimensions," in *Digest of the Topical Meeting on Signal Recovery and Synthesis with Incomplete Information and Partial Constraints* (Optical Society of America, Washington D.C., 1983).

J. R. Fienup,
"Reconstruction of an object from the modulus of its Fourier transform," Opt. Lett. **3**, 27-29 (1978).

J. R. Fienup,
"Space object imaging through the turbulent atmosphere," Opt. Eng. **18**, 529-534 (1979).

J. R. Fienup,
"Reconstruction and synthesis application of an iterative algorithm," in *Transformations in Optical Signal Processing*, W. T. Rhodes, J. R. Fienup, and B. E. A. Saleh, eds., SPIE-The International Society for Optical Engineering **373**, 147-160 (1981a)

J. R. Fienup,
"Image reconstruction for stellar interferometry," in *Current Trends in Optics*, Arechi and Aussenegg, eds. (Taylor & Francis, London, 1981b), p. 95.

J. R. Fienup,
"Phase retrieval algorithms: a comparison," Appl. Opt. **21**, 2758-2769 (1982).

J. R. Fienup,
"Phase retrieval in astronomy," in *Digest of the Topical Meeting on Signal Recovery and Synthesis with Incomplete Information and Partial Constraints* (Optical Society of America, Washington D.C., 1983).

J. R. Fienup and C. C. Wackerman,
"Phase-retrieval stagnation problems and solutions," J. Opt. Soc. Am. A **3**, 1897-1907 (1986).

J. R. Fienup,
"Phase retrieval: Algorithm improvements, uniqueness, and complex objects," in *Digest of the Topical Meeting on Signal Recovery & Synthesis II* (Optical Society of America, Washington D.C., 1986a).

J. R. Fienup,
"Phase retrieval using boundary conditions,"J. Opt. Soc. Am. A **3**, 284-288 (1986b).

B. R. Frieden,
"Restoring with maximum likelihood and maximum entropy," J. Opt. Soc. Am. **62**, 511-518 (1972).

W. R. Fright and R. H. T. Bates,
"Fourier phase problems are uniquely solvable in more than one dimension II: Computaional examples for two dimensions,"Optik **62**, 219-230 (1982).

K. L. Garden and R. H. T. Bates,
"Fourier phase problems are uniquely solvable in more than one dimension II: One dimensional considerations,"Optik **62**, 131-142 (1982).

R. W. Gerchberg and W. O. Saxton,
"A Practical Algorithm for the Determination of Phase from Image and Diffraction Plane Pictures," Optik, **35**, 237-246 (1972).

R. W. Gerchberg and W. O. Saxton,
"Comment on 'A method for the solution of the phase problem in electron mcroscopy'," J. Phys. D: Appl. Phys. **6**, L31-L32 (1973).

P. D. Gianino and J. L. Horner
"Additional properties of the phase-only correlation filter," Opt. Eng. **23**, 695-697 (1984).

J. W. Goodman,
Introduction to Fourier Optics, (McGraw-Hill, New York, 1968).

J. W. Goodman,
Statistical Optics, (John Wiley & Sons, New York, 1985).

F. Gori,
"Fresnel transform and sampling theorem," Opt. Comm. **39**, 293-297 (1981).

I. S. Gradshteyn and I. M. Ryzhik,
Tables of Integrals, Series, and Products, (Academic Press, New York, 1980).

A. H. Greenaway,
"Proposal for phase recovery from a single intensity distibution," Opt. Lett. **1**, 10-12 (1977).

M. H. Hayes,
"Signal recovery from phase or magnitude," Ph. D. Dissertation, Massachusetts Institute of Technology (1981).

M. H. Hayes,
"The Reconstruction of a multidimensional sequence from the phase or magnitude of its Fourier transform," IEEE Trans. Acoust. Speech Signal Process. **ASSP-30**, 140-154 (1982).

M. H. Hayes,
"The unique reconstruction of multidimensional sequences from Fourier transform magnitude and phase," in *Image Recovery: Theory and Applications*, H. Stark, ed., (Academic Press, Orlando, 1987).

M. H. Hayes, J. S. Lim, and A. V. Oppenheim,
"Signal reconstruction from phase or magnitude," IEEE Trans. Acoust. Speech Signal Process. **ASSP-28**, 672-680 (1980).

M. H. Hayes, J. S. Lim, and A. V. Oppenheim,
"Iterative procedure for signal reconstruction from Fourier transform phase," Opt. Eng. **21**, 122-127 (1982).

M. H. Hayes and J. H. McClellan,
"Reducible polynomials in more than one variable," Proc. IEEE **70**, 197-198 (1982).

T. Haque and R. A. Meyer,
"Iterative reconstruction of images from Fourier-transform phase using moments," Opt. Lett. **11**, 764-766 (1986).

J. L. Horner and P. D. Gianino,
"Phase-only matched filtering," Appl. Opt. **23**, 812-816 (1984).

T. S. Huang, J. W. Burnett, and A. G. Jeczky,
"The importance of phase in image processing filters," IEEE Trans. Acoust., Speech, Signal Processing, **ASSP-23**, 529-542 (1975).

A. M. J. Huiser and P. van Toorn,
"Ambiguity of the phase-reconstruction problem," Opt. Lett. **5**, 499-501 (1980).

D. Kermisch,
"Image reconstruction from phase information only," J. Opt. Soc. Am. **60**, 15-17 (1970).

P. Kierdron,
"On the 2-D solution ambiguity of the phase recovery problem," Optik **59**, 303-309 (1981).

P. Kierdron,
"Conditions sufficient for one-dimensional unique recovery of the phase under the assumption that the intensity distributions: $|f(x)|^2$ and $|df(x)/dx|^2$ are known," Optica Applicata **10**, 149-154 (1980).

R. E. Kinzly, R. C. Haas, and P. G. Roetling,
"Designing filters for image processing to recover detail," in *Image Information Recovery*, SPIE Seminar Proceedings **16**, 97-104 (1969).

D. Kohler and L. Mandel,
"Operational approach to the phase problem in optical coherence," J. Opt. Soc. Am. **60**, 280-281 (1970).

D. Kohler and L. Mandel,
"Source reconstruction from the modulus of the correlation function: a practical approach to the phase problem of optical coherence theory," J. Opt. Soc. Am. **63**, 126-134 (1973).

L. B. Lesem, P. M. Hirsch, and J. A. Jordan, Jr.,
"The kinoform: A new wavefront reconstruction device," IBM J. Res. Develop 13, 150-155 (1969).

A. Levi and H. Stark,
"Signal restoration from phase by projections onto convex sets," J. Opt. Soc. Am. 73, 810-822 (1983).

A. Levi and H. Stark,
"Image restoration by the method of generalized projections with application to restoration from magnitude," J. Opt. Soc. Am. A 1,932-943 (1984).

C. L. Mehta,
"Determination of spectral profiles from correlation measurements," Nuovo Cimento 36, 202-205 (1965).

C. L. Mehta,
"New approach to the phase problem in optical coherence theory," J. Opt. Soc. Am. 58, 1233-1234 (1968).

A. A. Michelson,
"On the application of interference-methods to spectroscopic measurements-I," Phil. Mag. 31, 338-345 (1891).

A. A. Michelson,
"On the application of interference-methods to spectroscopic measurements-II," Phil. Mag. 34, 280-298 (1892).

D. L. Misell and P. A. Childs,
"Deconvolution in two dimensions with particular reference to the electron microscope," J. Phys. D: Appl. Phys. 5, 1760-1768 (1972).

D. L. Misell,
"A method for the solution of the phase problem in electron microscopy," J. Phys. D: Appl. Phys. 6, L6-L9 (1973a).

D. L. Misell,
"An examination of an iterative method for the solution of the phase problem in optics and electron optics: I. Test calculations," J. Phys. D: Appl. Phys. 6, 2200-2216 (1973b).

D. L. Misell,
"An examination of an iterative method for the solution of the phase problem in optics and electron optics: II. Sources of error," J. Phys. D: Appl. Phys. 6, 2217-2225 (1973c).

P. J. Napier and R. H. T. Bates,
"Inferring phase information from modulus information in two-dimensional aperture synthesis," Astron. Astrophys. Suppl. 15, 427-430 (1974).

M. Nieto-Vesperinas,
"Dispersion relations in two dimensions: Application to the phase problem," Optik **56**, 377-384 (1980).

H. M. Nussenzveig,
"Phase problem in coherence theory," J. Math. Physics **8**, 561-572 (1967).

E. L. O'Neill and A. Walther,
"The question of phase in image formation," Opt. Acta. **10**, 33-40 (1963).

A. V. Oppenheim, J. S. Lim, G. E. Kopec, and S. C. Pohlig,
"Phase in speech and pictures," Proc. IEEE Int. Conf. Acoust., Speech, and Signal Processing, 632-637, (1979).

A. V. Oppenheim, M. H. Hayes and J. S. Lim,
"Iterative procedure for signal reconstruction from phase," in *1980 International Optical Computing Conference*, W.T. Rhodes, ed., Proc. Soc. Photo-Opt. Instrum. Eng. **231**, 121-129 (1980).

A. V. Oppenheim and J. S. Lim,
"The importance of phase in signals," Proc. IEEE **69**, 529-541 (1981).

A. V. Oppenheim, M. H. Hayes, and J. S. Lim,
"Iterative procedure for signal reconstruction from phase," Opt. Eng. 21, 122-127 (1982).

A. V. Oppenheim, J. S. Lim, and S. R. Curtis,
"Signal synthesis and reconstruction from partial Fourier-domain information," J. Opt. Soc. Am. 73, 1413-1420 (1983).

A. V. Oppenheim and J. S. Lim,
"Signal reconstruction from partial Fourier domain information," in *Digest of the Topical Meeting on Signal Recovery and Synthesis with Incomplete Information and Partial Constraints* (Optical Society of America, Washington D.C., 1983).

A. Papoulis,
Probability, Random Variables, and Stochastic Processes, (McGraw-Hill, New York, 1965).

W. Pearlman and R. Gray,
"Source coding of the discrete Fourier transform," IEEE Trans. Inform. Theory **IT-24**, 683-692 (1978).

W. K. Pratt,
Digital Image Processing, (John Wiley & Sons, New York, 1978)

Lord Rayleigh,
"On the interference band of approximately homogeneous light; in a letter to Prof. A. Michelson," Phil. Mag. **34**, 407-411 (1892).

R. Rolleston and N. George,
"Image reconstruction from partial Fresnel zone information," Appl. Opt. **25**, 178-183 (1986).

R. Rolleston and N. George,
"Stationary phase approximations in Fresnel zone magnitude-only reconstructions," J. Opt. Soc. Am. A **4**, 148-153 (1987).

G. Ross, M. A. Fiddy, and H. Moezzi,
"The solution to the inverse scattering problem, based on the fast zero location from two measurements," Optica Acta **27**, 1433-1444 (1980).

B. E. A. Saleh,
"Image synthesis: Discovery instead of recovery," in *Image Recovery: Theory and Applications*, H. Stark, ed., (Academic Press, Orlando, 1987).

J. L. C. Sanz and T. S. Huang,
"Unique reconstruction of a band-limited multidimensional signal from its phase or magnitude," J. Opt. Soc. Am. **73**, 1446-1450 (1983).

M. S. Scivier and M. A. Fiddy,
"Phase ambiguities and the zeros of multidimensional band-limited functions," J. Opt. Soc. Am. A **2**, 693-697 (1985).

R. M. Scott,
The Practical Applications of Modulation Transfer Functions, (Perkin-Elmer Corp, Norwalk, CT, 1963).

J. L. Seligson,
"Phase measurements in the focal region of an aberrated lens," Ph. D. Dissertation, University of Rochester (1981).

M. I. Sezan and H. Stark,
"Image restoration by the method of convex projections: Part 2-Applications and numerical results," IEEE Trans. Med. Imag. **MI-1**, 95-101 (1982).

H. Stark, ed.,
Image Recovery: Theory and Applications, (Academic Press, Orlando, 1987).

J. S. Toll,
"Causality and the dispersion relations: Logical foundations," Phys. Rev. **104**, 1760-1770 (1956).

A. VanderLugt,
"Fresnel transforms and Bragg cell processors," App. Opt. **24**, 3846-3859 (1985).

P. L. Van Hove,
"Signal reconstruction from Fourier transform amplitude," M. S. Dissertation, Massachusetts Institute of Technology (1982).

P. L. Van Hove, J. S. Lim, and A. V. Oppenheim,
"Signal reconstruction from Fourier transform amplitude," in *Digest of the Topical Meeting on Signal Recovery and Synthesis with Incomplete Information and Partial Constraints* (Optical Society of America, Washington D.C., 1983).

N. G. Van Kampen,
"An asymptotic treatment of diffraction problems," Physica **14**, 575-589 (1949).

N. G. Van Kampen,
"An asymptotic treatment of diffraction problems II," Physica **16**, 817-821 (1950).

A. Walther,
"The question of phase retrieval in optics." Opt. Acta. 10, 41-49 (1963).

E. Wolf,
"Is a complete determination of the energy spectrum of light possible from measurements of the degree of coherence?," Proc. Phy. Soc. **80**, 1269-1272 (1962).

D. C. Youla and H. Webb,
"Image restoration by the method of convex projections: Part 1-Theory," IEEE Trans. Med. Imag. MI-1, 81-94 (1982).

Appendix A

Aberrated Wavefront Illumination

An alternative view of the optical Fresnel zone transform described in Sect. 2.2 will be presented in this appendix. The image reconstruction algorithms discussed in Chapt. 2 assumed that the object , which is real-valued and non-negative, is illuminated by a coherent plane wave. Consider the optical transform system shown in Fig. A-1. In this case, the

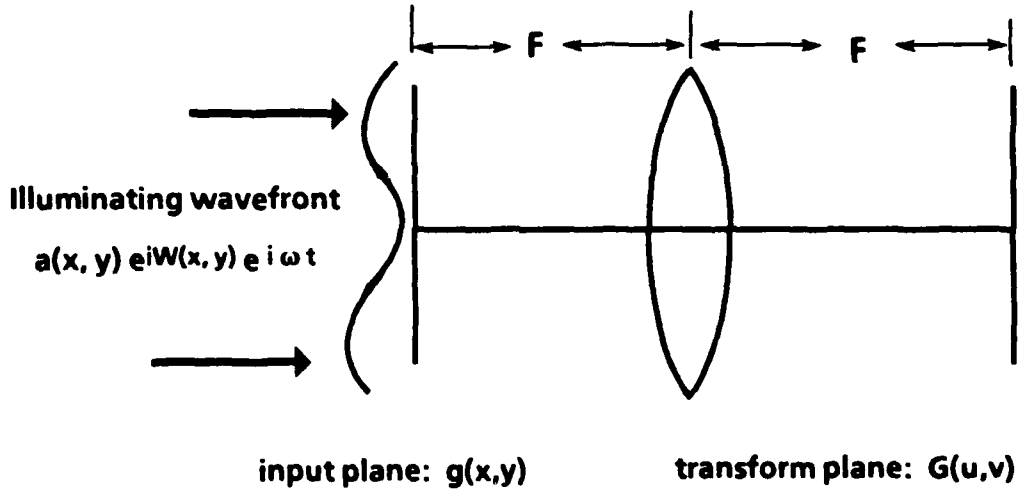

Fig. A-1 Coherent optical Fourier transform system.

object is known to be real-valued and non-negative, the Fourier transform plane is located in the back focal plane of the lens, and the illuminating wavefront has an amplitude and phase described by the function, a(x,y)exp{iW(x,y)}.

The scalar components of the electric field in the front and back focal planes of the lens are related through a Fourier transform pair. If the amplitude transmittance of the image is denoted by g(x,y), and the scalar component of the field in the transform plane is denoted by $G(f_x, f_y)$, then the Fourier transform relation which relates the fields in the front and back focal planes of the lens is given by

$$G(f_x, f_y) = \int_{-\infty}^{+\infty}\int_{-\infty}^{+\infty} g(x,y)a(x,y)e^{i\,W(x,y)}\, e^{-i\,2\pi(f_x x + f_y y)}\, dxdy\,, \tag{A-1}$$

and the inverse transform is given by

$$g(x,y) = \frac{1}{a(x,y)}e^{-i\,W(x,y)} \int_{-\infty}^{+\infty}\int_{-\infty}^{+\infty} G(f_x, f_y)\, e^{+i\,2\pi(f_x x + f_y y)}\, df_x df_y\,, \tag{A-2}$$

where the spatial frequency variables f_x and f_y have been defined as

$$f_x = -u/\lambda F \quad and \quad f_y = -v/\lambda F\,. \tag{A-3}$$

Notice that if a(x,y) = 1.0 and $W(x,y) = -\pi a_1(x^2 + y^2)$, then Eqs. (A-1) and (A-2) reduce to the Fresnel zone transform pair described in Chapt. 2.

It is now possible to apply the reconstruction techniques described in Chapt. 2 to the case of a generalized illuminating wavefront. Consider a phase function for the illuminating wavefront which contains the 5 primary aberrations; the phase of this wavefront can be written as

$$W(x,y) = 2\pi\{A(x^2 + y^2)^2 + By(x^2 + y^2) + C(x^2 + 3y^2)$$

$$+ D(x^2 + y^2) + Ey + Fx\}\,, \tag{A-5}$$

where A is the number of waves of spherical, B is the number of waves of

coma, C is the number of waves of astigmatism, D is the number of waves of defocus, E is the number of waves of tilt about the x-axis, and F is the number of waves of tilt about the y-axis.

The original 256 X 256 X 8-bit digitized image used in the following reconstruction experiments is shown in Fig. A-2.

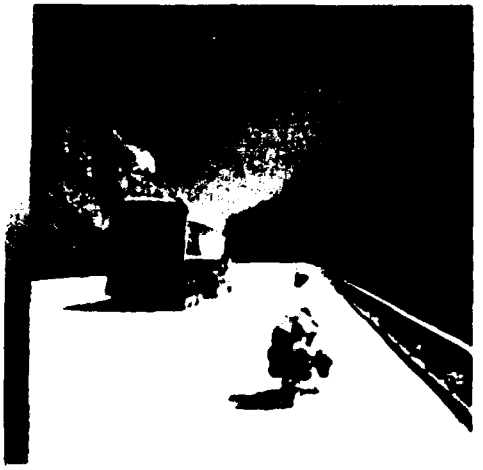

Fig. A-2 Original digitized image used in the reconstruction experiments. The image has 256 X 256 pixels with 8 bits/pixel.

The magnitude and phase of the Fourier transform when there is a small amount of aberration present in the illuminating wavefront is shown in Fig. A-3. For this example: $a(x,y) = 1.0$, $A = 0.4$, $B = 0.3$, $C = -0.4$, $D = -0.1$, $E = 0.0$, and $F = 0.0$. Note that the magnitude information shown in Fig. A-3(a) appears to have a polar symmetry; this is the case for the Fourier magnitude of a real-valued object. The phase information shown in Fig. A-3(b) has no distinct pattern. The magnitude and phase information from this Fourier transform with an aberrated illumination

wavefront is very similar to the information one would obtain from a Fourier transform obtained with plane wave illumination.

The magnitude-only and phase-only reconstructions are shown in Fig. A-4. The magnitude-only reconstruction after 10 iterations, shown in Fig. A-4(a), is easily recognized and is about the same quality as a magnitude-only reconstruction after 5 iterations from Fresnel zone data at 3.0 Fresnel zones. The phase-only reconstruction after 5 iterations, shown in Fig. A-4(b), is very good. In the phase-only reconstruction the edges are recovered very quickly, and as the iterations continue the low frequency areas of the picture are slowly improved.

A second set of reconstruction experiments was performed with the parameters $a(x,y) = 1.0$, $A = 4.0$, $B = 3.0$, $C = -4.0$, $D = -1.0$, $E = 0.0$, and $F = 0.0$. The magnitude and phase of of this Fourier transform are shown in Fig A-5. Notice that the magnitude information shown in Fig. A-5(a) is more spread out than in the case of a Fourier transform obtained with plane wave illumination, and that there is no longer any symmetry to the magnitude data. The phase information shown in Fig. A-5(b) has small regions which show a slowly varying structure in the phase data.

The two reconstruction from this data are shown in Fig A-6. After 10 iterations the magnitude-only reconstruction shown in Fig. A-6(a) is fairly good, and is about the same quality as a magnitude-only reconstructionafter 5 iterations from Fresnel zone data at 5.0 Fresnel zones. The phase-only reconstruction after 5 iteration shown in Fig. A-6(b) is very good.

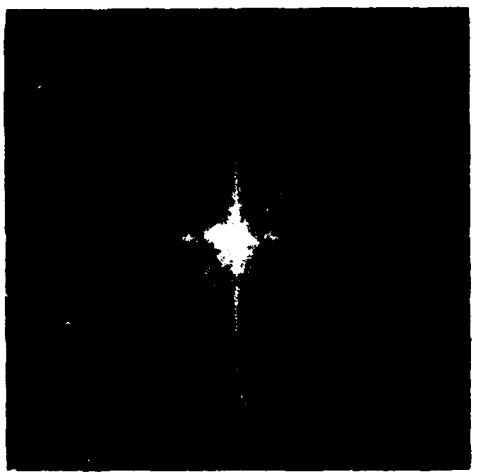

(a) Magnitude

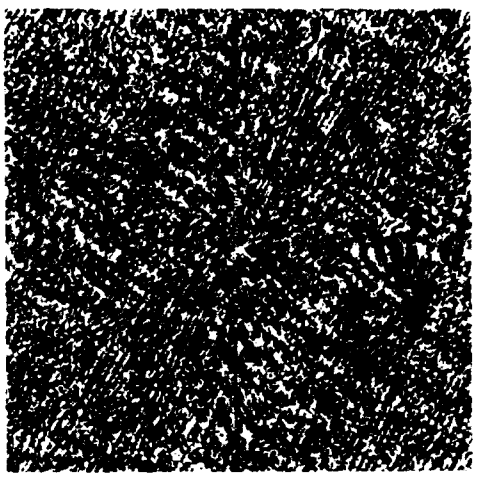

(b) Phase

Fig. A-3 (a)magnitude and (b) phase of Fourier transform using an aberrated wavefront with a(x, y) = 0.1, A = 0.4, B = 0.3, C = -0.4, D = -0.1, E = 0.0, and F = 0.0.

(a) Magnitude-only Reconstruction

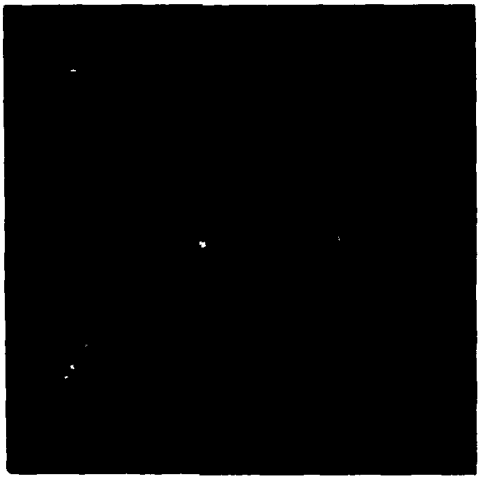

(b) Phase-only Reconstruction

Fig. A-4 (a)Magnitude-only reconstruction after ten iterations. (b)Phase-only reconstruction after five iterations.

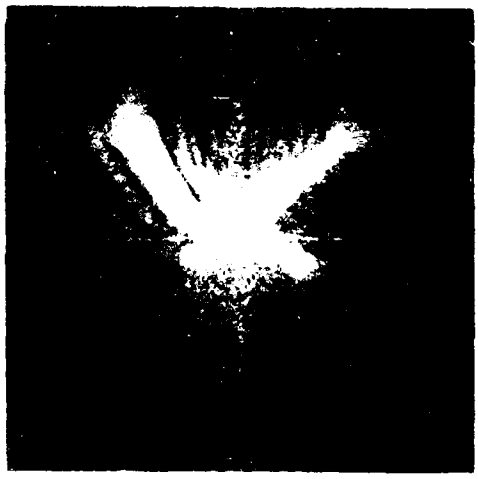

(a) Magnitude

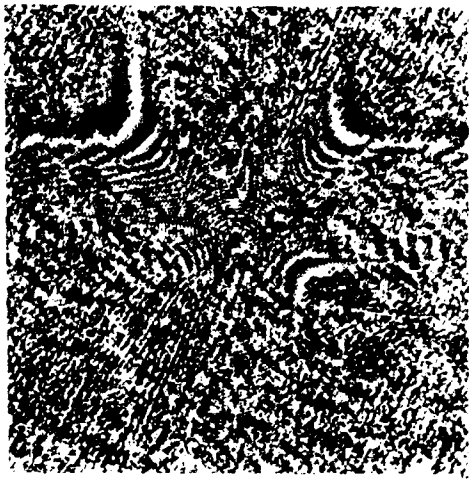

(b) Phase

Fig. A-5 (a)magnitude and (b) phase of Fourier transform using an aberrated wavefront with $a(x, y) = 1.0$, $A = 4.0$, $B = 3.0$, $C = -4.0$, $D = -1.0$, $E = 0.0$, and $F = 0.0$.

(a) Magnitude-only Reconstruction

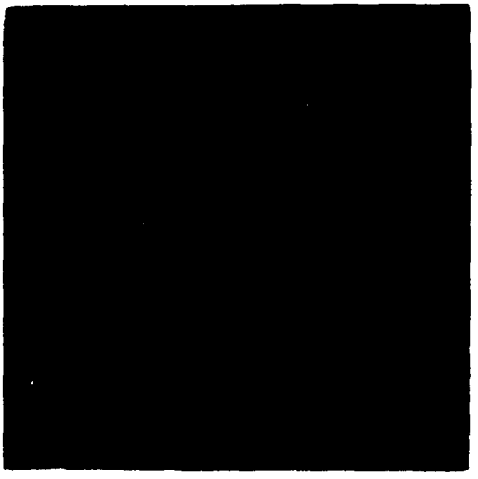

(b) Phase-only Reconstruction

Fig. A-6 (a)Magnitude-only reconstruction after ten iterations. (b)Phase-only reconstruction after five iterations.

A coherent optical system which has an aberrated wavefront illuminating a real-valued, non-negative object has been discussed in this appendix. Two examples of the resulting magnitude and phase of the Fourier transform have been presented. Through these examples, it was demonstrated that it is possible to recover an image in just a few iterations from either the phase-only or magnitude-only part of the Fourier transform, if the form of the aberrated illuminating wavefront is known. For a set number of iterations there is an increase in the quality of the reconstructed image obtained from magnitude-only data as the aberrations on the illuminating wavefront become more severe. In reconstructing from phase-only data, a good reconstruction is obtained which is fairly insensitive to the amount of aberration on the illuminating wavefront.

In reconstructing an image from Fresnel zone data, it is assumed that the unknown image is real-valued, non-negative, has a known size, and that the given data comes from a known region in the Fresnel zone of a coherent optical processor. In reconstructing an image from partial Fourier transform data obtained from a coherent optical system with a known aberrated illumination wavefront, the unknown image is again assumed to be real-valued, non-negative, and to have a known size. This unknown image corresponds to the magnitude of the wavefront in the front focal plane of a coherent optical processor. The Fresnel zone transform discussed throughout the body of this dissertation is a special case of the Fourier transform relationship, obtained with an aberrated wavefront, discussed in this appendix.